ARMY RESEARCH LABORATORY

Second Workshop on the Electromagnetics of Combat Induced Atmospheric Obscurants

CIAO II

Volume II: Apendices

by W. Michael Farmer
New Mexico State University

Robert A. Sutherland
Survivability/Lethality Analysis Directorate

ARL-TR-833 September 1996

Sponsored in cooperation with the U.S. Joint Program Office for Special Technology Countermeasures, Dahlgren, VA. 24 October 1994; revised November 1994; December 1994.

NOTICES

Disclaimers

The findings in this report are not to be construed as an official Department of the Army position, unless so designated by other authorized documents.

The citation of trade names and names of manufacturers in this report is not to be construed as an official Government indorsement or approval of commercial products or services referenced herein.

Destruction Notice

When this document is no longer needed, destroy it by any method that will prevent disclosure of its contents or reconstruction of the document.

REPORT DOCUMENTATION PAGE

Form Approved
OMB No. 0704-0188

1. AGENCY USE ONLY (Leave Blank)	2. REPORT DATE	3. REPORT TYPE AND DATES COVERED
	September 1996	Final

4. TITLE AND SUBTITLE

Second Workshop on the Electromagnetics of Combat Induced Atmospheric Obscurants (CIAO II) Volume II: Apendices

5. FUNDING NUMBERS

6. AUTHOR(S)

W. Michael Farmer (NMSU)
Robert A. Sutherland (ARL)

7. PERFORMING ORGANIZATION NAMES(s) AND ADDRESS(ES)

U.S. Army Research Laboratory
Survivability/Lethality Analysis Directorate
ATTN: AMSRL-SL-CA
White Sands Missile Range, NM 88002-5513

8. PERFORMING ORGANIZATION REPORT NUMBER

ARL-TR-833

9. SPONSORING/MONITORING AGENCY NAMES(S) AND ADDRESS(ES)

U.S. Army Research Laboratory
2800 Powder Mill Road
Adelphi, MD 20783-1145

10. SPONSORING/MONITORING AGENCY REPORT NUMBER

11. SUPPLEMENTARY NOTES

12a. DISTRIBUTION/AVAILABILITY STATEMENT

Approved for public release; distribution is unlimited.

12b. DISTRIBUTION CODE

A

13. ABSTRACT (Maximum 200 words)

This is the second of a two part report summarizingthe results of the Combat Induces Atmospheric Obscurants (CIAO) workshops held during 2 through 5 November 1993 and 10 through 24 July 1994, under joint sponsorship by the U.S. Army Research Laboratory and the U.S. Joint Porjects Office for Special Technology Countermeasures. Volume I is a technical summary giving the highlights of the workshops and major conclusions. Volume II gives details of the various reports and investigations from the two worksships (CIAO I and CIAO II). In Apprendix A we summarize results from the first workshop (CIAO I). Appendix B is a bibliography of technical papers on the subject of millimeter wave obscurants, one of the major topics of the workshops. Appendix C give the results of a modeling exercise to determine single particle electromagnetic scattering and absorption properties and Appendix D summarized field measurements capabilities.

14. SUBJECT TERMS

electromagnetics, atmospherics, obscurants, extinction, scattering, absorption, polarizaton, Mueller matrix.

15. NUMBER OF PAGES

115

16. PRICE CODE

17. SECURITY CLASSIFICATION OF REPORT	17. SECURITY CLASSIFICATION OF THIS PAGE	17. SECURITY CLASSIFICATION OF ABSTRACT	20. LIMITATION OF ABSTRACT
UNCLASSIFIED	UNCLASSIFIED	UNCLASSIFIED	UNCLASSIFIED

Preface

This volume contains Appendices A through D that were referenced in Volume I: Technical Summary of the CIAO II workshop results. Appendix A provides overviews of the CIAO I and CIAO II workshops, participants and summaries of papers presented at the CIAO I workshop. Appendix B provides an extensive bibliography of millimeter wave data reports for laboratory, field, and operational measurements. Appendix C compares results from the model comparison exercise conducted for the CIAO II workshop. Appendix D provides a review of existing measurement techniques and facilities where these techniques are employed.

Contents

Contents

Preface 1

Appendix A: CIAO I and CIAO II Overviews 5
1. Purpose and Scope 7
1.1 CIAO I Workshop Participants 8
1.2 CIAO II Workshop Participants 12
1.3 CIAO I Presentation Overviews 14
1.3.1 Model Presentation Overviews 14
1.3.2 Model Application Presentation Overviews 29
1.3.3. Experimental Evaluation and Analyses Overviews 37

Appendix B: Bibliography (Millimeter Wave Database) 43
1. General Millimeter Wave Obscurant Bibliography 45
2. ISST Data Base Summary 55

Appendix C: Results from CIAO II Modeling Exercise 63
1. Purpose and Scope 65
2. Description of the Problem 65
3. Results for Fibers (Cylinders) 66
4. Results for Flakes (Disks) 67

Appendix D: Review of Existing Measurement Techniques 75
1. Purpose and Scope 77
2. Multispectral Extinction Field Measurements 77
3. Multispectral Extinction Data Analyses 79
4. Radar Measurements 85
5. Data Sources 89
5.1 Facilities 91
5.2 Scattering Properties 92
5.3 Particle Orientation Distribution 95
5.4 Particle Number Density Size Distributions after Atmospheric Release 98
5.5 Material Dielectric Constants 98
5.6 Obscurant Characteristic Polarizations 101

Distribution 107

Figures

C-1. Intermediate data for the flake example showing cross-sections and asymmetry parameter as a funciton disk orientation 70
C-2. Plots of the disk ensemble averaged polarimetric phase functions 71
D-1. Typical Tansmissometer system in a ffield test scenario for the measurement of multispectral extinction 78
D-2. Relative error in measured mass extinction coefficient for 05 uncertainty in transmittance and selected relative uncertainties in concentration length 81

D-3. Example regression plot of multispectral optical depths to determine relative mass extinction coefficients 84
D-4. Elevation (side) view sketch of a typical radar field set-up 86
D-5. Typical A-Scope display for cloud attenuation and scattering measurement . . . 87
D-6. Calculated α and α_s (m^2/gm) versus number of fibers in a bundle 88
D-7. ISST microwave scattering facility 93
D-8. HARC bistatic RADAR microwave scattering facility 93
D-9. HARC data comparisons 94
D-10. United Kingdom 94 Ghz polar nephelometer 96
D-11. Example of Chermring polar nephelometer calibration data 97
D-12. Three microphotographs of graphite fibers (materials discussed at the CIAO II workshop) showing end on views of fiber candidates for milimeter wave obscurants 99
D-13. Photomicrographs 100
D-14. Laboratory measured 35 Ghz mass extinction coefficient as a function of aerosol mass concentration for 25-μm diameter, 3.1-mm long aluminized glass fibers 102
D-15. Change in signal return from a calibrated target due to dissemination of 1.5 mm aluminized glass fibers 103
D-16. Change in signal return due to dissemination of 4.0 mm aluminized glass fibers 103
D-17. Change in signal return from a calibrated target due to dissemination of 4.0-mm long nickel coated graphite fibers 104

Tables

B-1. Selected Microwave Scattering Data (Rough Particles & Target Parameters) . . 55
B-2. Selected Microwave Scattering Data (Finite Cylinders & Target Parameters) . . 56
B-3. Selected Microwave Scattering Data (Circular Disks, Square Plate & Target Parameters) 57
C-1. Input data for the modeling exercise 68
C-2. Results of the CIAO II workshop modeling exercise 68
C-3. Intermediate results 69
C-4. Summary of results for the disk modeling exercise 69
D-1. Summary of obscurant data sources for evaluation of electromagnetic wave ropagation odels 90

Appendix A

CIAO I and CIAO II Workshop Overviews

1. Purpose and Scope

Appendix A provides overviews of the CIAO I and CIAO II workshops. A summary abstract of the work discussed and problems posed by the participants is provided.

First, CIAO I and CIAO II participants and their mailing addresses are given. Next, presentation overviews from CIAO I that summarize the thrust of the research discussed during this workshop follow. CIAO II did not use a paper presentation format and results from the discussions held during that workshop are described in Volume 1 of this report. The CIAO I presentation overviews are organized into three areas: 1) model development, 2) model application, and 3) experimental evaluation. Presentations on model development discuss the development of models of scattering and absorption from first principle physical assumptions. Papers on model applications discuss the application of previously developed models to the analyses of experimental data or particular problems. Papers on experimental evaluation discuss experimental methods and analyses.

1.1 CIAO I Workshop Participants

ARTHUR, MICHAEL D., DR.
Naval Surface Warfare Center
Code J41
Dahlgren, VA 22448-5000

ARTHUR, JOY
U.S. Army Research Laboratory
Electronic Warfare Division
ATTN: AMSRL-SL-ES
White Sands Missile Range, NM
88002-5501

AYRES, SCARLETT D.
U.S. Army Research Laboratory
Battlefield Environment Directorate
ATTN: AMSRL-BE-E
White Sands Missile Range, NM
88002-5501

BELL, ROBERT DR.
Earth and Physical Sciences
University of Texas-San Antonio
San Antonio, TX 78249

BLANCHARD, ANDREW J.
Houston Advanced Research Center
4800 Research Forest Drive
The Woodlands, TX 77381

BOHREN, CRAIG DR.
Department of Meteorology
The Pennsylvania State University
508 Walker Building
University Park, PA 16802

BOWERS, JAMES F.
Commander
U.S. Army Dugway Proving Ground
ATTN: STEDP-MT-M
Dugway, UT 84022-5000

BREWER, RALPH J. DR.
OptiMetrics, Inc.
106 E. Idaho, Suite C
Las Cruces, NM 88005

BRUCE, DOROTHY A. DR.
U.S. Army Research Laboratory
Battlefield Environment Directorate
ATTN: AMSRL-BE-A
White Sands Missile Range, NM
88002-5501

BUSIC, JOHN F.
Naval Surface Warfare Center
Code J41
Dahlgren, VA 22448-5000

BULLARD, BRIAN
Science and Technology Corporation
555 Telshor Boulevard, Suite 200
Las Cruces, NM 88001

BUTTERFIELD, JOSEPH E.
U.S. Army Research Laboratory
Battlefield Environment Directorate
ATTN: AMSRL-BE-A
White Sands Missile Range, NM
88002-5501

CAMERON, WILLIAM L. DR.
Boeing Defense & Space Group
P.O. Box 3999
Mail Stop 8H-51
Seattle, WA 98124-2499

CHAPMAN, J. RODRICK
Engineering Technology Inc.
3275 Progress Drive, Suite D
Orlando, FL 32826

COHOON, DAVID K. DR.
Director
U.S. Army Edgewood Research,
Development & Engineering Center
ATTN: SCBRD-RTB, Building E5951
Aberdeen Proving Ground, MD 21010-5423

CRAIN, JOHN N.
Science and Technology Corporation
555 Telshor Boulevard, Suite 200
Las Cruces, NM 88001-0000

DAUM, GAELEN R.
14789 Dash Way
Poway, CA 92064

DAVIS, ROGER E. DR.
Science and Technology Corporation
555 Telshor Boulevard, Suite 200
Las Cruces, NM 88001

DE ANTONIO, MICHAEL D.
Physics Department
New Mexico State University
Box 30001, Department 3D
Las Cruces, NM 88003-001

DUNGEY, CLIFTON E. CPT
Air Force Institute of Technology/ENP
2950 P Street, Building 640
Wright Patterson AFB, OH 45433-7765

EVANS, BLAIR DR.
Defense Research Establishment - Valcartier
2459 Pie XI Boulevard, North
P.O. Box 8800
Courcelette Quebec, GOA 1RO
CANADA

FARMER, W. MICHAEL DR.
The Bionetics Corporation
First National Bank Tower
500 South Main, Suite 900
Las Cruces, NM 88004

FARRELL, RICHARD A. DR.
Applied Physics Laboratory
The Johns Hopkins University
Johns Hopkins Road
Laurel, MD 20723

FLATAU, PIOTR DR.
Scripps Institute of Oceanography
University of California-San Diego
Mail Code 0221
La Jolla, CA 92093

FLORES, BEN
University of Texas at El Paso
500 West University
El Paso, TX 79968

FRATAMICO, JOHN DR.
Science Applications, Inc.
Mail Stop C6
10260 Campus Point Drive
San Diego, CA 92121

FREUND, DAVID E.
Applied Physics Laboratory
The John Hopkins University
John Hopkins Road
Laurel, MD 20723

FULLER, KIRK A.
Department of Atmospheric Science
Colorado State University
Fort Collins, CO 80523

GARVEY, DENNIS
U.S. Army Research Laboratory
Battlefield Environment Directorate
ATTN: AMSRL-BE-E
White Sands Missile Range, NM
88002-5501

GILLESPIE, JAMES B. DR.
U.S. Army Research Laboratory
Battlefield Environment Directorate
ATTN: AMSRL-BE-E
White Sands Missile Range, NM
88002-5501

GILLESPIE, PATTI L. DR.
U.S. Army Research Laboratory
Battlefield Environment Directorate
ATTN: AMSRL-BE-S
White Sands Missile Range, NM
88002-5501

GOEDECKE, GEORGE DR.
Physics Department
New Mexico State University
Box 30001, Department 3D
Las Cruces, NM 88003-0001

GOLDBERG, IRA B. DR.
Rockwell Science Center
1049 Camino dos Rios
Thousand Oaks, CA 91360

GOMEZ, RICHARD B. DR.
Topographic Engineering Center
ATTN: CETEC-ZC
Fort Belvoir, VA 22060-5546

GREENLEAF, WILLIAM
Commander
U.S. Army Missile Command
ATTN: AMSMI-RD-GC-T
Redstone Arsenal, AL 35898

HALE, JEFF
Director
U.S. Army Edgewood Research,
Development & Engineering Center
ATTN: SCBRD-RTB
Building 3331, Room 209
Aberdeen Proving Ground, MD 21010-5423

HANZO, ARTHUR E.
Engineering Technology Inc.
3275 Progress Drive, Suite D
Orlando, FL 32826

HORST, MARGRET M.
Georgia Tech Research Institute
Georgia Institute of Technology
Signatures Technology Laboratory
Atlanta, GA 30332-0800

KENNEDY, BRUCE W.
Physical Sciences Laboratory
New Mexico State University
P.O. Box 30002
Las Cruces, NM 88003-0002

KENNEDY, JOHN DR.
Naval Surface Warfare Center
Code J41
Dahlgren, VA 22448-5000

KLETT, JAMES D.
PAR Associates
4507 Mockingbird Street
Las Cruces, NM 88001

LAMB, LOWELL D. DR.
Department of Physics
University of Arizona
1118 E. 4th Street
Tucson, AZ 85721

LAX, MELVIN
Physics Department
City College of New York
New York, NY 10031

LINES, RAYMOND T.
U.S. Army Research Laboratory
Battlefield Environment Directorate
ATTN: AMSRL-BE-E
White Sands Missile Range, NM
88002-5501

MACKOWSKI, DANIEL
Department of Mechanical Engineering
Auburn University
Auburn, AL 36849

MILLARD, BRADLEY
U.S. Army Research Laboratory
Battlefield Environment Directorate
ATTN: AMSRL-BE-E
White Sands Missile Range, NM
88002-5501

MORGAN, PAUL
Engineering Technology Inc.
3275 Progress Drive, Suite D
Orlando, FL 32826

MULHOLLAND, GEORGE W.
National Institute of Standards & Technology
Building 224, Room B356
Gaithersburg, MD 20899

NASH, PAT DR.
Earth and Physical Sciences
University of Texas-San Antonio
San Antonio, TX 78249

NEWMAN, EDWARD H. DR.
Department of Electrical Engineering
ElectroScience Laboratory
Ohio State University
Columbus, OH 43212

NILES, FRANKLIN E. DR.
U.S. Army Research Laboratory
Battlefield Environment Directorate
ATTN: AMSRL-BE-S
White Sands Missile Range, NM
88002-5501

OTA, CLEM
Science and Technology Corporation
555 Telshor Boulevard, Suite 200
Las Cruces, NM 88001-0000

PEDERSEN, JEANNE C. DR.
Pedersen Research Inc.
212 High Street
Newburyport, MA 01950

PELLEGRINO, PAUL
Physics Department
New Mexico State University
Box 30001, Department 3D
Las Cruces, NM 88003-0001

PENDLETON, DAVID DR.
U.S. Army Research Laboratory
Battlefield Environment Directorate
ATTN: AMSRL-BE-E
White Sands Missile Range, NM
88002-5501

PERRY, BEN
Georgia Tech Research Institute
Georgia Institute of Technology
SEAL/RSD/5-108
7220 Richardson Road
Smyrna, GA 30332-0800

SERNA, JOSE M.
Physical Science Laboratory
New Mexico State University
Box 30002
Las Cruces, NM 88003-0002

SMITH, FREDERICK G.
OptiMetrics, Inc.
3115 Professional Drive
Ann Arbor, MI 48104-5131

SMITH, JACK
Department of Electrical Engineering
University of Texas at El Paso
500 West University
El Paso, TX 79968

SOTO, SYLVIA
U.S. Army Research Laboratory
Battlefield Environment Directorate
ATTN: AMSRL-BE-S
White Sands Missile Range, NM
88002-5501

SUTHERLAND, ROBERT A. DR.
U.S. Army Research Laboratory
Battlefield Environment Directorate
ATTN: AMSRL-BE-S
White Sands Missile Range, NM
88002-5501

THURSTON, MICHAEL J.
U.S. Army Research Laboratory
Battlefield Environment Directorate
ATTN: AMSRL-BE-E
White Sands Missile Range, NM
88002-5501

WATERMAN, PETER C. DR.
Pedersen Research Inc.
8 Baron Park Lane, Suite 26
Burlington, MA 01803

YEE, YOUNG P.
U.S. Army Research Laboratory
Battlefield Environment Directorate
ATTN: AMSRL-BE-M
White Sands Missile Range, NM
88002-5501

1.2 CIAO II Workshop Participants

ARTHUR, MICHAEL D., DR.
Naval Surface Warfare Center
Code J41
Dahlgren, VA 22448-5000

BLANCHARD, ANDREW J.
Houston Advanced Research Center
4800 Research Forest Drive
The Woodlands, TX 77381

BUSHONG, PHIL DR.
Naval Surface Warfare Center
Code J41
Dahlgren, VA 22448-5000

BUTTERS, BRIAN
Chemring, Ltd.
Alchen Works
Fratton Trading Estate
Portsmouth P0485X
UNITED KINDGOM

CAMERON, WILLIAM L. DR.
Boeing Defense & Space Group
P.O. Box 3999, Mail Stop 8H-51
Seattle, WA 98124-2499

EVANS, BLAIR DR.
Defense Research Establishment - Valcartier
2459 Pie XI Boulevard, North
P.O. Box 8800
Courcelette Quebec, GOA 1RO
CANADA

FARMER, W. MICHAEL DR.
The Bionetics Corporation
First National Bank Tower
500 South Main, Suite 900
Las Cruces, NM 88004

FARRELL, RICHARD A., DR.
Applied Physics Laboratory
The Johns Hopkins University
Johns Hopkins Road
Laurel, MD 20723

FLATAU, PIOTR DR.
Scripps Institute of Oceanography
University of California-San Diego
Mail Code 0221
La Jolla, CA 92093

FULLER, KIRK A.
Department of Atmospheric Science
Colorado State University
Fort Collins, CO 80523

GOLDBERG, IRA B. DR.
Rockwell Science Center
1049 Camino dos Rios
Thousand Oaks, CA 91360

HOOCK, DON DR.
U.S. Army Research Laboratory
ATTN: AMSRL-BE-S
Battlefield Environment Directorate
White Sands Missile Range, NM
88002-5501

KENNEDY, BRUCE
New Mexico State University
Physical Science Laboratory
Box 30002
Las Cruces, NM 88003-0002

KLETT, JAMES D.
PAR Associates
4507 Mockingbird Street
Las Cruces, NM 88001

MILLARD, BRAD
U.S. Army Research Laboratory
ATTN: AMSRL-BE-E
Battlefield Environment Directorate
White Sands Missile Range, NM
88002-5501

PERRY, BEN
Georgia Tech Research Institute
Georgia Institute of Technology
SEAL/RSD/5-108
7220 Richardson Road
Smyrna, GA 30332-0800

RICHARDSON, ROBERT E., JR DR.
Naval Surface Warfare Center
Code J41
Dahlgren, VA 22448-5000

RUSSELL, LISLE H., DR.
Naval Surface Warfare Center
Code J407
Dahlgren, VA 22448-5000

SMALLEY, HOWARD
Commander
U.S. Army Edgewood Research
Development and
Engineering Center
ATTN: SCBRD-ENB
Edgewood, MD 21010-5346

SUTHERLAND, ROBERT A., DR.
U.S. Army Research Laboratory
Battlefield Environment Directorate
ATTN: AMSRL-BE-E
White Sands Missile Range, NM
88002-5501

WATERMAN, PETER C. DR.
Pedersen Research Inc.
8 Baron Park Lane, Suite 26
Burlington, MA 01803

WHITE, JOHN
Commander
U.S. Army Edgewood Research
Development and
Engineering Center
Attn:SCBRD-ENB
Edgewood, MD 21010-5346

1.3 CIAO I Presentation Overviews

The CIAO I presentation overviews are organized into three areas: 1) model development, 2) model application, and 3) experimental evaluation. Papers on model development discuss the development of models for scattering and absorption from first principle physical assumptions. Papers on model applications discuss the application of previously developed models to the analyses of experimental data or particular problems. Papers on experimental evaluation discuss experimental methods and analyses.

1.3.1 Model Presentation Overviews

Overviews presented in this section represent those describing model development. In overviews representing the work of more than one author, the workshop presenter is underlined.

ADVANCED COMPUTATIONAL TECHNIQUES

by

Dr. John Fratamico
Science Applications International Corporation
San Diego, CA

Dr. Fratamico's experience is in the design and development of Stealth weapons platforms. His talk was focused on software and hardware optimization techniques developed in stealth technology that may have application to atmospheric physics problems. The specific scattering technique referenced is the three dimensional method of moments (3D-MoM). This is a technique that spans the full gamut of material properties, material complexities and shapes. Advanced computational techniques addressed effects that can broaden the particle size and range to encompass as broad a range of material parameters as possible.

The first topic considered was the antenna type problem where the wavelength is large compared to the particle size. For this case, the impedance boundary condition formulation is appropriate as one may vary not only material properties but also the impedance loading. Computationally, the formulation should avoid _·n'B terms when the particle size is much smaller that a wavelength; avoid B·n'B terms; and force the impedance terms near the diagonal of the matrix.

A typical out-of-core impedance matrix might consist of 100,000 x 100,000 fully complex elements. This requires approximately 100 gigabytes of storage. The MoM solution requires on the order of N^3 floating point operations and N^2 I/O operations. Efficient algorithms for interleaving these operations on both parallel and vector architecture's were discussed.

Another important point addressed was the limits of excursion from an exactly solved problem that may be pursued via perturbation techniques. If the problem can be reconfigured such that the known problem is pushed into the lower right corner of the MoM matrix, then one can obtain the scattered fields for the perturbed problem without solving the intermediate step for the surface currents. This reduces computer run time by a factor of approximately 1/1,000.

THE DISCRETE DIPOLE APPROXIMATION FOR SCATTERING CALCULATIONS

by

Bruce T. Draine
Princeton University Observatory

and

Piotr J. Flatau
Scripps Institution of Oceanography

March 1994

The discrete dipole approximation (DDA) is an approximation of a continuum target by a finite array of polarizable points. The points acquire dipole moments in response to the local electric field. An array of polarizable points can accurately approximate the response of a continuum target on length scales large compared to the dipole separation. For a finite array of point dipoles, the scattering problem can be solved essentially exactly. The only "approximation" in the DDA is the replacement of the continuum target by an array of N point dipoles. The replacement requires specification of both the vector locations of the dipoles and the dipole polarizabilities. There is a close correspondence between the DDA and discretizations based on the "digitized Green's function" method or the "volume integral equation" formulation. In the low frequency limit where the interdipole spacing or side of a cubical subvolume is much less than an incident wavelength the DDA has been shown to be formally equivalent to digitized Green's function and volume integral formulations. However, workers developing these formulations encountered difficulties in attempting to compute second order corrections whereas DDA permits rigorous derivation of second order corrections. The principle limitation of the DDA is in handling the target boundaries since the DDA array has a minimum length scale equal to the interdipole spacing. For targets with large values of the refractive index, the accuracy of the DDA suffers. In this case the DDA can seriously overestimate the absorption cross-section, even in the dc. limit. When the absolute value of the refractive index is much greater than one other techniques may be superior to the DDA.

Fast Fourier transform (FFT) methods can greatly accelerate the computations required to solve the scattering problem, but only if the dipoles are located on a periodic lattice. With FFT methods calculations can be performed on a workstation for numbers of dipoles (e.g. ~ 10^5) much greater than the largest values (~ 10^4) which could be handled without FFT methods. We have used FFT methods accepting the requirement of a periodic lattice and further assumed cubic lattices.

There have been questions of the best method for assigning dipole polarizabilities. One approach is to use the "Claussius-Mossotti" polarizabilities which is exact for an infinite cubic lattice in the limit that the interdipole spacing is much less than a wavelength.

Extensive DDA calculations for spheres comparing different prescriptions for the dipole polarizability confirms that the lattice dispersion relation developed analytically by Draine and Goodman for an infinite lattice of polarizable points appears to be the best when the product of the absolute value of the index of refraction, wave vector, and interdipole spacing is less than 1.

By locating dipoles on a lattice, computational memory requirements are approximately linearly dependent on N, the number of dipoles. For example, the program DDSCAT has a total memory requirement of approximately $0.58(N_xN_yN_z/1000)$ Mbytes, where N_x x N_y x N_z is the rectangular volume containing all the N dipoles. CPU requirements are also significant for large targets. For example, on a Sun 4/50 (Sparcstation IPX), a single CCG iteration requires approximately $3.0(N_xN_yN_z/1000)$ cpu seconds. Between 10 and 100 iterations are typically required to solve for a single incident direction and polarization. It is for this reason that T-matrix methods which exploit efficient procedures for orientational averaging are competitive for some target geometries as well as recursive T-matrix algorithms currently developed by Chew.

At this time there is no known way to predict precisely the accuracy of DDA calculations. Computations for the extinction efficiency with moderately refracting spheres performed using DDA and compared with exact Mie theory calculations show errors are less than 3% for size parameters less than 12 and an index of refraction of 1.33 +0.01i. For an index of refraction of 2+i, the error in the absorption efficiency is about 4% when dipole numbers are greater than 10^4. Computations for the error in the differential scattering cross-sections are within 20% for all scattering directions for an index of refraction of 1.33+0.01i and within 30% for 2+i.

The DDA has been applied to calculations of scattering and absorption by rough and porous particles, interstellar graphite particles, aggregate particles, inhomogeneous particles, structures on surfaces, microwave scattering by ice crystals, single scattering properties of ice crystals, and scattering at plane boundaries perturbed by roughness.

DIGITIZED GREEN'S FUNCTION APPROACH TO SCATTERING FROM ARBITRARY STRUCTURES

by

Dr. George Geodecke
New Mexico State University
Las Cruces, NM

The digitized Green's function approach to scattering from complex objects was discussed. The method is completely general and, in principle, is capable of calculating absorption and scattering by waves of all kinds from localized scatterers of arbitrary shape, size and morphology. Mathematically, the digitized Green's function approach is closely related to the coupled dipole method (Purcell and Pennypacker, AP J 186, 705-714 1973).

The development discussed at this conference included the proper way to include self-terms and depolarization dyadics into the formalism. It was shown that the solutions automatically obey the Optical Theorem. Two specific applications were discussed: 1) structures with smoothly varying constants; and 2) structures with a few sharp, cutoff surfaces such as soot or snowflakes.

Areas identified as needing further research included incorporating a Born series approximation, better accounting for near neighbor interactions, and using a variable cell size over the parameter space. Limitations of the technique were also discussed. These are basically related to computation time and storage limitations. These issues were also addressed by Dr. John Fratamico.

SIMPLIFIED TREATMENT OF THE EXTENDED QUASISTATIC THEORY FOR ABSORPTION BY CONDUCTING FIBERS

by

Norman Pedersen, Jeanne Pedersen,
and Peter Waterman
Panametrics, Inc.

26 June 1989

An elementary treatment of electromagnetic wave absorption by conducting fibers is developed assuming the fibers are prolate spheroids, the quasistatic approximation, that wavelengths are greater than 20μm. We note that even in the low frequency limit, the problem of analytically calculating the electric field distribution within a right circular cylinder has not been solved in closed form. The quasistatic approximation requires the cylinder length to be much less than an incident wavelength. However, in spite of the assumptions made in the analysis, accurate results for absorption by very thin fibers are obtained over very wide ranges of meaningful wavelengths and easily obtained particle dimensions. In many cases, one or more of the limiting assumptions can be relaxed without adverse results.

For randomly oriented fibers of high aspect ratio, the absorption cross-section has the following features:

1. When the product of the depolarization factor and imaginary component of the dielectric constant squared is much less than 1, large values of particle material electrical conductivity produce large values of the absorption cross-section per unit volume.

2. Conditions for feature 1, can be achieved by making particle aspect ratio large.

3. High values of absorption cross-section per unit volume obtained using features 1 and 2 are the result of a non-resonant condition that can be met over a wide range of frequencies.

The quasistatic approximation has been extended to provide an analysis of the absorption cross-section when the particle length approaches or exceeds the free space wavelength of the incident radiation. The extended quasistatic approximation assumes the effective cylinder half-length is half a wavelength. This assumption cannot be supported on strict theoretical grounds but has been found to provide accurate and useful results in many cases. The result of our analysis with this approximation is to slightly modify the depolarization factor used in quasistatic approximation computations. The advantage of the Extended Quasistatic result is that it allows one to use analytic methods in obtaining closed form approximate solutions to practical problems.

INTEGRAL EQUATION ANALYSES OF ARTIFICIAL DIELECTRICS

by

Dr. Edward Newman
Ohio State University
Columbus, OH

The electromagnetic analysis of artificial dielectrics is one of the fundamental building blocks of Low Observable (Stealth) Technology. Dr. Newman and his group at Ohio State University are the premier leaders in the unclassified research into this area. The techniques discussed are important and directly applicable to problems in atmospheric physics. The electromagnetic analysis of an artificial dielectric and the electromagnetic analysis of a heterogeneous smoke/obscurant cloud are intimately intertwined.

This paper focuses on two mathematical techniques: 1) the formulation of the relevant integral equations, and 2) their solution by Method of Moments (MoM) techniques. Calculated results are shown to compare favorably with measurements for three cases: 1) a fixed array of dipoles, 2) a fixed array of crosses, and a 3) composite weave. These are directly applicable to the Low Observables problems of conformal antennas, band-pass radomes, and wing leading edge treatments, respectively. The extension to the complex artificial dielectric properties of a heterogeneous aerosol/particulate cloud is apparent.

The examples discussed in this paper address the effects on the effective permittivity due to the host medium, the scattering medium, the frequency, the effective lattice spacing of the artificial dielectric, the scatterer shape and the polarization and angle of the incident wave. For the undriven case, it is shown that the resulting integral equations are homogeneous and the root corresponds to a different polarization of the incident wave.

It is demonstrated by comparison with experimental results that the techniques described accurately account for complex shapes of the individual scatterers and the mutual coupling between them. It is explicitly shown that the mutual coupling between individual particles is adequately accounted for by increasing the number of expansion functions used on the MoM solution to the integral equations.

WAVELET TRANSFORMS IN THE T-MATRIX THEORY OF ELECTROMAGNETIC SCATTERING

by

Dr. Patrick L. Nash
University of Texas at San Antonio
San Antonio, TX

The construction of the T-matrix requires the numerical evaluation of many surface integrals involving the tensor products of the vector spherical harmonics and the angular dependent factors describing the boundaries of the scattering particles. The wavelet transform approximates these square integrable functions with smoothed versions of these functions. This results in a matrix formulation that lends itself to a multi-wavelength resolution analysis of the scattering problem under consideration.

This paper presents results obtained from using a generalized two-dimensional wavelet transform and an approximate matrix inversion technique. Iterations of the wavelet transform on an n x n matrix are shown to yield a sparse and easily solvable problem even in the case where the initial diagonal elements are arbitrary (and even singular).

LIGHT SCATTERING FROM AGGLOMERATES: COUPLED ELECTRIC AND MAGNETIC DIPOLE METHOD

by

George W. Mulholland
National Institute of Standards and Technology (NIST)
Gaithersburg, MD

This is an outgrowth of a fire research program at NIST. Of particular interest is the growth of soot and smoke particulate. It is shown that the absorption cross section of a complex, fractal soot particulate is approximately given by the absorption cross section of the basic building-block structure times the number of these building blocks in the agglomerate. It is usually sufficient to use a sphere as the basic building block and to model the agglomerate as a collection of touching spheres. No multiple scattering within the agglomerate is considered.

Inclusion of a magnetic dipole term in the solution is shown to essentially double the range of size parameter for which the technique yields sufficiently accurate results. The solution of the coupled equations is achieved by iteration of approximate solutions to self-consistency. The results obtained compare favorably to the exact solution obtained by Fuller (within 5% for size parameters less that unity).

The scattering and extinction cross sections, the differential scattering cross section and the polarization ratio are calculated for agglomerates consisting of 17, 52, and 165 primary spheres for soot-like and silica-like agglomerates are generated by a computer simulation of Brownian dynamics in flame growth. A comparison was made among the Rayleigh-Debye, Coupled Electric Dipole, and Coupled Electric and Magnetic Dipole techniques. It is further shown that the polarization ratio computed by the Coupled Electric and Magnetic Dipole technique is sensitive to the primary sphere size independent of the size of the agglomerate particle.

VARIATIONAL SCATTERING TECHNIQUES

by

Dr. Richard A. Farrell
John Hopkins Applied Physics Laboratory
Johns Hopkins University, MD

Variational techniques are a class of solutions to electromagnetic scattering problems which have the advantage of quadratic convergence to the exact solution. On the other hand, the technique is limited by the accuracy of the initial guess of the form of the solution. As such, though in principle the variational technique is completely general, in practice it is most useful when the problem at hand is an extrapolation of a problem whose solution is known from other techniques. An advantage of this approach is that the variational technique can supply accurate results at all wavelengths. Of particular interest to atmospheric physics is the fact that the Schwinger variational principle yields a formalism that is directly applicable to a stochastic ensemble of simple scatterers such as often occurs in CIAO.

The work discussed here extends the range of validity of the variational technique to long wavelengths via the incident field approximation and to short wavelengths via the Kirchoff approximation. It is shown by comparison with measurement that this approach yields accurate results for both random and fixed agglomerations of simple scatterers, provided that the trial function takes proper account of the refractive effects of dielectrics, the boundary conditions and shadowing effects and the existence of creeping waves.

The paper shows conclusively that the variational technique can be reliably extended to stochastic distributions of simple scatterers and to near-field scattering problems, and that these solutions are valid at all wavelength/particle ratios.

COMPOSITE LIMIT ANALYSIS OF ELECTROMAGNETIC CROSS SECTIONS OF ISOMETRIC, PLANAR AND CYLINDRICAL PARTICLES

by

Janon Embury
(Presented by David Cohoon)
U.S. Army Edgewood Reseach

The purpose of this research is to study the effects of particle size distributions and particle shape distributions on extinction. The model developed is completely general, however it assumes that the concentration of the particulate is small enough that multiple scattering effects within the cloud may be ignored.

Fibers and hollow spherical shells are discussed in detail, as well as a variety of distribution functions. The model developed leads to an understanding of the levels of extinction that may be expected for clouds of artificial aerosols of varying shape, size, conductivity and orientation.

THE SCATTERING OF ELECTROMAGNETIC RADIATION BY NONCONNECTED, HETEROGENEOUS, BIANISOTROPIC STRUCTURES

by

David Cohoon
U.S. Army Edgewood Research
Development and Engineering Center
Edgewood, MD

Computation times and storage requirements limit the size and complexity of problems that can practically be considered. Volume integral equation techniques alleviate this difficulty somewhat. This work describes a technique developed for solving electromagnetic interaction problems that can give answers to machine precision by using the concept of an exact finite rank integral equation whose solution is exactly the projection of the integral operator onto a space of approximate solutions of the original, infinite rank, integral equations.

The integral equations discussed are valid for heterogeneous, bianisotropic structures which are not necessarily connected. It is proven that this technique will always converge to the solution, but the issue of how quickly it converges is not settled. The technique is completely general but still new enough to be untried on problems of practical interest. While the method is very intriguing, there is much development work yet to be done.

LIGHT SCATTERING BY INHOMOGENEOUS SPHERES: APPROXIMATE SOLUTIONS USING A VOLUME CURRENT METHOD

by

Steven Hill
and Hasan Saleheen
New Mexico State University

It is of interest to compute the scatter from spheres containing small foreign inclusions (See for example the summary of work presented by Ron Pinnick). A technique called the "volume current method" (VCM) has been developed to perform the computations. The VCM assumes approximate solutions for the polarization currents of small inclusions found within the primary sphere, then computes the resulting electromagnetic fields and ultimately the scattering magnitudes by integrals over the induced currents for each inclusion. The results have been compared with the separation of variables code developed by Kirk Fuller (see the summary for Kirk Fuller's work) to establish a measure of result reasonableness and the two methods are shown to be reasonably consistent. However, it should be pointed out that neither method has been experimentally verified.

Two comparison cases are considered between the VCM method and the separation of variables: nonresonant spheres, and near resonance spheres. For the nonresonant sphere case, an inclusion comparable in size to the host is assumed. In this case the VCM prediction agrees within 5 percent of that predicted by the separation of variables method. For the case where the inclusion is much less than the host diameter and oriented within the host for maximum scatter there is almost perfect agreement between the two models.

When the host sphere is near resonance in size, it is important that an effective average refractive index be used that accounts for both host and inclusions. The VCM and separation of variables method agree well in predicting the resonant peak. The scatter magnitudes agree well.

It is found that at large scatter angles the differences between scatter from a host without inclusions and host with inclusions are large. This suggests that observations of scatter magnitude can be used to detect biological aerosols.

The VCM analysis conducted thus far assumes scatter observed at 90° relative to the incident beam. Future work should consider additional scatter angles and system sensitivities.

ALGEBRAIC APPROXIMATIONS OF EXTINCTION EFFICIENCY FOR NON-SPHERICAL PARTICLES

by

Blair Evans
Defense Research Establishment
Val Cartier, Canada

The immediate objective of this work is to significantly reduce the computational burden in calculating the extinction from non-spherical particles. The longer term objective is to alleviate the remaining constraints in the theoretical consideration of non-spherical aerosols and obscurants of either natural or artificial origin.

An analytic semi-empirical approximation for the extinction efficiency for randomly oriented spheroids has been developed and compared with the extended boundary condition or T-matrix method. The basic approach is to orthogonalize as much as possible the scattering physics into well-defined regimes. For small physical and optical sizes, the electrostatics (Rayleigh) approximation is used. For larger and very large optical sizes we still use the electrostatics approximation but with the optical constants transformed to include the effects of the magnetic dipole. In the large physical size regime, the analysis uses a diffraction (anomalous diffraction) component and what can loosely be described as edge effects. The diffraction component is modeled by the anomalous diffraction approximation developed by Van de Hulst. The edge effect (Fock theory) component is modeled by extending a technique introduced by Jones. This component is further generalized to have proper behavior at small optical sizes and large indices. The gap between the large and small particle regimes is bridged by a binomial form similar to the "generalized mean."

The approximation has been verified for complex refractive indices, $m = n - ik$, where $1 \leq n \leq \infty$ and $0 \leq k \leq \infty$ and aspect ratios from 0.2 to 5. After extensive error analysis and comparisons with other verified models such as the T-matrix and the Mie theory, it is concluded that the approximation is uniformly valid over all size parameters and aspect ratios. Errors relative to the T-matrix range between 1 and 35 percent. The largest errors occur for k values greater than 1, and for real refractive indices near 1. Least errors, 1 percent or less are found in comparisons with the Mie theory.

All approximate computations for the extinction efficiency in this study were produced at a rate greater than 10^4 times faster than the T-matrix code. Since the T-matrix computation times scale at least as the cube of the optical size and the analytic approximation is optical size dependent, larger size parameters or larger refractive indices lead to larger speed-up factors.

Approximation limitations for $n<1$ and/or $k<0$ have not been modeled since new and significant physical phenomena arise (e.g. total internal reflections and optical gain). Even n modestly less than one can cause problems. Another limitation occurs for $2 \leq k \leq 10$ and large particles. In this region, the absorption is not well modeled. If this effect was properly accounted for, absorption and scattering efficiencies could be globally and readily obtained by using the same approach.

THE CORPUSCULAR VIEW OF LIGHT

by

Mel Lax
City College of New York

The corpuscular view of light promoted by Newton was discredited by Descartes because it appeared to require an increase in the velocity of light in a dielectric medium (using qualitative arguments based on the direction of bending). The quantitative arguments, as summarized by **Kline and Kay (1965)** and by **Luneburg (1966)** seem to yield the same conclusion but they are based on interpreting an artificial parameter τ as the time. To reinstate the corpuscular view of light we must find the correct parallelism between mechanics and light, not the usual one chosen by Hamilton.

Kline, M. and Kay, I.W. (1965), *Electromagnetic Theory and Geometrical Optics*, Wiley-Interscience, Sec. 2.6

Luneburg, R. K., (1966) *Mathematical Theory of Optics*, University of California Press.

1.3.2 Model Application Presentation Overviews

Overviews presented in this section represent those papers describing model applications.

CHAFF MODELING AND SIMULATION

by

Robert J. Puskar, Ph.D.
Mission Research Corporation

Electromagnetic scattering by chaff dipoles has been under investigation for almost 40 years. Individual dipole scattering is well understood, scattering from clouds of dipoles is not. All the dipoles do not scatter independently except for very long times after release. This means linear addition of scatter from single dipoles is inappropriate. Furthermore, aerodynamic studies show dipoles have preferred orientations after release into the atmosphere. Thus, estimating scatter from randomly oriented particles is inappropriate. The most accurate way to predict chaff cloud radar cross-section (RCS) is to numerically solve the integral equation governing scattering. This works for very small chaff clouds. Only small numbers of dipoles can be handled in this way because of computational requirements. However, the statistical properties derived from this type of analysis are valid for large clouds. Other scattering parameters that can be modeled in this way include frequency bandwidth, bistatic scattering, and polarization response.

In any chaff cloud model, the effects of dispensing, dispersal, blooming, diffusion, and agglomeration should be included. No such model exists. One of the most detailed chaff aerodynamic models, a 6 degree-of-freedom dipole trajectory program that predicts individual dipole trajectories based on particle aerodynamic coefficients. It does not handle clouds of dipoles. To a large extent, this aspect of chaff cloud modeling relies on empirically derived data.

There are four basic types of chaff models in use in the electronic warfare community. The first type is a chaff signature simulation and is used to analyze and study chaff radar signatures in fine detail. The second is a chaff/radar effectiveness model and is used primarily to evaluate the effects of chaff on radar system performance. The third and fourth types are used to study the aerodynamic and electromagnetic scattering characteristics of chaff respectively. Nine different models used in these categories are described in this work.

There are three primary modes in which chaff is now used: saturation, self-protection, and confusion/deception. The way chaff is used can be extremely important in determining effectiveness, especially in the self-protection mode which is now the most common use for chaff. Saturation chaff refers to the practice of producing a huge corridor of chaff to mask the penetration of other aircraft. This practice is not likely to be used in the future because of tactics now used for penetration by the USAF. Confusion/deception refers to the generation of false radar targets. The effectiveness of this mode is very difficult to evaluate. There no longer seems to be significant effort by the USAF to use chaff in a confusion/deception mode. In an Army battlefield situation it could have major effects.

BACKSCATTERING BY NONSPHERICAL HYDROMETERS AS CALCULATED BY THE COUPLED DIPOLE METHOD: AN APPLICATION IN RADAR METEOROLOGY

by

Clifton E. Dungey
Department of Engineering Physics
Air Force Institute of Technology
Wright-Patterson AFB OH 45433-7765

and

Craig F. Bohren
Department of Meteorology
The Pennsylvania State University
University Park, Pennsylvania 16802

The ability of the coupled dipole method (also called the "Discrete Dipole Approximation" by Flatau) to calculate backscattering by nonspherical particles is demonstrated. For spheres smaller than the size which produces the first backscattering minimum as a function of size parameter, small shape variations in the dipole array do not affect the accuracy of the calculation. Conversely, when spheres are larger than the size which produces the first minimum, backscattering calculations lose accuracy. For particles with an aspect ratio of at least 5:1 and small size parameter, the backscattering calculation is relatively insensitive to the exact cross-sectional shape of the particle, i.e. hexagonal column, cylinder, etc. Backscattering calculations for ice spheres, hexagonal columns, and plates are presented. Polarization effects are analyzed using principles associated with the Mueller matrix.

We find identification of ice crystal size distribution depends on several factors. First, the size distribution is assumed continuous. A discontinuous size distribution produces gaps in the Doppler shift spectrum used for backscatter analysis that could be mistaken for a backscattering minimum. Second, for our theory to be applicable, ice crystals must not be aggregated. Backscatter computations have only been made for plates and columns; scattering by aggregates may obscure the desired backscattering minima. Third, the optical depth of the ice cloud must not be too large. Otherwise, the back scattered signal will be a result of multiple scattering events. Our procedure for identifying ice crystals is based on single scattering.

Our results show it is feasible to estimate size distribution for hexagonal columns and plates using millimeter wave radar. In general, the size of the ice crystals dictates the wavelength best suited for obtaining the first backscattering minimum. However, at shorter wavelengths attenuation by atmospheric water vapor may limit system performance.

LIGHT SCATTERING BY AGGREGATES AND INHOMOGENEOUS SPHERES

by

Kirk A. Fuller
Department of Atmospheric Science
Colorado State University

Electromagnetic scattering by agglomerations of spheres or by spherical hosts possessing such agglomerates or eccentrically located spheres can be solved within a single theoretical framework. The theory uses a repeated application of the same principles employed in the Lorenz-Mie treatment of light scattering by single homogeneous spheres. The approach is to first transform a plane wave incident on a spherical particle into vector spherical harmonic waves that can be matched directly to the spherical geometry. The Mie coefficients for the expansion can then be interpreted as being analogous to Fresnel reflection and transmission coefficients for a plane wave incident on a planar slab of material. To extend the theory to an ensemble of spheres of arbitrary number and size, the scattered fields from each sphere are added coherently by using the addition theorem for vector spherical harmonics and applying the proper boundary conditions for each particle. This approach requires the solution of a set of coupled equations and represents the practical computational limit on the number of particles in an aggregate which can be evaluated.

The procedure has been applied to the computation of the extinction cross-section of small carbon particles on the surface of sulfate droplets. The extinction cross-section varies with the carbon particle position on the droplet surface relative to the plane of incidence and the incident polarization. When the particle in or near the focal volume of the drop scattering is enhanced, when the particle is removed from the focal volume area scatter is reduced. For an average over all orientations and polarizations, the absorption characteristics of the carbon particles do not change much relative to the free particles. Placing the carbon grain inside a droplet shows that the absorption cross-section decreases as the particle moves from the center of the drop to the surface when averaged over all polarizations and orientations.

When the procedure is applied to a linear chain of spheres and an average is performed over all orientations and incident polarizations, the ratio of aggregate to single equivalent sphere cross-sections increases by about 50% for carbon particles and about 300% if the material is aluminum.

The solution procedure developed for computing cross-sections for aggregates of spheres is very powerful and accurate. For example, it yields a solution that is much simpler than previously computed when applied to the coated sphere problem. The analysis yields expressions in terms of the Mie coefficients solution for a single sphere that are analogous to the reflection and transmission coefficients for a thin film. The procedure for solving the extinction from aggregates provides a method for testing the accuracy of approximations used for solving the scatter from irregularly shaped particles.

COMPUTATION OF RADIATIVE CROSS SECTIONS OF SPHERE CLUSTERS

by

Daniel MacKowski
Auburn University

The motivation for this work is the modeling of absorption, scattering, and extinction of super spherical agglomerates such as carbonaceous soot arising during combustion processes. The analytical formulation of the solution to Maxwell's equations for this problem is similar to that of Kirk Fuller where a superposition of vector spherical harmonic expansions about each of the spheres is used. The analysis shows that simple recurrence relationships can be used to obtain the vector spherical harmonic addition coefficients. It is found for this problem that it is simpler to compute the scattering cross-section from the difference of the extinction and absorption cross-sections, than is normally done by computing the scattering and extinction cross-sections first. Random particle orientations can be addressed simply by using a T matrix (not the T-matrix for extinction computations) that is developed in the problem formulation. Comparisons of analytical predictions with previously acquired data show agreement within about 30 percent for the extinction efficiency.

For visible and infrared wavelengths, and size parameters much less than 1, computational results show that more than just the dipole terms are needed for the computation. For example, computations for a binary cluster with size parameter of 0.01, shows that as the complex index of refraction increases so does the number of terms required to specify the absorption efficiency. However, using the electrostatic approximation (Rayleigh approximation) for the same case shows that the absorption efficiency is constant for complex index of refraction when the size parameter is less than about 0.1, which is as expected. A similar problem is found for particles consisting of large numbers of small size parameter spheres in an aggregate. It is believed that the differences in the analytical results arise because a pair of dipoles act together more like a spheroid, than a simple dipole pair.

An approximation for the extinction by spherical aggregates has been developed by considering interactions only between pairs of dipoles. The approximation gives a closed form solution that is a slight under prediction of the absorption cross-section computed for multiple particle interactions beyond pairs only. An appropriate characteristic size of the aggregate is found to be the radius of gyration divided by the number of fundamental particles in the aggregate raised to the 1/3 power.

ORIENTATION EFFECTS OF FALLING NON-SPHERICAL PARTICLES

by

James Klett
PAR Associates

Prediction of falling non-spherical particle orientation is addressed by a heuristic model that assumes the particles are subject to isotropic turbulence within or below the inertial subrange, i.e. the Kolmogorov spectrum of eddies, depending on particle size. The RMS tilt angle of a small eccentricity spheroidal particle is determined by Langevin-type averaging over its equation of motion. The calculation takes into account the first order restoring torque arising when the stable fall mode is perturbed by either thermal or turbulent fluctuations. An approximate expression for the variance of an assumed Gaussian orientation distribution for small tilt angles and small Reynolds numbers is obtained by invoking dimensional constraints concerning the nature of the main flow and turbulent stresses, and by assuming turbulent and thermal fluctuations are uncorrelated. The expression is then generalized to provide a semi-quantitative, nearly Gaussian orientation distribution for arbitrary tilt angles, particle aspect ratios, Reynolds numbers, and particle sizes relative to the Kolmogorov microscale length. The analysis applies to particles that can be modeled as spheroids, disks, and cylinders, as well as ice crystal hexagonal plates and columns.

The principal analytical result is an orientation distribution of the form $p(\theta) = Z(\beta) \exp(-\beta \sin^2(\theta))$, where Z is the normalization constant, and where β is

$$\beta = \frac{(1-y)m(1+N_{Re}^{\gamma})v_{\infty}^{2}}{kT+m(1+N_{Re,t}^{\gamma})v_t^2}$$

θ is the tilt angle measured from the stable position, y is the particle aspect ratio, m is the effective mass term representing the mass of air in a volume about 54 percent of the particle volume, N_{Re} is the particle Reynolds number, γ is a number of O(1), v_{∞} is the particle terminal speed, k is Boltzmann's constant, T is absolute temperature, $N_{Re,t}$ is the Reynolds number of turbulent eddies of scale size equal to the particle maximum dimension, and v_t is the corresponding magnitude of the turbulent eddy fluctuating velocity. The kT term in the denominator of β represents the disorienting effects of Brownian motion, and the limiting form of the distribution for the case of vanishing turbulence coincides with the distribution due to thermal effects obtained by Fraser (JOSA, 69, 1112 (1979)). According to the model, turbulence can significantly affect the orientational order of some aerosols. For example, for the case of carbon and glass fibers of 3mm length and density 2.5g/cm^3, falling in mildly turbulent air (characterized by a turbulent energy dissipation rate of 10 cm^3/sec^2), a transition from orderly fall to random tumbling is predicted if the diameters of the fibers are reduced from 10μm to 5μm. This result is consistent with field observations (W. Michael Farmer, private communication, 1991).

SIMPLE MODEL AND MEASUREMENTS FOR MODEL VALIDATION IN THE MM/CM WAVELENGTH REGION

by

Ira Goldberg
Rockwell International Space Center

A simple semi-empirical approach is developed to evaluate the attenuation and scattering in the mm and cm wavelength regions of particulate dispersed in air. The approach involves an improved Maxwell-Garnett type model to calculate the attenuation as a function of frequency. The ensemble of particles is treated as an artificial dielectric in which the aspect ratio and the conductivity are the input variables. These calculations are compared to data measured on a suspension of ellipsoids. Several materials have been studied: carbon cylinders, nickel coated carbon, aluminum coated glass and iron coated glass. The best fit to the experimental data is obtained by using the measured effective conductivity of the fibers rather than the bulk conductivity. The effective conductivity is generally about 10% lower than the bulk conductivity.

Validation is done by measuring the absorption and scattering by a fluid suspension of filaments uniformly dispersed in a fixed volume tank. Measurements are taken in the range from 2-20 GHz and from 26-140 GHz. The measurement technique allows the concentration dependence to be accurately determined and effects of random versus aligned orientation to be considered. Experience has shown that the experimental setup is reproducible.

The main conclusion drawn from this work is that the modified Maxwell-Garnett model provides a quick and accurate computational tool whose predictions agree well with the measured performance.

MM WAVE POLARIZATION FEATURES FOR AUTOMATIC TARGET RECOGNITION AND DETECTION

by

William Cameron
The Boeing Co
Seattle, WA

MM wave target signatures are recognized by spatially resolving the constituent scatterers. The maximum degree of discrimination is achieved by using polarization effects to identify the individual scatterer types and orientations. These scatterer types and orientations are extracted from the polarization scattering matrix by transforming it into a vector for subsequent analysis. It is shown that for symmetric scatterers, the responses can be represented as points contained in the unit disc of the complex plane.

These methods are applied to measured signatures of simple polarimetric scatterers to determine the scatterer type and orientation. Several types of examples are discussed in detail.

1.3.3 Experimental Evaluation and Analyses Overviews

Overviews presented in this section represent those papers describing experimental evaluation and analyses of models.

THE SCATTERING OF INFRARED RADIATION BY IRREGULAR PARTICLES ON SURFACES

by

Lowell D. Lamb, Julie D. Lorentzen, and Donald R. Huffman
Department of Physics, University of Arizona
Tucson, Arizona

Mueller scattering-matrix elements were measured for 50 irregular SiC particles on a NaCl substrate. The measurements were made with a polarization-modulated, angle-scanning, infrared scattering instrument that has a tunable wavelength CO_2 laser as its source of illumination. The particles were illuminated individually at two wavelengths (9.25 and 10.66μm), and a small angular region of the scattered light was collected by a Cassegrain telescope held at a fixed angle. Because the electromagnetic behavior of SiC changes dramatically as the illumination wavelength is varied from "insulating" at 9.25μm to "metallic" at 10.66μm, it was possible to measure the scattering of pairs of systems which, except for particle composition, were identical in every way. Hence, the need to physically remove one particle and replace it with another and the many potential sources of experimental error which would accompany replacement of the particle were eliminated. Comparison of a statistical analysis of the data to a sum-of-fields model suggests that measurements of the polarization states of light scattered from irregular particles on surfaces could be used potentially in practical applications to discriminate between compositional classes of particles.

LIGHT SCATTERING FROM ASSEMBLIES OF SCATTERS: APPLICATIONS TO THE CORNEA OF THE EYE

by

D.E. Freund, R.L. McCally and R.A. Farrell
The Johns Hopkins University
Applied Physics Laboratory
Johns Hopkins Road
Laurel, MD 20723

When making comparisons between theory and experiment, care must be taken to assure that the quantity explicitly computed corresponds to what is measured, and that the analysis model does not neglect any of the relevant physical processes governing the experimental data. Two examples based on our research using scattered light to probe the ultrastructure of the cornea are presented to illustrate the importance of these considerations. We show how it is not always easy to recognize when one or the other is being violated.

The first example shows the importance of computing quantities that correspond to what is measured. In particular it shows that calculations performed over an extremely small subregion give rise to a diffraction term that depends only on the size and shape of the subregion and not on the scatterers contained within. The computed results (visible transmittance through the cornea) disagreed with experimental data that probed a macroscopic region in which only the scattering from the assembly of scatterers was measured. However, by recomputing the scattered intensity to more nearly match the experimental conditions under which the data were acquired by eliminating the diffraction term, we obtained excellent agreement between theory and experiment.

The second example shows the importance of assuring the idealized model contains all the relevant physical processes. In this example the model gives good results for total scattering cross-section but poor results for the angular scattering cross-section. This example is particularly striking because the total scattering cross-section was obtained by first computing the angular scattering cross-section and then numerically integrating to obtain the total scattering cross-section. We found that only when the model was refined to include highly significant orientation effects of the constituent scatterers did theoretical predictions agree with the measurements.

PARAMETRIC SENSITIVITY STUDIES OF A VARIATIONAL MODEL FOR MILLIMETER WAVE OBSCURANTS

by

W. Michael Farmer
Bruce Kennedy
The Physical Sciences Laboratory
New Mexico State University

A sensitivity analysis was performed on the commonly used Pedersen-Waterman "extended quasistatic" model to predict the extinction cross-section for high aspect ratio cylinders. The analysis was applied to Dixon 1102 graphite and aluminum millimeter wave obscurants. The objectives of the study were to determine the impact of uncertainty in input data on model prediction capability and to identify the most significant experimental parameters that affect model prediction. Study results show that model uncertainty is strongly dependent on particle material, and is relatively insensitive to variations in particle length. For the particle diameters and lengths considered in this study, 10% relative uncertainty in dielectric constants and length for graphite was found to yield higher relative uncertainty in extinction cross-section predictions at frequencies below about 60 GHz than aluminum. Above 60 GHz, aluminum extinction cross-section predictions yielded higher relative uncertainties than graphite. Uncertainty in model predictions are near the uncertainties in particle length, all other factors having no relative uncertainty. For aluminum, relative uncertainty in model predictions is essentially due to the imaginary component of the dielectric constant for frequencies below 40GHz. For graphite, the real and imaginary components make nearly equal contributions for frequencies as high as 10GHz, and then become dominated by the imaginary component of the dielectric constant. The relative uncertainty in transmission as a result of uncertainties in extinction cross-section predictions was found to increase as transmission decreases and to increase as frequency decreases.

Study results clearly demonstrate that model predictions are generally only as accurate as input values. The analysis shows that model prediction uncertainty typically varies between 1.5 and 2.5 times that of the input parameters. However, for frequencies in the 60-100GHz range, relative uncertainty in extinction cross-sections for aluminum due to relative uncertainty in dielectric constant are significantly less than the relative uncertainty of the input values.

For reliable model predictions it is important that relative uncertainty in the prediction be estimated as a function of the relative uncertainty of model input parameters. The model may be a perfect representation of physical reality and still fare poorly in its predictive capability simply because of the uncertainty in model inputs and because of the model's sensitivity to those inputs.

SUPPRESSION OF SCATTERING RESONANCES IN INHOMOGENEOUS MICRODROPLETS

by

Ron Pinnick
U.S. Army Research Laboratory
Battlefield Environment Directorate
White Sands Missile Range, NM 88002-5501

This work considers the prediction and experimental measurement of the scatter from liquid droplets containing much smaller randomly distributed spherical inclusions. Particles of this type include atmospheric hydrometers that have scavenged small solid aerosols, e.g. sulfate based droplets containing carbon particles, dust particles with individual mineral inclusions, and liquid droplets bearing biological materials. It is this latter case which is the primary objective for analysis in this study.

For this study, glycerol droplets 2-10 μm in diameter are levitated and suspended in an electric field trap and illuminated with a laser. Scatter from the droplet is observed at 90° relative to the incident beam. The droplet diameter slowly changes through evaporation over observational periods of minutes to hours. The droplet diameter is precisely sized, with an uncertainty of less than $\pm$10nm, using scattering resonances predicted by Mie theory. Theory and experiment are in sufficient agreement that over 80 observed resonance cycles can be matched with theoretical predictions.

When the glycerol droplet is impregnated with 10^3 to 10^6 latex spheres having diameters of the order of 60nm, the resonance amplitude decreases and is broadened. These effects are observed to increase in magnitude as the size of the added latex inclusions increases. The signal is also observed to fluctuate in time with the presence of latex inclusions, whereas for the pure glycerol drop the signal does not have the temporal fluctuation component.

In an attempt to explain the experimental observations, the computer code developed for predicting scatter by spherical aggregates (see the summary of Kirk Fuller's work) was used to compute scatter effects by a single small inclusion as it drifted through high intensity illumination regions inside the glycerol droplet. The scatter predicted for this case is insufficient to explain the experimental results. To obtain sufficient scatter magnitude would require an agglomeration of about 11 latex spheres. This is not believed to be likely to occur. A second possible explanation considers coherent scatter by pairs of latex particles that produce homodyne Doppler shift interference that temporally modulates the signal. Analysis of this effect is in process. Regardless of the correct physical explanation, the observed phenomena suggest the possibility that resonance scatter has the potential for distinguishing particles with and without inclusions. This is a technique worth consideration for the detection of biological aerosols.

Appendix B

Bibliography
(Millimeter Wave Database)

1. General Millimeter Wave Obscurant Bibliography

The following bibliography represents reports and refereed journal publications that have been selected to provide a reasonable overview of the state of data sources and data bases for data with which to evaluate electromagnetic wave scattering and propagation models not generally published in the open literature. The bibliography is divided into sections that parallel those discussed in section 5. Many of the technical report references listed for millimeter wave and microwave chaff were extracted from the bibliography assembled by Gary Grider at Wright-Patterson Air Force Base.

OBSCURANT BIBLIOGRAPHY

OBSCURANT PARAMETERS - LABORATORY MEASURMENTS

Anderson, David H., 1988: "Fiber Aerosol Electromagnetic Extinction Coefficients," Proceedings of the Smoke and Obscurants Symposium XII, Vol. I (In Confidential Section), OPM SMOKE/OBSCURANTS TECHNICAL REPORT, AMCPEO-CNS-CT-001-88, .

Anderson, David A., Janon F. Embury, and R. Frickel, 1990: "Millimeter Wave Aerosol Measurements at CRDEC," Proceedings of the Smoke and Obscurants Symposium XIV, Vol. I pp.107 - 118, CRDEC-CR-092.

Bruce, C.W., et al, 1991: "Trans-spectral absorption and scattering of electromagnetic radiation by diesel soot," Appl. Optics, **30**, pp.1537-1546.

Dybbs, A., A. Rutstein, J. Kral, J. Embury, R. Wright, and D. Anderson, 1990: "A Pneumatic Method for Disseminating of Fibrous Material in Laboratory Aerosol Chamber," Proceedings of the Smoke and Obscurants Symposium XIV, Vol. I, pp.137-146, CRDEC-CR-092.

Giles Roy, A.P., B. Drouin, and R. Gagnon, 1988: "Laboratory Evaluation of Smoke Grenades at Submillimetric Wavelengths," Proceedings of the Smoke and Obscurants Symposium XII, Vol. I, pp. 49 - 56, OPM SMOKE/OBSCURANTS TECHNICAL REPORT, AMCPEO-CNS-CT-001-88.

Hoyle, C.D., and D.J. Olsen, and L.R. Whitney, 1989: "Millimeter Wave Characterization of Particles Suspended in Liquids and Predictions for Aerosols," Proceedings of the Smoke and Obscurants Symposium XIII, Vol. I (In Confidential Section), OPM SMOKE/OBSCURANTS TECHNICAL REPORT, AMCPM-SMK-CT-001-89.

Labrum, N. R., 1952: "Some experiments on centimeter-wavelength scattering by small obstacles," Journal of Applied Physics, **23**, pp.1320-1323.

Olsen, R.L., and M.M.Z. Kharadly, 1976: "Experimental investigation of the scattering of electromagnetic waves from a model random medium of discrete scatterers," Radio Science, **11**, pp.39-48.

Poulson, Grahame W., Nigel J. Cronin, Niel A. Martin, and Brian C. F. Butters, 1990: "A Novel Millimetre Wave Scattering Measurement Facility," Proceedings of the Smoke and Obscurants Symposium XIV, Vol. I pp.93 - 106, CRDEC-CR-092.

Rutstein, A., A. Dybbs, J. Kral, and J. Hale, 1990: "Wind Tunnel Testing of Fiber Separation Ejector Prototype," Proceedings of the Smoke and Obscurants Symposium XIV, Vol. I, pp.177-180, CRDEC-CR-092.

Scheuneman, Winfred H., and W. Michael Farmer, 1988: "A Sedimentation Technique for the Determination of the Mass Extinction Coefficient of Millimeter Screening Smokes," Proceedings of the Smoke and Obscurants Symposium XII, Vol. I, pp. 57 - 66, OPM SMOKE/OBSCURANTS TECHNICAL REPORT, AMCPEO-CNS-CT-001-88.

Wang, R.T., J.M. Greenberg, and D.W. Schuerman, 1981: "Experimental Results of Dependent Light Scattering by Two Spheres," Opt. Lett. **6**, 543.

Wright, Robert J., and Robert W. Doherty, 1990: "Mass Concentration Measurements for Large Particulates, $D^{ae} > 15$ Micrometers," Proceedings of the Smoke and Obscurants Symposium XIV, Vol. I, pp.31-50, CRDEC-CR-092.

OBSCURANT PARAMETERS - FIELD MEASUREMENTS

Ben-David, Avishai, 1993: "Backscattering and polarization ratio for cylindrical graphite fibers CO_2 laser wavelengths," Applied Optics, **32**, pp.6777-6783.

Bleiweiss, Max P.,Charles Bruce, Jeffrey Hale, and William C. Parnell, 1990: "Mass Densities for EA5968 Clouds Derived from Radar Measurements," Proceedings of the Smoke and Obscurants Symposium XIV, Vol. I (In Confidential Section), CRDEC-CR-092.

Bruce, C.W., et al, 1990(a):"Attenuation at a wavelength of 0.86 cm due to fibrous aerosols," Appl. Phys. lett., **56**, pp.791-792.

Bruce, C.W., et al, 1990(b): "Millimeter wavelength attenuation efficiencies of fibrous aerosols," Proceedings of the Smoke and Obscurants Symposium XIV, Vol. I, pp.119-127, CRDEC-CR-092.

Fox, Jay A., and Cynthia R. Gautier, 1991: "Effects of Battlefield Obscurants on Laser Rangefinders Operating at 1.06μm and 1.54μm", Proceedings of the Smoke/Obscurants Symposium XV, Vol.II, CRDEC-CR-115, Aberdeen Proving Ground MD 21010-5423.

Hoock, Donald W., 1991: "Theoretical and Measured Fractal Dimensions for Battlefield Aerosol Cloud Visualization and Transmission", Proceedings of the 1991 Battlefield Atmospherics Conference, Ft. Bliss, TX, 3-6 December 1991. Sponsored by the Atmospheric Sciences Laboratory, U.S. Army Laboratory Command, White Sands Missile Range, NM.

Kennedy, Bruce W., and W. Michael Farmer, 1992: "Calibration and Uncertainties of Smoke Characterization Systems", Summary Report completed Dec. 1992, under P.O. 20629PR from the Physical Science Laboratory under Government Contract DAAD07-91-C-0139.

Kennedy, Bruce W., Brian A. Locke, Walter Klimek, and Robert Laughman, 1990: "Large-Area and Self-Screening Smokes and Obscurants (LASSO), (Smoke Week XII) Quick Look Report," STC Technical Report 4056, Science and Technology Corporation, Las Cruces, NM.

Locke, Brian A., and John Crain, 1991: Excerpts from Smoke Week XIII quick look report and data from the Atmospheric and Optical Data Library, Science and Technology Corporation, Las Cruces, NM.

Mijangos, Adrian, 1991: "Test Report Measurements of Millimeter Wave Obscurants Smoke Week XIII," Millimeter Wave Systems Division, Eglin AFB, FL (1991).

Parnell, William C., 1988: "Millimeter Wave RCS Measurements of Multispectral Obscurants EA5968," Proceedings of the Smoke and Obscurants Symposium XII, Vol. I (In Secret Section), OPM SMOKE/OBSCURANTS TECHNICAL REPORT, AMCPEO-CNS-CT-001-88.

Roberts, Lt. Pete, and Adrian Mijangos, 1990: "Test Report Measurements of Millimeter Wave Obscurants at Smoke Week XII," Millimeter Wave Systems Division, Eglin AFB, FL, Spence, Tony and Craig Lewis, 1990: "Obscurant Concentration Measurements System (Nephelometer) Field Test Data Report for Smoke Week XII Test," Physical Science Laboratory, Las Cruces, NM.

Stratton, Suzanne R., and Donald G. Bauerle, 1989: "A Method for Characterization of Radar Chaff Grenades," Proceedings of the Smoke and Obscurants Symposium XIII, Vol. I pp. 181-196, OPM SMOKE/OBSCURANTS TECHNICAL REPORT, AMCPM-SMK-CT-001-89.

OBSCURANT MATERIALS CHARACTERISTICS

Anderson, David A., and Janon F. Embury, 1990: "Microwave Dielectric Constant Measurements," Proceedings of the Smoke and Obscurants Symposium XIV, Vol. I pp.85-93, CRDEC-CR-092.

Bell, Robert J, Mark A. Ordal, and Ralph W. Alexander, Jr, 1985: "Equations linking different sets of optical properties for nonmagnetic materials," Applied Optics, **24**, pp.3680-3682.

Cole, K.S., and Cole R.H.,1941: "Dispersion and absorption in dielectrics, I. Alternating current characteristics", J. Chem Phys, **9**,341-351.

Dulcie, L.L., et al.,1991: "Electrical resistivity and surface coating integrity of carbon and composite fibers", Proc. Smoke and Obscurants Symp. XIV, CRDEC-CR-092,U.S. Army Chemical Research and Development Center, Aberdeen Proving Ground MD, 119-127. Hagemann, H.J., W. Gudat, and C. Kunz, 1975: "Optical constants from the far infrared to the x-ray region: Mg, Al, Cu, Ag, Au, Bi, C, and Al_2O_3," JOSA, **65**, pp.742-744.

Hemmati, Hamid, John C. Mather, and William L. Eichhorn, 1985: "Submillimeter and millimeter wave characterization of absorbing materials," Applied Optics, **24**, pp.4489-4492.

Ordal, M.A., et al, 1983: "Optical properties of the metals Al, Co, Cu, Au, Fe, Pb, Ni, Pb, Ag, Ti, and W in the infrared and far infrared," Applied Optics, **22**, pp.1099-1119.

Ordal, M.A., et al, 1985: "Optical properties of fourteen metals in the infrared and far infrared: Al, Co, Cu, Au, Fe, Pb, Ni, Pb, Pt, Ag, Ti, V, and W," Applied Optics, **24**, pp.4493-4499.

Ordal, M.A., et al, 1987: "Optical properties of Au, Ni, and Pb at submillimeter wavelengths," Applied Optics, **26**, pp.744-752,.

Ordal, M.A., et al, 1988: "Optical properties of Al, Fe, Ti, Ta, W and Mo at submillimeter wavelengths," Applied Optics, **27**, pp.1203-1209.

Querry, M.R., 1985: Optical constants. Technical Report CRDC-CR-85034, U.S. Army Chemical Research and Development Center, Aberdeen Proving Ground MD.

Querry, M.R., 1987: Optical constants of minerals and other materials from the millimeter to ultraviolet. Technical Report CRDEC-CR-8809, U.S. Army Chemical Research Engineering and Development Center, Aberdeen Proving Ground MD.

Stead, Michael and George Simonis, 1989: "Near millimeter wave characterization of dual mode materials," Applied Optics, **28**, pp.1874-1876.

MMW/RADAR HYDROMETER CHARACTERISTICS

Brussaard, G., 1976: "A meteorological model for rain-induced cross-polarization," IEEE Transactions Antennas Propagation, **AP-24**, pp.5-11.

Cho, H.R., J.V. Iribarne, and W.G. Richards, 1981: "On the orientation of ice crystals in a cumulonimbous cloud," Journal of Atmospheric Science, **38**, pp.1111-1114.

Harris, D.A., T. M. Teo, 1981: "Extinction cross-section measurements on single falling water drops at 100 GHz," Electronics Letters, **17**, pp.7-8.

Holt, A. R., 1982: "The scattering of electromagnetic waves by single hydrometers," Radio Science, **17**, pp.929-945.

Ishimaru, A. and R.L.-T. Cheung, 1980: "Multiple-scattering effect on radiometric determination of rain attenuation at millimeter wavelengths," Radio Science, **15**, pp.507-516.

Oguchi, Tomohiro, 1983: "Electromagnetic Wave Propagation and Scattering in Rain and Other Hydrometers," Proceedings of the IEEE, **71**, pp.1029-1078.

Olsen, R. L., 1981: "Cross-polarization during precipitation on terrestial links: A review," Radio Science, **16**, pp.761-779.

Olsen, R. L., 1982: "A review of theories of coherent radio wave propagation through precipitation media of randomly oriented scatterers and the role of multiple scattering," Radio Science, 17, pp.913-928.

Pounder, E.R.,1965: *The Physics of Ice*, Pergamon, New York.

Ray, Peter S., 1972, "Broadband complex refractive indices of ice and water," Applied Optics, **11**, pp.1836-1845.

Sadiku, Matthew N.O., 1985: "Refractive index of snow at microwave frequencies," Applied Optics, **24**, pp.572-575.

Semplak, R. A., 1974: "Measurements of rain-induced polarization rotation at 30.9 GHz," Radio Science, **9**, pp. 425-429.

Senior, T.B.A., and H. Weil, 1977: "Electromagnetic scattering and absorption by thin walled dielectric cylinders with applications to ice crystals," Applied Optics, **16**, pp.2979-2985.

Yeh, C., R. Woo, A. Ishimaru, and J. Armstrong, 1982: "Scattering by single ice needles and plates at 30 GHz," Radio Science, 17, pp.1503-1510.

Zavody, A. M., 1974: "Effect of scattering by rain on radiometer measurements at millimeter wavelengths," Proceedings of Inst. Elec. Eng.,**121**,pp.257-263.

MMW/RADAR CHAFF/TARGET CHARACTERISTICS

Ananthanarayanan, Karimpuzha S., February 1976, "Effective Electromagnetic Properties of Lossy Ferrite Composite Media," USAF Report, Unclassified, AFAL-TR-75-91.

Arthur, J.L., December 1981, "Dipole Breakage Effect on Theoretical Chaff Radar Cross Section," USA Report, Unclassified, DELEW-M-TR-81-40

Arthur, J.L., and Edward Zarret, August 1983, "Chaff Polarization," USA Report, Unclassified, DELEW-M-TR-83-8.

Author Not Listed, 26 June 1967, "Scattering by Thin Wires," Ohio State University Interim Technical Report, Unclassified, Interim TR 2409-1.

Author Not Listed, 30 October 1967, "Scattering by Perfectly Conducting Circular Wire Arcs," Ohio State University Interim Technical Report, Unclassified, ESD-TR-561, Interim TR 2409-2.

Author Not Listed, February 1973, "Chaff Cloud Signature I Measurements Program," Hyco Technical Report, Confidential, AFAL-TR-73-57, AD#525550.

Author Not Listed, August 1974, "Chaff Cloud Signature II Measurements Program," Hyco Technical Report, Unclassified AFAL-TR-74-59, AD#923520L.

Author Not Listed, November 1975, "Chaff Aerodynamics," USAF Report, Unclassified, AFAL-TR-75-81, AD#A019525.

Author Not Listed, December, 1977, "Aerosol Chaff Optical Cross Sections," USAF Report, Unclassified, AFAL-TR-77-221, AD#B028592L.

Author Not Listed, 15 August 1977, "Testing of Chaff Radar Cross-Section," Unclassified, MIL-STD-2071 (AS).

Author Not Listed, May 1978, "Chaff RCS Measurements and Calculation," Ohio State University Technical Report, Unclassified, AFAL-TR-79-1114, AD#A080989.

Author Not Listed, December 1978, "High Efficiency Chaff, Volumes I and II," Tracor Technical Report, Secret, AFAL-TR-78-203.

Author Not Listed, July 1979, "Green's Function Technique for Near-Zone Scattering By Cylindrical Wires with Finite Conductivity," Ohio State University Technical Report, Unclassified.

Author Not Listed, September 1979, "Broadband Chaff," Tracor Technical Report, Secret, AFAL-TR-79-1126, AD#C021577.

Author Not Listed, July 1982, "Millimeter Wave Chaff Analysis," Tracor Technical Report, Secret/No Forn, T82-AU-30-SNF.

Avrin, J.S., and M.V. McCafferty, September 1973, "Chaff Cloud Dynamics," KMS Technology Center, Technical Report, Unclassified, AFAL-TR-73-286.

Bahret, W.F., and R. Garbacz, April 1972, "Practical Consideration of Absorptive Chaff," USAF Report, Secret, AFAL-TR-72-39, AD#520170.

Begley, M.E., 28 June 1990, "Jammer Illuminated Chaff (JAFF)," Georgia Institute of Technology, Technical Report, Secret/No Forn/Winintel, GTRI TM-A8200-075-11.

Breithaupt, R.W., 13 February 1967, "Bistatic Scattering By a Thin, Lossy Cylindrical Wire," Canadian Defense Research Establishment, Unclassified.

Carpenter, Albert G., December 1970, "Effects of Cloud of Thin Metallic Dipoles Upon Search Radars," USAF Report, Secret/No Forn.

Cowart, Gregory, 24 October 1986, "Comparison of the Theoretical RCS of Loop and Dipole Chaff," USN Technical Report, Confidential, NRL Technical Memorandum Report 5867.

Davenport, D.E., August 1980, "Dipole Breakage Investigation," PhD Dissertation and USA Report, Unclassified, DELEW-M-TR-81-37 MB-R-80/20. Contract No. DAAD07-80-C-0117.

Diggs, J.F., and W.T. Davis, 3 October 1969, "Cross-Section Studies of X-Band Chaff," USN Technical Report, Unclassified, NRL Report 6923.

Edwards, J.L. and E.C. Burdette, January 1975, "Radar Cross-Section of Chaff," Georgia Institute of Technology, Technical Report, Confidential, ECOM-5697.

Garbacz, R.J., 15 January 1961, "The Bistatic Scattering from a Class of Lossy Dielectric Spheres with Surface Impedance Boundary Conditions," Ohio State University Technical Report, TR 925-5, Contract AF 30(602)-2042.

Jiusto, James E., and William J. Eadie, May 1963, "Terminal Fall Velocity of Radar Chaff," Unclassified, JGR, Vol. 68, pp. 2858-2861.

Kawano, Tadasu and Leon Peters, Jr., 15 November 1963, "An Application of Modified Geometrical Optics Method for Bistatic Radar Cross Sections of Dielectric Bodies," Ohio State University Technical Report, Unclassified, AFCRL-64-296, Scientific Report No.24.

Knott, E.F., D.J. Lewinski, and S.D. Hunt, September 1981, "Chaff Theoretical/Analytical Characterization and Validation Program," Georgia Institute of Technology, Technical Report, Unclassified, DELEW-M-TR-82-7.

Kutsch, Victor J., December 1977, "Long-Term Persistence of Chaff Echoes over Water," USN Technical Report, Confidential, NRL Memorandum Report 3656.
Lee, W.C.Y. et al, 15 August 1964, "Modified Geometrical Optics for Electromagnetic Scattering by Gytropic Bodies," Ohio State University Technical Report, Unclassified, AFCRL-64-901, Scientific Report No. 30.

Mack, Richard B., August 1977, "Measured Backscatter Modulation From Linearly Oscillating Metal Disks," USAF Report, RADC-TR-77-285.

Martin, E.E., August 1986, "ECM Chaff Measurements Millimeter Wave Radar Support," Georgia Institute of Technology Technical Report, Unclassified, Georgia Tech-TM-A4070-560.

Mihora, D.J., 3 October 1974, "Photogrammetry of Minute Chaff Elements in a Quiescent Test Chamber," Astro Research Corp Techincal Report, Unclassified, ARC-TM-320. AF Contract No. F33615074-C-1052.

Mostrom, R.A., et al., November 1975, "Thin Film Chaff Measurement Techniques (Ultrafines)," AVCO Technical Report, Secret, AFCRL-TR-75-0611.

Nigro, F., et al, October 1976, "Radar Cross Section Modulation Study," AVCO Technical Report, Secret, AVSD -0089-76-RR and SAMSO-TR-76-138.

Olin, I.D., and E.E. Maine, Jr., September 1966, "Characteristics of Radar Return from Chaff," USN Technical Report, Confidential, NRL Report 6434.

Otto, Donald V., 23 December 1968, "Bistatic Scattering by Radially Inhomogeneous Imperfectly Conducting Wires of Arbitrary Length," Ohio State University Technical Report, Unclassified, TR 2584-3.

Peebles, Peyton Z., November 1983, "Radar Chaff: A Bibliography," University of Florida Technical Report, Unclassified, HDL-CR-83-107-5, AD#A135928.

Peebles, Peyton Z., June 1983, "Bistatic RCS of Chaff," University of Florida Technical Report, Unclassified, HDL-CR-83-107-6, AD#A133967.

Peebles, Peyton Z., March 1984, "Bistatic RCS of Horizontally Oriented Chaff," University of Florida Technical Report, Unclassified, HDL-CR-84-062-2, AD#A140903.

Pratt, Thomas, et al, January 1993, "Standoff Chaff ECM Analysis," Georgia Institute of Technology, Technical Report, Secret, WL-TR-93-1042.

Prickett, M.J., et al, November 1979, "Dynamic Chaff Measurements Using Wideband Coherent Radar," USN Technical Report, Confidential, NOSC TR-486.

Porter, M.C., August 1968, "Conductive Fiber Development," AVCO Technical Report, Confidential, AVSSD-0153-68-RR.

Puskar, Robert, July 1975, "Chaff Cloud RCS Studies and Measurements Using a High Resolution Radar," USAF Technical Report, Unclassified, AFAL-TR-74-337, AD#B007252L.

Pyati, Vittal, April 1975, "Statistics of Electro-Magnetic Scattering from Chaff Clouds," USAF Technical Report, Unclassified, AFAL-TR-74-296, AD#A013929.

Richmond, Jack H., et al, 19 February 1970, "Scattering Characteristics of Some Thin Wire Elements," Ohio State University Technical Report 2584-8, AD#865406.

Richmond, Jack H., 1976, "Admittance of Infinitely-Long Cylindrical Wire with Finite Conductivity and Magnetic-Frill Excitation," Ohio State University Technical Report, Unclassified, F33615-76-C-1024.

Sammartino, John, and Christopher Moss, 17 October 1989, "Measurements on the Bistatic RCS and Spectral Spreading of Airborne Self-Protection Chaff," USN Technical Report, Confidential, NRL Memorandum Report 6561.

Schwab, L.M., 13 February 1968, "Double Crossed Dipole Chaff Elements," Ohio State University Technical Report, Unclassified, R.F. 2584.

Schwab, L.M., 11 March 1968, "Reactively Loaded Crossed Dipoles for Chaff Applications," Ohio State University Technical Report, Unclassified, TR 2584-1.

Sinclair, I.P.W., and S.Y.K. Tam, March 1982, "RCS Measurements on Chaff in a Wind Tunnel," Canadian Defense Research Establishment, DSS File No. 13SR.3238044.

Thiele, Gary A., 9 November 1967, "RCS of Open Circular Loops," Ohio State University Technical Report, Unclassified, ESD-TR-67-568, and TR No. 2409-3.

Thiele, Gary A, 21 June 1968, "Scattering by Imperfectly Conducting Wires of Arbitrary Shape," Ohio State University Technical Report, Unclassified, ESD-TR-68-202, and TR-2409-6.

Thomas, David T., 1 August 1962, "Scattering By Plasma and Dielectric Bodies," Ohio State University Technical Report, Unclassified, AFCRL-62-735. Report No. 1116-20.

Thompson, Lane A, July 1976 "Unichaff," USAF Report, Secret/No Forn, ADTC-TR-76-41.

Turpin, Richard H., 28 May 1969, "Average Backscattering Cross-Section of Wires for Arbitrary Transmitter and Receiver Polarizations," Ohio State University Technical Report, ESD-TR-69-160, and TR - 2409/Subcontract No. 359.

Walker, D.R., R.J. Tolosko, and Joseph Hyman, February 1966, "Chaff Aerodynamics," AVCO Technical Report, Secret, AD#375607.

Wickliff, R.G., June 1971, "Scattering From Some Finite Arrays of Randomly Oriented Coupled Dipole Elements," Ohio State University Technical Report, Unclassified, AFAL-TR-2584-12

Wilken, John, July 1982, "The Measurement of Dipole Angle Distribution," Cryptec Technical Report, Unclassified, AD#A145965.

Winkler, C., March 1972, "Diagnostic Studies of Chaff by High Resolution Radar - Theoretical," Australian Ministry of Defense, Unclassified.

THEORETICAL PAPERS WITH OBSCURANT DATA APPLICATIONS

Canosa, J., and H.R. Penafiel, 1973: "A direct solution of the radiative transfer equation: Application to Rayleigh and Mie Atmospheres," Journal of Quantitative Spectroscopy and Radiative Transfer, **13**, pp.21-39.

Daum, G.R., 1985: The theory of multispectral screening, Technical Report BRL-TR-2693, U.S. Army Ballistic Research Laboratory, Aberdeen Proving Ground MD.

Dave, J.V., and J. Canosa, 1974: "A direct solution of the radiative transfer equation: Application to atmospheric models with arbitrary vertical nonhomogeneities," Journal of Atmospheric Science, 31, pp.1089-1101.

Dingle, R.B.,1950: Proc. Roy. Soc., A201, 545.

Hong, S.T., and A. Ishimaru, 1976: "Two frequency mutual coherence function, coherence bandwidth, and coherence time of millimeter and optical waves in rain, fog, and turbulence," Radio Science, **11**, pp.551-559.

Nelson, A., and L. Eyges, 1976: "Electromagnetic scattering from dielectric rods of arbitrary cross-section," Journal of the Optical Society of America, **66**, pp.254-259.

Pedersen, N.E., P.C. Waterman and J.C. Pedersen, 1986: "Absorption and Scattering by Conductive Fibers: Basic Theory and Comparison with Asymptotic Results," Proceedings of the 1985 Scientific Conference on Obscuration and Aerosol Research, Edited by Ronald H. Kohl, CRDEC-SP-86019, pp. 441-473.

Perry, Benjamin, and Hale Jeff, 1989: "Effectiveness Analysis of Radar Obscurant Material Against Soviet Battlefield Surveillance Radar Systems," Proceedings of the Smoke and Obscurants Symposium XIII, Vol. I (In Secret Noforn Section), OPM SMOKE/OBSCURANTS TECHNICAL REPORT, AMCPM-SMK-CT-001-89.

Uzunoglu, N. K., N. G. Alexopoulos, and J. G. Fikioris, 1978: "Scattering from thin and finite dielectric fibers," Journel of the Optical Society of America, **68**, pp.194-197.

Weil, H., and C. M. Chu, 1976: "Scattering and absorption of electromagnetic radiation by thin dielectric discs," Applied Optics, **15**, pp.1832-1836.

BIBLIOGRAPHY

Farmer, W. Michael, and Bruce W. Kennedy (1991), "Electro-Magnetic Properties of Radar/MMW Obscurants," Final Report: 23 July - 15 Dec 1991 Under U.S. Army Research Office Delivery Order 2758.

Farmer, W. Michael, and Bruce W. Kennedy (1994), "Particle Length and Diameter Effects on Extinction and Dispersion Parameters of Field Produced Millimeter Wave Obscurants," Technical Report Prepared for Physical Science Laboratory Under W.A.O. 93-3.2-1.

Farmer, W. Michael, and Bruce W. Kennedy (1994), "Parametric Sensitivity Studies of a Variational Model for Millimeter Wave Obscurants," Technical Report Prepared for Physical Science Laboratory Under W.A.O. 93-3.2-1.

Farmer, W. Michael, and Bruce W. Kennedy (1993), "Exotic Battlefield Aerosols Testing," Technical Report Prepared for Physical Science Laboratory Under Purchase Order 20629PR.

Farmer, W. Michael, and Robert Sutherland (1993), "An Evaluation of Models For Dielectric Constants of Millimeter Wave Obscurant Materials," Proceedings of the Smoke/Obscurants Symposium XVII (VOL. 1), ERDEC-CR-080, Aberdeen Proving Ground, Maryland 21010-5423.

Farmer, W. Michael (1994), "Data Bases and Sources for Validation of Millimeter Wave and Microwave Obscurant Propagation Models," Technical Report Prepared for Physical Science Laboratory Under W.A.O. 93-3.2-1.

Kennedy, Bruce W., W. Michael Farmer, and Karen Hutchison (1994), "Analysis of Smoke/Obscurant Mixtures," Technical Report Prepared for Physical Science Laboratory Under W.A.O. 93-3.2-1.

Kennedy, Bruce W. and W. Michael Farmer (1993), "Selected Analysis From Recent Millimeter Wave Obscurant Field Tests," Proceedings of the Smoke/Obscurants Symposium XVII (VOL. 1), ERDEC-CR-080, Aberdeen Proving Ground, Maryland 21010-5423.

Kennedy, Bruce W., and W. Michael Farmer (1992), "Calibration and Uncertainties of Smoke Characterization Systems," Technical Report Prepared for Physical Science Laboratory Under W.A.O. 92-3.2-1.

Kennedy, Bruce W., and W. Michael Farmer (1991), "Analysis of Millimeter Wave Obscurants At Smoke Week XII and XIII," Final Report: 23 July - 15 Dec 1991 Under U.S. Army Research Office Delivery Order 2758.

Kennedy, Bruce W. and W. Michael Farmer (1994), "Millimeter Wave Trials Analytical Data Compilation," Data Base Instruction Set For CIAO Analytical Test and Evaluation (CIAOATE) Data Sample. Technical Report Prepared for Physical Science Laboratory Under W.A.O. 93-3.2-1.

2. ISST Data Base Summary

This appendix contains a brief summary of scattering measurements made at the Institute of Space Science and Technology, Gainsville, FL. As provided by Dr. Ru Wang.

TABLE B-1. Selected Microwave Scattering Data for Rough Particles and the Target Parameters

ID #	Target Shape	d_o(cm) Outer Diam.	d_i(cm) Inner Diam.	l_{lng}(cm) Longer Length	l_{sht}(cm) Shorter Length	x_v Volume Equiv. Size	$m=m'-im''$ Refractive Index	Extinc-tion P-Q Data	Angular Scatt Data PO	RO
1	A	3.782	1.891	3.777	1.885	3.650	1.610-*i*0.004	1♣	3♦	1♦
2	A	5.692	2.856	5.692	2.843	5.499	1.610-*i*0.004	1♣	3♦	1♦
3	A	7.607	3.809	7.620	3.793	7.346	1.610-*i*0.004	1♣	3♦	1♦
4	A	8.905	4.482	8.956	4.482	8.626	1.610-*i*0.004	1♣	3♦	1♦
5	A	3.439	2.144	3.490	2.228	3.592	1.256-*i*0.003	1♣	3♦	1♦
6	A	5.354	2.702	5.377	2.686	5.184	1.388-*i*0.005	1♣	3♦	1♦,♥
7	B		1.529	4.580	3.053	4.257	1.366-*i*0.005	1♣	3♦	1♦,♠
8	B		2.187	6.538	4.314	6.069	1.367-*i*0.005	1♣	3♦	1♦,♥
9	B		2.754	8.161	5.582	7.694	1.360-*i*0.005	1♣	3♦	1♦
10	B		4.622	13.854	9.260	12.882	1.353-*i*0.005	1♣	3♦	1♦

Legend:

(1) Target Shape:

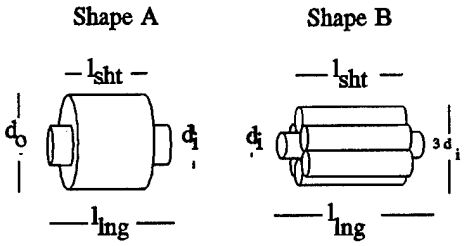

(2) PO: Data for a Preferentially Oriented particle. RO: Averaged data over Radom Orientations.

(3) References where the marked data are cited or described:
- ♣: Wang, R. T., 1984 in Proc (1)
- ♦: Wang, R. T., 1984, in Proc (2)
- ♥: Wang, R. T., 1992, "Scattering..."
- ♠: Wang, R. T., 1992, "Extinction..."

Table B-2. Selected Microwave Scattering Data for Finite Cylinders and the Target Parameters

ID #	*a* radius (cm)	*l* length (cm)	*p=l/(2a)* aspect ratio	*ka=2π a/λ* cylinder size parameter	x_v volume-equival. size param.	*m=m'-lm"* refractive index	Extinc-tion P-Q Data	Angular Scatt. Data PO	Angular Scatt. Data RO	Scatt. Intensity vs. Azim. Sweep
1	.849	3.400	2.002	1.676	2.418	1.610-*i*.004	1			
2	.955	3.828	2.004	1.885	2.720	"	1			
3	1.058	4.240	2.003	2.089	3.014	"	1			
4	1.165	4.670	2.004	2.299	3.318	"	1			
5	1.270	5.100	2.008	2.506	3.620	"	1	3	1	6♥
6	1.376	5.512	2.002	2.717	3.920	"	1			
7	1.482	5.940	2.003	2.926	4.222	"	1			
8	1.590	6.365	2.002	3.137	4.526	"	1			
9	1.799	7.206	2.003	3.551	5.123	"	1			
10	2.012	8.050	2.001	3.970	5.727	"	1			
11	2.118	8.485	2.004	4.179	6.031	"	1			
12	2.328	9.328	2.004	4.594	6.630	"	1			
13	2.540	10.185	2.004	5.014	7.237	"	1			
14	1.304	5.014	1.922	2.574	3.663	1.322-*i*.005	1			
15	1.302	5.032	1.932	2.570	3.671	1.416-*i*.005	1			
16	2.490	10.056	2.019	4.914	7.112	1.321-*i*.005	1			
17	2.512	10.046	2.000	4.958	7.118	1.442-*i*.005	1			
18	.785	6.282	4.001	1.549	2.816	1.610-*i*.004	1♣,♠	3	1 ,♦,*	
19	.964	7.712	4.000	1.903	3.457	"	1♠	3	1	
20	1.204	9.636	4.002	2.376	4.320	"	1♣,♠	3	1	
21	1.457	11.656	4.000	2.876	5.225	"	1♣,♠	3	1	
22	1.157	9.256	4.000	2.284	4.150	1.335-*i*.005	1	3	1	6♥,+
23	1.620	12.970	4.002	3.198	5.812	1.390-*i*.005	1			
24	.635	10.110	7.961	1.253	2.816	1.610-*i*.004	1	(round-ends cyl)		
25	1.144	18.334	8.009	2.259	5.174	1.333-*i*.005	1			
26	.744	18.260	12.26	1.469	3.878	1.327-*i*.005	1	3♠	1	6♥,*

Legend:

(1) PO: Data for a preferentially oriented cylinder.
RO: Averaged data over randon orientaions.

(2) References where the marked data are cited or described:
: Schuerman, D. W. , R. T. Wang , 1981
♦: P. e. Geller, 1985
♠: Wang, W. X., and R. T. Wang
♣: Wang, R. T. and D. W. Schuerman, 1981
♥: Wang, R. T., and Y. L. Xu, 1985
+: J. I.Hage, 1991

Table B-3. Selected Microwave Scattering Data for Circular Disks & Square Plate and the Target Parameters

ID #	a(cm) radius or edge length	t(cm) thick-ness	$p=t/(2a)$ aspect ratio	$ka=2\pi a/\lambda$	x_v volume-equival. size param	$m=m'-im''$ refractive index	Extinc-tion P-Q Data	Angular Scattering Data PO	RO	Scatt. Intensity versus Azimuth
1	1.8978	0.4711	0.1241	3.746	2.139	1.610-i.004	1			
2	1.8862	0.9484	0.2514	3.723	2.690	1.380-i.005	1			
3	1.924	0.962	0.250	3.797	2.738	1.610-i.004	1♣,♦	3	1	
4	2.361	1.180	0.250	4.660	3.360	1.610-i.004	1♣,♦	3	1	
5	2.950	1.476	0.250	5.822	5.123	1.610-i.004	1♣,♦	3	1	
6	3.569	1.784	0.250	7.044	6.198	1.610-i.004	1♣,♦	3	1	
7	2.497	2.537	0.500	4.928	4.501	1.318-i.005	1			
8	(Square Plate): 4.7612cm x 4.7612cm									
x 0.9492cm					3.405	1.366-i.005				1♥

Legend:

(1) PO: Data for a preferentially oriented disk.
RO: Averaged data over random orientations.

(2) References where the marked data are cited or described:

: Schuerman, D. W., R. T. Wang , 1981
♣: Wang, R. T., and D. W. Schuerman; Wang, R. T., 1982 "Extinction..."
♦: Wang, W. X., and R. T. Wang, 1982 "Corrections..." ; Wang, W. X., and R. T. Wang, 1987 "Theoretical..."
♥: Hage, J. I., 1991

References

Barber, P. W., and S. C. Hill, 1990, Light Scattering by Particles: Computational Methods, World Scientific Publishing, Singapore.

Chylek, P., V. Srivastava, R. G. Pinnick, and R. T. Wang, 1988, "Scattering of Electromagnetic Waves by Composite Spherical Particles: Experiment and Effective Medium Theory Approximations," Appl. Opt. **27**, 2396-2404.

Fuller, K. A., and G. W. Kattawar, 1988, "Consummate solution to the problem of classical electromagnetic scattering by an ensemble of spheres. I: Linear chains," Opt. Lett. **13**, 90-92.

Fuller, K. A., G. W. Kattawar, and R. T. Wang, 1986, "Electromagnetic Scattering from Two Dielectric Spheres: Further Comparisons Between Theory and Experiment," Appl. Opt. **25**, 2521-2529 (1986).

Fuller, K. A., and G. W. Kattawar, 1988,"Consummate solution to the problem of classical electromagnetic scattering by an ensemble of spheres. II: Clusters of arbitrary configuration," Opt. Lett. **13**, 1063-1065.

Geller, P. E., T. G. Tsuei, and P. W. Barber, 1985, "Information content of the scattering matrix for spheroidal particles." Appl. Opt. 24, 2391-2396.

Greenberg, J. M., N. E. Pedersen, and J. C. Pedersen, 1961,"Microwave Analog to the Scattering of Light by Nonspherical Particles," J. Appl. Phys. **32**, 233-242.

Greenberg, J. M., R. T. Wang, and L. Bangs, Mar 29, 1971, "Extinction by Rough Particles and the Use of Mie Theory," Nature, Phys. Sci., 230, 110-112.

Hage, J. I., J. M. Greenberg and R. T. Wang, 1991, "Scattering from Arbitrarily Shaped Particles: Theory and Experiment," Appl. Opt. **30**, 1141-1152.

Haracz, R. D., L. D. Cohen, A. Cohen, and R. T. Wang, 1987, "Scattering of Linearly Polarized Microwave Radiation from a Dielectric Helix," Appl. Opt. **26**, 4632-4638.

Kattawar, G. W., and C. E. Dean, 1983, "Electromagnetic scattering form two dielectric spheres: comparison between theory and experiment," Opt. Lett. **8**, 48-50.

Lind, A. C., R. T. Wang, and J. M. Greenberg, 1965, "Microwave Scattering by Nonspherical Particles," Appl. Opt. **4**, 1555-1561.

Roberts, S., and A. von Hippel, 1946, "A New Method of Measuring Dielectric Constant and Loss in the Range of Centimeter Waves," J. Appl. Phys. **17**, 610-616.

Schuerman, D. W., and R. T. Wang, 1981, "Experimental Results of Multiple Scattering," U.S. Army CAL Contractor Rept. ARCSL-CR-81003, Aberdeen, MD.

Schuerman, D. W., R. T. Wang, B. A. S. Gustafson, and R. W. Schaefer, 1981, "Systematic Studies of Light Scattering. I: Particle Shape," Appl. Opt. **20**, 4039-4050.

Schuerman, D. W., 1980, "The Microwave Analog Facility at SUNYA: Capabilities and Current Programs," in *Light Scattering by Irregularly Shaped Particles*, D. W. Schuerman. ed., Plenum, New York, NM, pp. 227-232. (See also an article in this same book: R. T. Wang, "Extinction Signatures of Non-spherical and Non-isotropic Particles," pp. 255-272.)

Stratton, J. A., 1981, *Electromagnetic Theory*, McGraw-Hill, New York, NM (1941), pp. 488-490
Van de Halst, H. C., 1957, *Light Scattering by Small Particles*, Wiley, New York, NY; Dover, NY.

Wang, R. T., and Y. L. Xu, 1986, "Specular Scattering by Finite Cylinders," in Proc. of the 1985 CRDC Scientific Conference on Obscuration and Aerosol Research, R. Kohl, ed., Army CRDEC-SP-86019, Aberdeen, MD, pp. 475-485.

Wang, R. T., Sept. 1986, "Electromagnetic Scattering from a Helix," DAAG29-81-D0100/TCN 85-597 Final Report, Army CRDEC-CR-86071, Aberdeen, MD.

Wang, R. T., and B. A. S. Gustafson, 1984, "Angular Scattering and Polarization by Randomly Oriented Dumbbells and Chains of Spheres," in *Proc. of the 1983 CRDC Scientific Conference on Obscuration and Aerosol Research*, J. Farmer and R. Kohl, eds, Army CRDC-SP-84009, Aberdeen, MD, pp. 237-247.

Wang, W. X., and R. T. Wang, 1987, "Corrections and Developments on the Theory of Scattering by Spheroid -- Comparison with experiments," J. Wave-Material Interaction **2**, 227-242.

Wang, R. T., 1984, "Extinction by Dumbbells and Chains of Spheres," in *Proc. of the 1983 CRDC Scientific Conference on Obscuration and Aerosol Research*, J. Farmer and R. Kohl, eds., Army CRDC-SP-84009, Aberdeen, MD, pp. 223-235.

Wang, W. X., and R. T. Wang, 1988, "Theoretical Calculation on Scattering by Spheroidal Particles and Comparisons with Microwave Extinction Measurements," in Proc. of the 1987 CRDEC Scientific Conference on Obscuration and Aerosol Research, E. H. Engquist and K. A. Sistek, Compilers, Army CRDEC-SP-88031, Edgewood, MD, pp. 473-487.

Wang, W. X., and R. T. Wang, 1988, "Light Scattering by Spheroidal Particles with High Aspect Ratio," J. Wave-Material Interaction **3**, 151-161.

Wang, R. T., 1988, "Status of the Microwave Scattering Facility (MSF) Upgrade," in *Proc. of the 1987 CRDEC Scientific Conference on Obscuration and Aerosol Research,* E. H. Engquist and K. A. Sistek, Compilers, Army CRDEC-SP-88031, Edgewood, MD, pp. 323-339.

Wang, R. T., J. M. Greenberg, and D. W. Schuerman, 1981, "Experimental Results of Dependent Light Scattering by Two Spheres," Opt. Lett. **6**, 543-545.

Wang, R. T., 1985, in *Proc. of the 1984 CRDC Scientific Conference on Obscuration and Aerosol Research*, J. Farmer and D. Stroud, eds. Army CRDC-SP-85007. Aberdeen, MD: (1) "Extinction by Rough Particles," pp. 315-326. (2) "Angular Scattering by Rough Particles," pp 327-363.

Wang, R. T., 1983, "Extinction Signatures by Randomly Oriented, Axisymmetric Particles," in *Pro. of the 1982 CSL Scientific Conference on Obscuration and Aerosol Research*, R. Kohl, ed., Army ARCSL-SP-83011, Aberdeen, MD, pp. 223-242.

Wang, R. T., and D. W. Schuerman, 1982, "Extinction by Randomly Oriented, Axisymmetic Particles," in *Proc. of the 1981 CSL Scientific Conference on Obscuration and Aerosol Research*, R. Kohl, ed., Army ARCSL-SP-82022, Aberdeen, MD, pp. 47-58.

Wang, R. T., 1992, "Scattering by Spheres of Narrow Size Distribution," in ***Proc. of the 1991 CRDEC Scientific Conference on Obscuration and Aerosol Research,*** Compiled by D. Clark, J. E. Rhodes and B. A. Claunch, Army CRDEC-SP-048, Edgewood, MD, pp. 227-238.

Wang, R. T., 1993, "Extinction and Angular Scattering by Rough Particles," in Proc. of the 1992 ERDEC Scientific Conference on Obscuration and Aerosol Research, J. E. Rhodes, Compiler, ERDEC-SP-006, Army Edgewood Research, Development and Engineering Center, Edgewood, MD, pp. 323-332.

Appendix C

Results From CIAO II Modeling Exercise

1. Purpose and Scope

This appendix summarizes the results of model computations made by CIAO II participants using the same aerosol sizes and materials complex index of refraction. The objective of this comparison was to determine how well different models computing the same electromagnetic wave scattering parameters agreed and to identify those areas where caution needs to be exercised in the use of these models.

Models developed for millimeter wave scattering and absorption by fibers and for infrared extinction by disks were exercised prior to the CIAO II workshop. Results were tabulated and compared for illumination by three millimeter wave wavelengths and for 10-μm (disks only). Results of the comparisons are tabulated and discussed.

2. Description of the Problem

As a part of the CIAO II workshop, members of the development community were invited to participate in a modeling exercise to determine the agreement among the various models in determining basic EM properties of non-spherical particles. This exercise was intended to serve as a baseline study from which to progress further. Two examples were chosen; one to address IR flakes (disks) and one for finite length fibers. All fiber calculations were performed for four wavelengths, one in the infrared and three in the millimeter wave band. Three fiber lengths were chosen to span the dipole, resonant, and diffraction regimes. In all cases, the fiber was assumed to be a 7-μm diameter cylinder and the flakes were assumed to be 10-μm diameter by 0.2-μm thick disks. Calculations for the flakes were performed at 10-μm wavelengths only. In all cases, the calculations were made assuming an ensemble average over a uniform particle orientation distribution giving what is referred to in the atmospheric propagation community as a tumble average of all quantities. The original computational plan called for computing all four polarization components as well as the phase function. However, for model output comparison purposes, we focus on the mass extinction coefficients for which field data are available for comparison. Details of the specific particle characteristics that were used in the exercise are summarized in table C-1. Table C-1 also gives values for the bulk conductivity and refractive indices, which happen to be characteristics of graphite.

Four models were compared in the millimeter wave regime for the fiber example: AWAS, JPO94M1, IPHASE, and P/W. AWAS is based upon a commercially available moment method supplied by Bob Richardson of the JPO. The JPO94M1 model was supplied by ARL (Klett and Sutherland) and is a modification of the IPHASE finite cylinder model developed by Blair Evans. The IPHASE model is, itself, based upon the variational approach published over the years in various stages of development by Pederson, Waterman, and Pederson (PWP). P/W is also based upon the PWP approach but it includes a special current function that eliminates certain errors found in the earlier versions as explained by Peter Waterman at CIAO I. In the IR regime (10-μm), two models were compared, IPHASE and JPO94S1, which are both based upon the infinite cylinder geometry using the formal solutions published in the literature by Bohren and Huffman (1983) and Kerker (1969).

Four models were compared for flakes: DDSCAT, IPHASE1, IPHASE2, and FLAKE. The DDSCAT model is based on the Discrete Dipole Approximation as developed by Piotr Flatau. The IPHASE models were supplied by Blair Evans and represent the oblate spheroid and anomalous diffraction approximations, respectively. The FLAKE model is also a part of the

IPHASE library. At the workshop, we also attempted to include results from the Discrete Green's Function (DGF) model of O'Brien and Goedecke but the model apparently was not able to handle the number of computations required for the particular geometries tested.

3. Results for Fibers (Cylinders)

For the 10-μm wavelength, IPHASE and JPO94S1 computational results yielded values for the mass extinction coefficient (m^2/g) of 0.195 and 0.178, respectively. The calculations in this region should be reasonably accurate because the diffraction regime contains numerous valid approximation methods (including the infinite cylinder).

The results were insensitive to the actual value of the fiber length because this is in the region of applicability for the infinite cylinder approximation. The difference between the two models, though slight (10 percent), may be due to the treatment of polarization in performing the ensemble averaging. This same problem arose in discussions involving the phase function. Several ideas presented at the workshop are currently being investigated to resolve the differences.

Results for the millimeter wave regime are summarized in table C-2 where all four applicable models were used. The mass extinction coefficient is the quantity compared at three millimeter wavelengths. For all table C-2 cases the mass extinction coefficient was determined from the calculated extinction cross-section and a bulk mass density of 1.78 g/cm^3, which is appropriate for graphite.

From inspection of the first three columns of table C-2, which correspond to the shortest fiber length (3.175mm), the results for the three variational models (JPO94M1, IPHASE2, P/W, and AWAS) are within 10 percent agreement. Earlier results for the IPHASE calculations as presented at the workshop were later found to be in error by a factor of $\pi/4 \sin(\theta)$ and are shown as a separate model that is identified as IPHASE1. The error was caused by an oversight in defining the solid angle for integration over the particle orientation. The results for the IPHASE1 model are listed for the sake of completeness because they were presented at the CIAO II workshop but they should otherwise be ignored. Previously reported values for AWAS were also later found to be in error and have been corrected here.

The results for the intermediate fiber length (6.35-mm) show a more marked disparity among the three variational models with the P/W results being significantly higher than the JPO94M1 or IPHASE2, at the shortest wavelength. Also the AWAS results, are generally in good agreement with all others. In cases where there is marked disparity among methods, the JPO94M1 and IPHASE2 results tend to agree with each other while the AWAS Method of Moments based code calculations tend to agree more closely with the Pedersen-Waterman results which use an improved current function. It is worth noting that, overall, the results for the two shorter wavelengths are in fair agreement with field data that estimate values of around 2 to 2.5 m^2/g.

Results for the longest fiber length (12.75-mm) show even greater disparities between the variational methods with the P/W results being over a factor of two higher than the JPO94M1 or IPHASE2. This is due to the improved treatment of the fiber current function employed by Waterman in the P/W formuation. The original version presented errors in certain wavelength regimes. However, the cause of this disparity and that with AWAS is still being investigated.

A word about the material parameter model for this calculation exercise is in order. For all of the microwave and mm-wave calculations, the carbon fiber electrical parameters were assumed to follow a Debye dielectric model rather than the Drude model where conductivity is essentially determined by its DC value and dielectric displacement current is negligible. While this is appropriate for comparison of different calculation tools, there is some doubt that the Debye model is the most appropriate for describing carbon fiber electrical behavior in the microwave and mm-wave regime. Differences between the two models become more severe as one goes lower in frequency. In other calculation and measurement exercises, the substitution of DC conductivity rather that Debye model based parameters appeared to yield results which were more nearly in agreement with measurement.

As a matter of completeness, table C-3 shows the results of some intermediate calculations supplied by Blair Evans using the various modules in the IPHASE library. Table C-3 includes results for the infinite cylinder, the finite cylinder, and the prolate spheroid covering all the cases suggested in the exercise where the various approaches are assumed valid.

4. Results for Flakes (Disks)

Results for IR (10-μm) flakes giving values for the mass extinction, absorption, and scattering coefficients (m^2/g) using the DDSCAT, IPHASE, and FLAKE approximations are summarized in table C-4.

Note that in table C-4 the DDSCAT method yielded a value of 2.40 for the scattering component and 1.08 for the absorption component giving an albedo of 0.43 as compared to a value of 0.3 for the FLAKE model. Currently, it is not clear why all methods are not in closer agreement. It is interesting to note that field measurements yield values ranging between 1 and 3 m^2/g, which are not signficantly greater than the spread in values in table C-4 if FLAKE results are excluded. An additional factor affecting the comparison of theoretical and experimental data are the validity of assumptions of disk size and shape for the IR flake materials.

Intermediate data showing plots of the extinction, absorption, and scattering cross-sections and phase function asymmetry factor as a function of orientation angle are shown in figure C-1. These plots were supplied by Pitor Flatau using data based upon the DDSCAT model, which is believed to be the most accurate representation of any of the models presented here. Even so, the DDSCAT mass extinction coefficient is about 20 percent higher than field measurements of graphite flakes.

The phase function plots of figure C-1 appear well behaved, beginning at some initial high value near zero (broadside) and diminish as the angle increases. The assymetry parameter varies from near zero (isotropic scattering) at the lower angles to near unity (strong forward scattering) at the higher angles. Plots of the modeled phase functions for the four polarization cases are plotted in figure C-2.

Table C-1. Input data for the modeling exercise

Incident Radiation	Particle Characteristics					
	Circular					
Disk	Fibers	Bulk Admittance mho/m		Complex Index of Refraction		
Wavelength	Diameter: 10μm					
Thickness: 0.2μ m	Diameter: 7μm					
Lengths:						
3.175, 6.35, and 12.7mm		σ	$jw\epsilon$	n	k	
10μm X	X	3.47 x 10^5	--	4.791	3.513	
3.19mm	NA	X	7.67×10^4	2.45×10^4	101	72.77
8.57mm	NA	X	4.87×10^4	4.18×10^4	165.7	75.69
18.75mm	NA	X	1.87×10^4	3.58×10^4	205.8	51.2

Table C-2. Results of the CIAO II workshop modeling exercise giving mass extinction coefficients for fiber lengths of 3.175-mm, 6.35-mm, and 12.75-mm.

MODEL	PREDICTED MASS EXTINCTION COEFFICIENTS, m^2/g								
	l = 3.175mm			l = 6.35mm			l = 12.75mm		
	λ_1	λ_2	λ_3	λ_1	λ_2	λ_3	λ_1	λ_2	λ_3
JPO94M1	2.56	1.74	0.206	1.65	3.63	0.80	1.36	1.74	1.31
IPHASE2	2.54	1.73	0.222	1.65	3.60	0.80	1.35	1.73	1.30
P/W	2.72	1.73	0.245	2.51	3.58	0.81	2.45	4.41	1.31
AWAS2	2.32	1.56	0.227	2.16	3.22	0.76	2.09	3.85	1.25
AWAS1				1.63	3.02	2.23			
IPHASE1	3.90	2.57	0.340	2.66	5.30	1.21	2.20	2.82	1.94

λ_1 = 3.19mm (94GHz); λ_2 = 8.57mm (35GHz); λ_3 = 18.75mm (16Ghz)

Table C3. Intermediate results supplied by Blair Evans; L_1 = 3.175mm, L_2 = 6.350mm, L_3 = 12.75mm

Model		Q_{ext}				Q_{sca}				Q_{abs}				α			
		10 μm	3.19 mm	8.57 mm	18.75 mm	10 μm	3.19 mm	8.57 mm	18.75 mm	10 μm	3.19 mm	8.57 mm	18.57 mm	10 μm	3.19 mm	8.57 mm	18.75 mm
∞ - Cylinder	∥	2.6977	58.274	112.81	43.180	1.9919	15.818	16.357	3.1897	.70578	42.456	96.451	39.991	.22276	4.8120	9.315	3.5655
	⊥	2.0326	.00238	2.07^{-4}	1.63^{-5}	1.2792	1.96^{-6}	1.00^{-7}	9.46^{-9}	.75341	.00238	2.07^{-4}	1.63^{-5}	.1678	1.96^{-5}	1.71^{-6}	1.34^{-6}
Finite Cylinder	L_1	.41176	30.757	20.929	2.688	.35068	7.345	1.418	2.691^{-6}	.00610	23.411	19.511	2.688	.02944	2.543	1.73	.2222
	L_2	.49937	19.096	43.572	9.782	.48865	4.5137	5.064	.2432	.01082	15.396	38.508	9.539	.03570	1.645	3.600	0.8082
	L_3	.49221	16.377	20.921	15.769	.48221	3.888	2.124	0.8456	.00925	12.490	18.797	14.923	.03511	1.353	1.328	1.307
Prolate Spheroid	L_1	2.4698	2.1950	1.2158	0.4651	-	-	-	-	-	-	-	-	.24154	.21354	.11945	.04519
	L_2	2.4700	2.1950	1.2158	0.4651	-	-	-	-	-	-	-	-	.24154	.21354	.11945	.04519
	L_3	2.4700	2.1950	1.2158	0.4651	-	-	-	-	-	-	-	-	.24154	.21354	.11945	.04519

Table C-4. Summary of results for the disk modeling exercise

Model	$\alpha_{abs}(m^2/g)$	$\alpha_{sca}(m^2/g)$	$\alpha_{ext}(m^2/g)$
DDSCAT	1.08	2.40	3.48
IPHASE 1			2.30
IPHASE 2			2.28
FLAKE	9.22	3.88	13.1

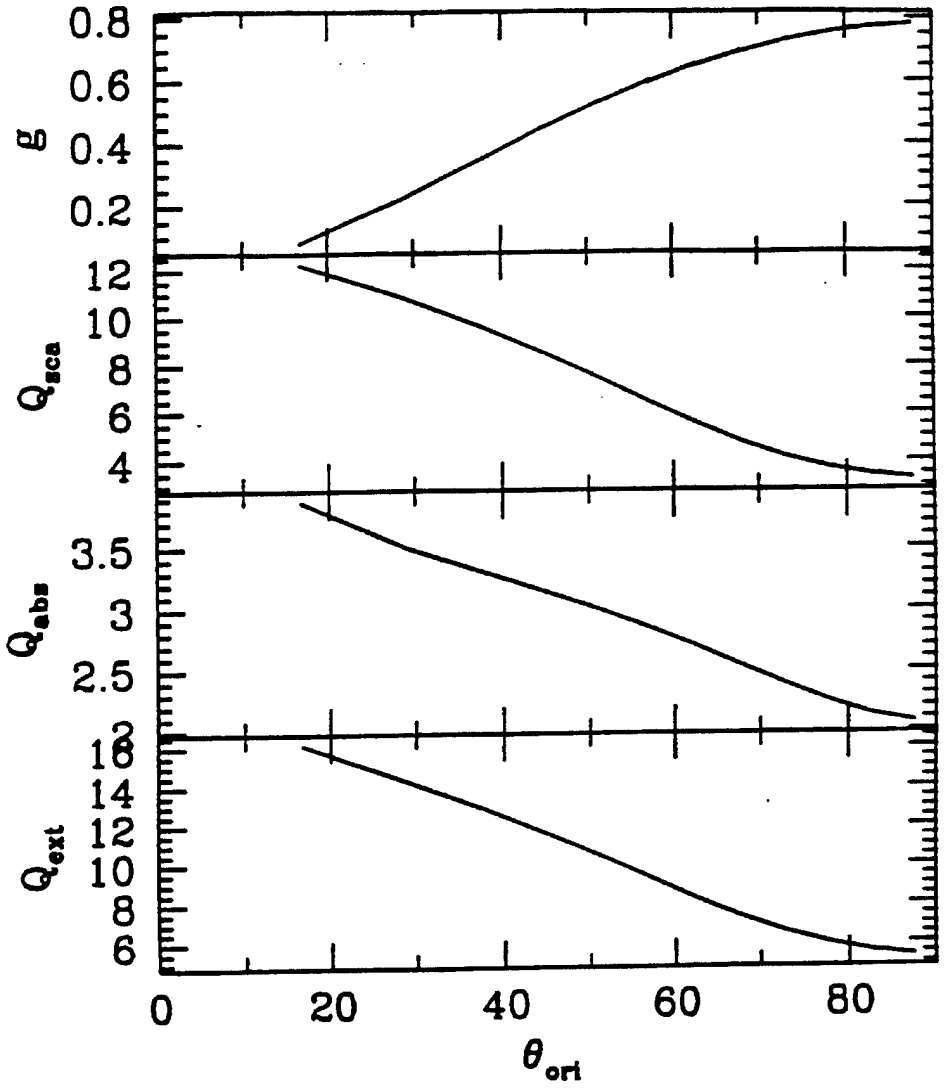

Figure C-1. Intermediate data for the flake example showing cross-sections and asymmetry parameter as a function disk orientation.

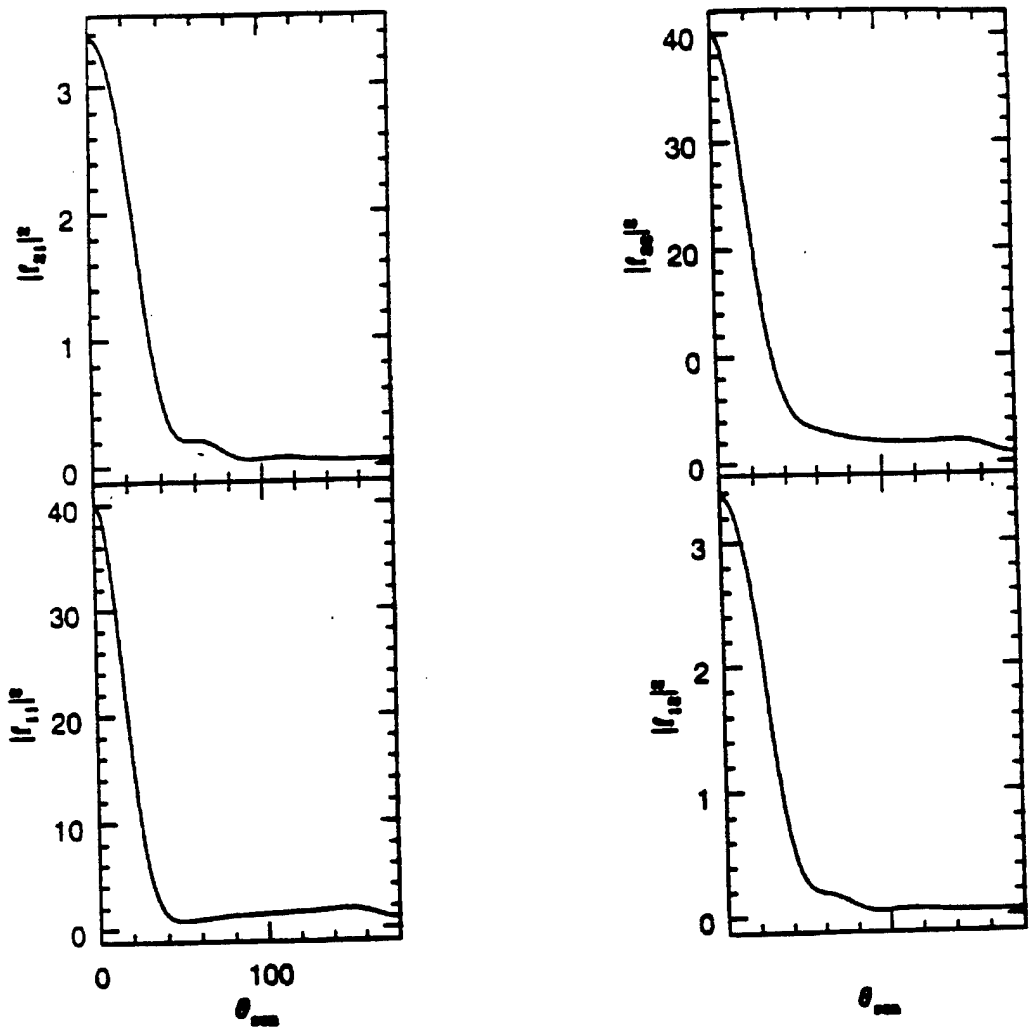

Figure C-2. Plots of the disk ensemble averaged polarimetric phase functions.

References

Bean, B.L., R.J., Brewer, A.E. Carver and J.P. Kahler, 1993, The Measurement and Analysis of Obscurant Cloud Transport, Deposition, and Exposure Effects, Summary Report completed Nov 1993 under contract number DAAA15-90-C-1081 Optimetrics Inc. Las Cruces, New Mexico.

Katrancha, M.F., and R.L. Richardson, 1995, Method of Moments Calculations of micro/mm-wave Properties of Fibrous Chaff and Obscurant Materials. Technical Report JTR-95/20 Naval Surface Warfare Center Dahlgren Division.

Moss, Perry, Ben and Karen, and Daniel Leatherwood, 1992: "Effects of Smoke on MMW Radar Measurements." GTRI Technical Report A-9007 prepared for U.S. Army Chemical, Research, Development and Engineering Center SMCCR-MUT, Aberdeen Proving Ground, MD, 21012-5423. Under Contract No. DAAA21-90-0020-009.

Moss, Perry, Ben and Karen, 1993, "Millimeter Wave Aerosol Obscurants Study" Vol II XM-56 mm-wave Module Data Analysis. GTRI Technical Report A-9279 prepared for U.S. Army Edgewood Research, Development, and Engineering Center, Aberdeen Proving Ground, MD 21012-5423.

Richardson, R.F., B. Steinbach, J.II. Jensen, and B.R. Cobb, 1992, X/Ku-Band Radar Measurement at Smoke Week XIII, Proceedings of the Smoke Obscurants Symposium.

Richardson, R., D. Anderson, J.F. Embury, and R. Frickel, 1990: "Millimeter Wave Aerosol Measurements at CRDEC" Proceedings of the Smoke and Obscurants Symposium XIV, April 1990 CRDEC-CR-092

Richardson. R. F., M.F. Katrancha and W.K. Cary, 1995, Millimeter-Wave Obscurant Chaff Properties: Measurement and Prediction Technical Report, JTR 95/5 Naval Surface Warfare Center Dahlgren Division.

Appendix D

Review of Existing Measurement Techniques

1. Purpose and Scope

This appendix describes experimental data and data analyses methods routinely used for evaluating obscuration models. Most of the data from field experiments that can be used to evaluate the accuracy of electromagnetic wave propagation model prediction are multispectral extinction. Effective electromagnetic wave propagation models must be able to predict this basic integral parameter. Multispectral extinction is used to estimate obscurant logistics requirements and to define the operational threshold of obscured sensors. Therefore, it is important to have a clear understanding of how multispectral extinction is normally analyzed and used to test propagation models.

The largest data base of field measurements available for model prediction comparisons is that for multispectral extinction. Experimental techniques for acquiring these data are reviewed, and methods of data analyses are discussed. It is shown how attenuation data are converted to mass extinction coefficients. Sources of experimental data are described and laboratories and agencies that have contributed significantly to obscurant data are discussed. The application of the experimental data base and measurement capability to validation of predictive models is described for the scattered electromagnetic vector field as a function of particle orientation, the orientation distribution of fibers in the atmosphere, particle number density after dissemination, the dielectric constant of obscurant materials, the obscurant characteristic polarization, and error models of instrumentation used to gather the data.

2. Multispectral Extinction Field Measurements

Figure D-1 shows a typical experimental arrangement for the measurement of multispectral extinction through an atmospheric obscurant. The obscurant aerosol is released upwind from a multispectral transmissometer line of sight. Typically, transmittance through the aerosol as it drifts through the line of sight is sampled at 1 to 10 Hz rates. The data are acquired as a function of time from some arbitrary zero reference. Each data point represents the average of a number of sampled points taken at a much higher rate than the sampling frequency.

The tranmissometer spectral range may be covered by a continuous broad band or by a series of narrow bands. Narrow band measurements are needed when the spectral extinction varies significantly within the measured band. Broad band measurements are sufficient when the spectral extinction is constant within the measured band.

Path lengths through obscurants are typically 10 to 100 m long. Line of sight path lengths (distance between transmitter and receiver) range between 500 and 3000 m. For visual to infrared bands, field test systems measure at 0.4 to 0.7, 1.06, 1.54, 3 to 5, 8 to 14, and 10.6μm wavelengths. At millimeter wavelengths, transmittances are obtained at 35 and 95 GHz.

To determine the mass extinction coefficient, the line of sight concentration length must be measured simultaneously with the transmittances. This is accomplished with an array of point mass concentration sensors or by transmittance at a wavelength for which the mass extinction coefficient is known. Point samplers are commonly used to measure visual to infrared obscurant mass concentrations. These devices are also used for measuring number density of millimeter wave obscurants.

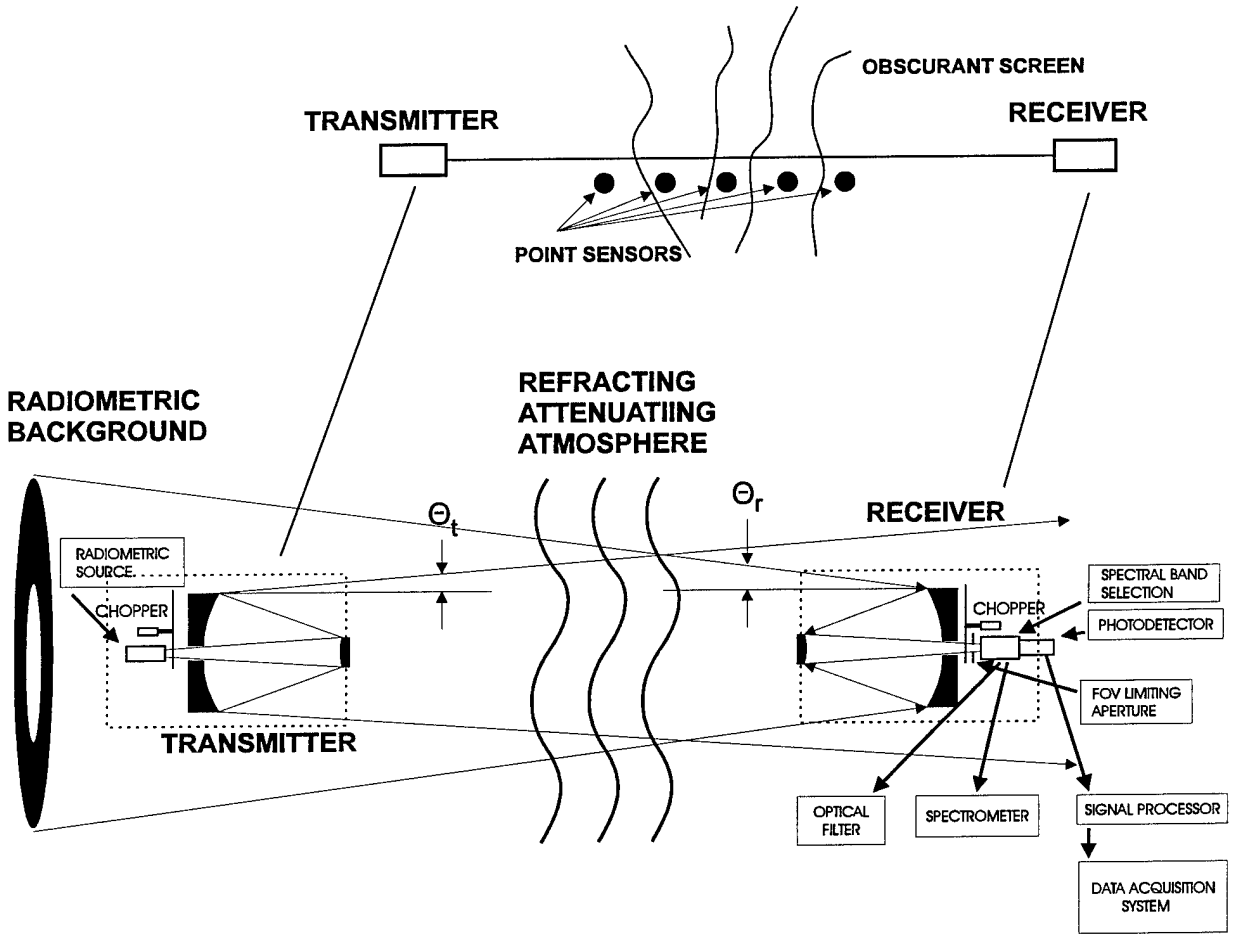

Figure D-1. Typical transmissometer system in a field test scenario for the measurement of multispectral extinction.

Errors in the concentration length measured with a sensor array arise because of inhomogeneities in the obscurant concentration distribution between samplers. These concentration length errors vary in magnitude from a few percent to factors of two. Concentration lengths measured with transmissometers are made for millimeter wave obscurants. In the case of millimeter wave obscurants, the mass extinction coefficient can be estimated within a few percent relative uncertainty using the geometric optical inversion (GOI) technique. The GOI technique works in this case because the particles are of a size that the extinction efficiency is approximately 2 at visual to infrared wavelengths.

3. Multispectral Extinction Data Analyses

For a well collimated transmissometer where data are produced that have no multi-scatter artifacts, the Beer-Bouguer transmission law can be applied to the data analyses. Minor manipulation of equation (1) in section 3, Volume I, shows that the Beer-Bouguer law transmission description for a homogeneously distributed obscurant material is

$$T=\exp(-\bar{\sigma}\rho_N L) \qquad \text{D-1}$$

where

T = the ratio of transmitted to incident irradiance

$\bar{\sigma}$ = the mean extinction cross section of the attenuating material

ρ_N = the aerosol particle number density

L = the path length

In equation, D-1, the extinction cross-section is a function of wavelength. The wavelength dependence is assumed in the following equations and not written explicitly.

Aerosol particle number densities are difficult to measure experimentally; therefore, it is common practice to transform the variables into those related to mass (which is straightforward to measure). The mass extinction coefficient α, is the mean extinction cross-section per mean particle mass. For spherical particles the mass extinction coefficient is

$$\alpha=\frac{\bar{\sigma}}{\frac{\pi}{6}\rho_o\mu_3} \qquad \text{(D-2)}$$

where

ρ_o = the material density of the obscurant

μ_3 = the third moment of the particle size distribution

The spherical particle mass concentration is

$$C=\frac{\pi}{6}\mu_3\rho_o\rho_N \tag{D-3}$$

Using equations (D-2) and (D-3) in equation (D-1) the expression normally used in obscurant analyses is as follows:

$$T=\exp(-\alpha CL) \tag{D-4}$$

The concentration length (CL), as shown in equation (D-1), is, in fact, an integral expression because the concentration is not homogeneously distributed along the transmittance line of sight. CL is

$$CL=\int_0^L C(l)\,dl \tag{D-5}$$

Field measurements produce values of T and CL. The mass extinction coefficient, predicted from electromagnetic wave propagation models, is from experimental data:

$$\alpha=\frac{-\ln(T)}{CL} \tag{D-6}$$

Although equations (D-1) to (D-6) are relatively simple, there are a number of subtle points that must be considered to effectively compare experimental results with theoretical predictions. First consider the impact of error in transmittance and concentration length on the relative uncertainty in mass extinction coefficient. The root-mean-square (RMS) relative uncertainty in mass extinction coefficient is

$$\sqrt{\left(\frac{\delta\alpha}{\bar{\alpha}}\right)^2}=\sqrt{\left(\frac{\delta T/\bar{T}}{\ln(T)}\right)^2+\left(\frac{\delta(CL)}{(CL)}\right)^2} \tag{D-7}$$

where $\delta x/x$ ($x = \alpha$) is the relative uncertainty in the variable, and a bar signifies a mean value. Figure D-2 plots the relative error in mass extinction coefficient as a function of transmittance and selected relative uncertainties in transmittance and CL.

Figure D-2 shows that the relative uncertainty varies with the transmittance and has a minimum value when the transmittance is about 0.37. The relative uncertainty in mass extinction coefficient increases rapidly near transmittances of 1 and when the transmittance is less than about 0.1. Therefore, the relative uncertainty in mass extinction must be determined by integrating equation (D-7) over the distribution of transmittance values obtained for the range of CL used in the estimate.

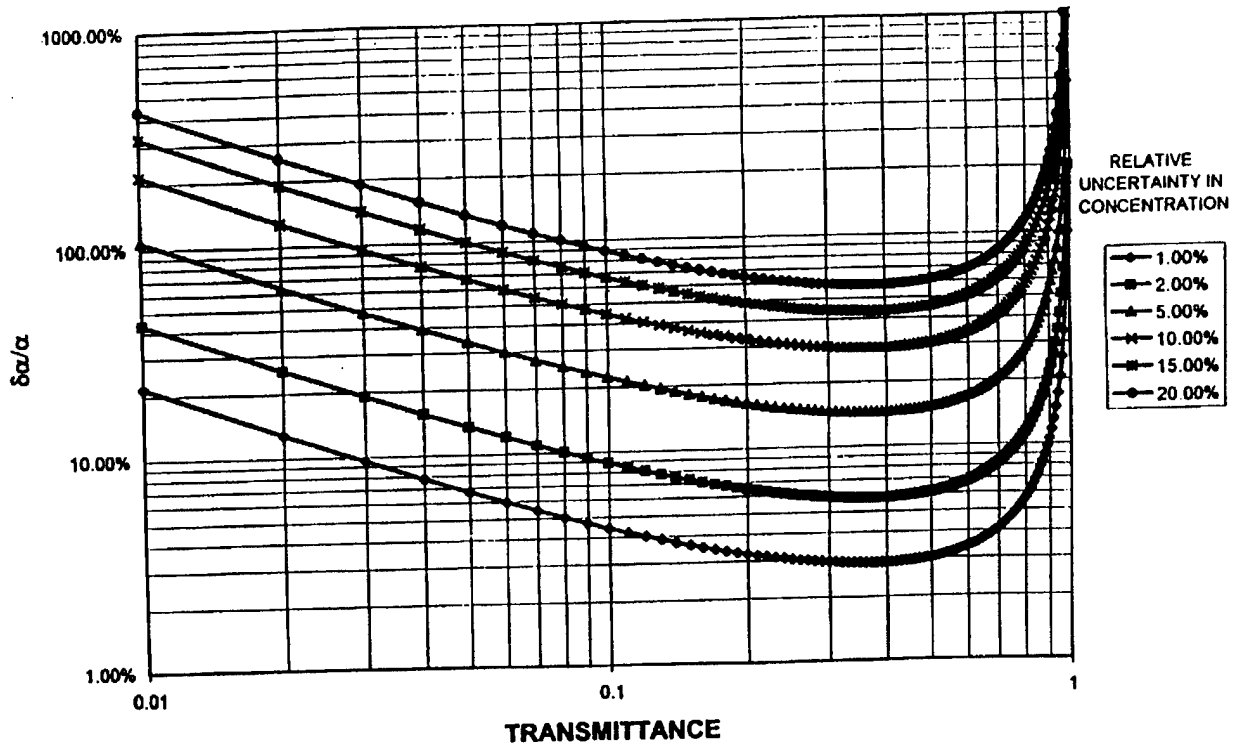

Figure D-2. Relative error in measured Mass extinction coefficient for 05 uncertainty in transmittance and selected relative uncertainties in concentration length.

The second point to consider in evaluating the mass extinction coefficient is its dependence on the obscurant particle size distribution. The shape of the particle size distribution defines the third moment μ_3 of the size distribution and is used to compute the mean value of the extinction cross-section in equation D-2. It is possible to experimentally determine the mass extinction coefficient through a measurement of the particle size distribution if the particle material density is known or assumed. However, particle size distribution measurements sample a very small volume of air relative to that of a transmissometer, and the size distribution measurement itself is very sensitive to sampling and measurement errors.

The analyses given by equations (D-1) to (D-7) is necessary if absolute values of mass extinction coefficient are to be determined. The uncertainties in CL measurements of many obscurants or particle size distribution measurements make the determination of absolute values of mass extinction coefficient difficult and these determinations often have a high level of uncertainty. Thus, methods using linear regressions of multispectral attenuation measurements have been developed that eliminate the need to directly measure concentration lengths. The following discussion outlines this method of determining relative mass extinction coefficients.

Assume that a transmissometer is capable of simultaneously measuring two or more spectral transmittances. The negative natural logarithm of a spectral transmittance is called the optical depth. The ratio of optical depths for two simultaneously measured transmittances is

$$\frac{-\ln(T(\lambda_1))}{-\ln(T(\lambda_1))} = \frac{\alpha(\lambda_1)CL}{\alpha(\lambda_2)CL} \tag{D-8}$$

Assume that the optical depth for λ_1 is the dependent variable. Equation (D-8) can then be written as a linear equation of the form

$$y = mx + b \tag{D-9}$$

where

$$y = -\ln(T(\lambda_1))$$
$$x = -\ln(T(\lambda_2))$$
$$m = \frac{\alpha(\lambda_1)}{\alpha(\lambda_2)}$$
$$b = 0$$

Much information is gained by plotting y versus x and performing a linear regression. First, if there is, in fact, in a linear relationship, then the Beer-Bouguer transmission law applies to the data. Second, the correlation coefficient from the regression is a measure of the noise and scatter of the data between the two spectral bands. The correlation coefficient provides a measure of data quality between the measurements. Third, if $b \neq 0$, then there is clear indication that the transmissometer is operating incorrectly or that data artifacts should be expected. Fourth, the slope from the regression is the ratio of mass extinction coefficients for the two spectral bands. Figure D-3 illustrates a typical regression plot of data measured in a field experiment. Information derivable from these type of analyses is of sufficient value that virtually all field measured transmittance data are now reviewed using this technique.

Evaluation of particle mass concentrations or number densities for millimeter wave and microwave obscurants in field tests is accomplished by measurements at an array of points along a line of sight using optical nephelometers calibrated to count single particles or to measure large numbers simultaneously for mass concentrations. Mean mass or number concentrations along a propagation path can be computed using the Geometric Optical Inversion (GOI) technique on optical (visible or infrared) transmittance data. The GOI can be used for millimeter wave or microwave obscurants when it is assumed the particles are much larger than an optical wavelength and are randomly oriented (see Wright and Butters in the Bibliography in appendix B). Under these assumptions, the mass extinction coefficient (extinction cross-section per particle mass) can be accurately estimated. It is

$$\alpha = \frac{2}{\rho_o D} \tag{D-10}$$

where ρ_o is the particle material density and D is the diameter. Equation (D-10) shows that the mass extinction coefficient is independent of incident wavelength and particle length when $D >> \lambda$. Equation (D-10) can be used in the Beer-Bouguer transmission law to obtain CL. The result is

$$CL = \frac{-\rho_o D \ln(T)}{2} \tag{D-11}$$

The weaknesses in estimating CL represented by equation (D-11) are 1) the particles must be randomly oriented, and 2) the transmission line of sight must be representative of the line of sight of the millimeter or microwave path. Furthermore, if number density is to be inferred from the CL then absolute path length through the obscurant is required and particle length must be known. Applications of the GOI technique to chamber measurements of millimeter wave and microwave obscurants are straightforward. Path lengths in the chamber are known. Turbulence in the chamber with mixing fans should assure random orientation. Particle releases in the chamber are sufficiently gentle so that particles are not broken and the size distributions are monodisperse in length and the particles are not agglomerated.

Uncertainties in the GOI technique include those determined by non-random particle orientation, particle length distributions, and particle agglomerations. Data for particle size distributions of millimeter wave and microwave obscurants are extremely limited. Analyses of transmittance data for field dispersions of these obscurants strongly suggest variations in size distributions result from variations in length (resulting from broken particles) and variations in diameter (agglomerated particles). Data reflecting direct measurement of these parameters in field measurements is sparse or, in some cases, nonexistent.

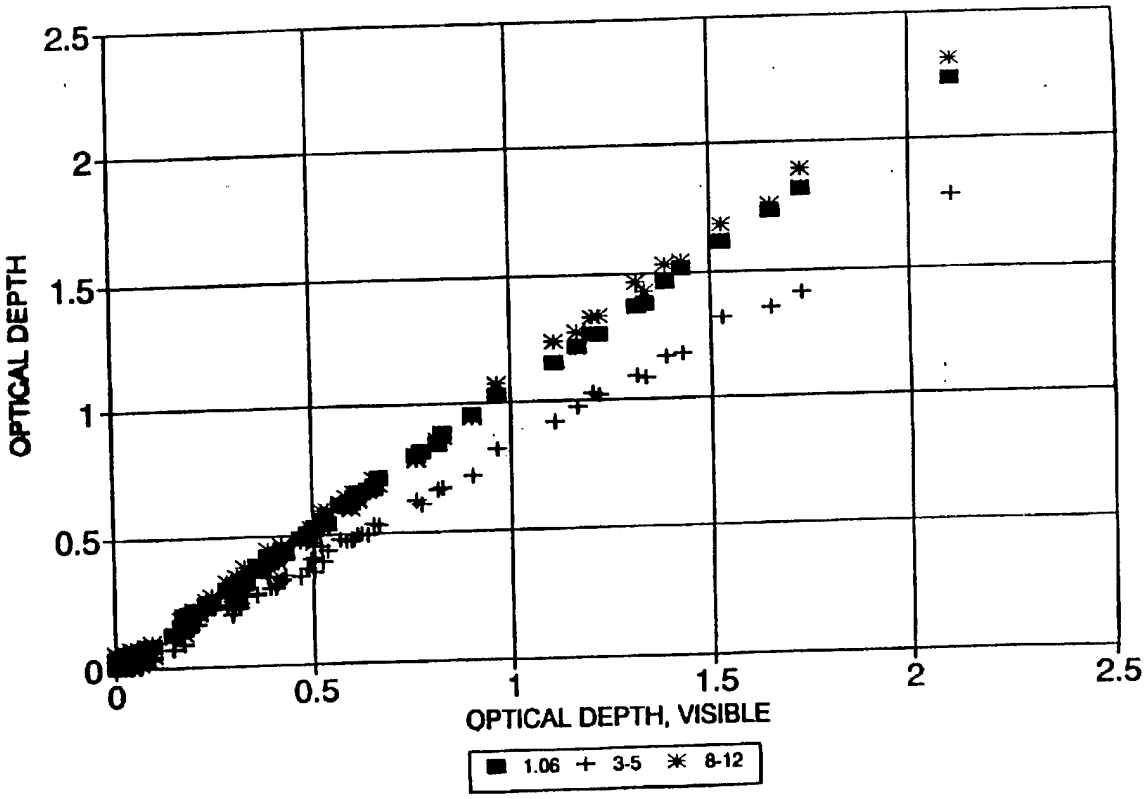

Figure D-3. Example regression plot of multispectral optical depths to determine relative mass extinction coefficients.

4. Radar Measurements

If the transmissometer is replaced by a radar such that scattering vs. range may be obtained, in addition to transmission, more complete information about the mass concentration in the cloud and a more complete overall picture to the dissemination may be obtained. However, radar measurement is more complicated than transmissometry. Issues involved in determining whether simple transmissometry or more complicated scattering measurement is required along with an overview of scattering measurement is described below.

Typically, the radar should be capable of range resolution on the order of 0.5 to 2 meter in order to determine the mass distribution in the cloud with suitable definition and also to aid in correcting for absorption of the signal with the cloud to determine the true scattering. Workers form NSWCDD (Richardson, 1995, Bean, 1993) have shown that these requirements may be easily met with FMCW radar architecture. Workers from GTRI and Eglin AFB (Perry, 1992, Mijangos, 1991) have performed similar measurements using a pulsed radar with a logarithmic receive. Figure D-4 shows an elevation view of a typical field-test installation. Several corner reflectors are placed down range so that the transmission and scattering are obtained simultaneously. The scattering measurement provides a 2-d map of material concentration. Spatial resolution is determined by the range resolution along the beam and the beamwidth along the direction of cloud motion. By using several corner reflectors at different elevations, an estimate (neglecting diffraction effects) of the vertical extent of the cloud may also be obtained. A typical A-scope display is shown in Figure D-5. When the cloud passes through the beam, its location along the beam and its extent are readily visible from the scattering return while the attenuation is observed directly by the reduction in signal level from the corner reflector peaks. the beamwidth of the radar beam must be carefully characterized so that the spot size is a known function of range. Further, it is desirable that the beam be narrow enough so that ground reflection effects and ground clutter are negligible. Ideally, the center of the beam should be at the same elevation as the nephelometer line.

Interestingly, the data obtainable from scattering measurement is complementary to nephelometer data. If one requires good spatial resolution of the material distribution in a cloud, and relies solely on nephelometers, a great many nephelometers are required since nephelometer lines are also required to be quite long. On the other hand, if one relies on the range resolution scattering for cloud material distribution measurement, the nephelometers may be relied upon for more normalization data to check for consistency of results. High range resolution and good normalization may be obtained without an infinite number of nephelometers.

With a suitably calibrated radar, (and corrections for attenuation within the cloud) one measures RCS per unit volume of cloud material. The pulse volume is determined by the spot size and the range resolution which is determined by the FFT block size and windowing function chosen for processing the FMCW radar burst.

Because of clumping effects, scattering measurement provides a better estimate of mass concentration in a cloud and a much better overall picture of the dissemination than absorption measurement alone, particularly for resistive obscurant materials. It is well known that materials do not always disseminate as single fibers but often clump together into multiple-fiber bundles where several (n) fibers are positioned together in a cord wood fashion. For typical parameter values clumping has profound influence on the absorption coefficient as shown in Figure D-6 but

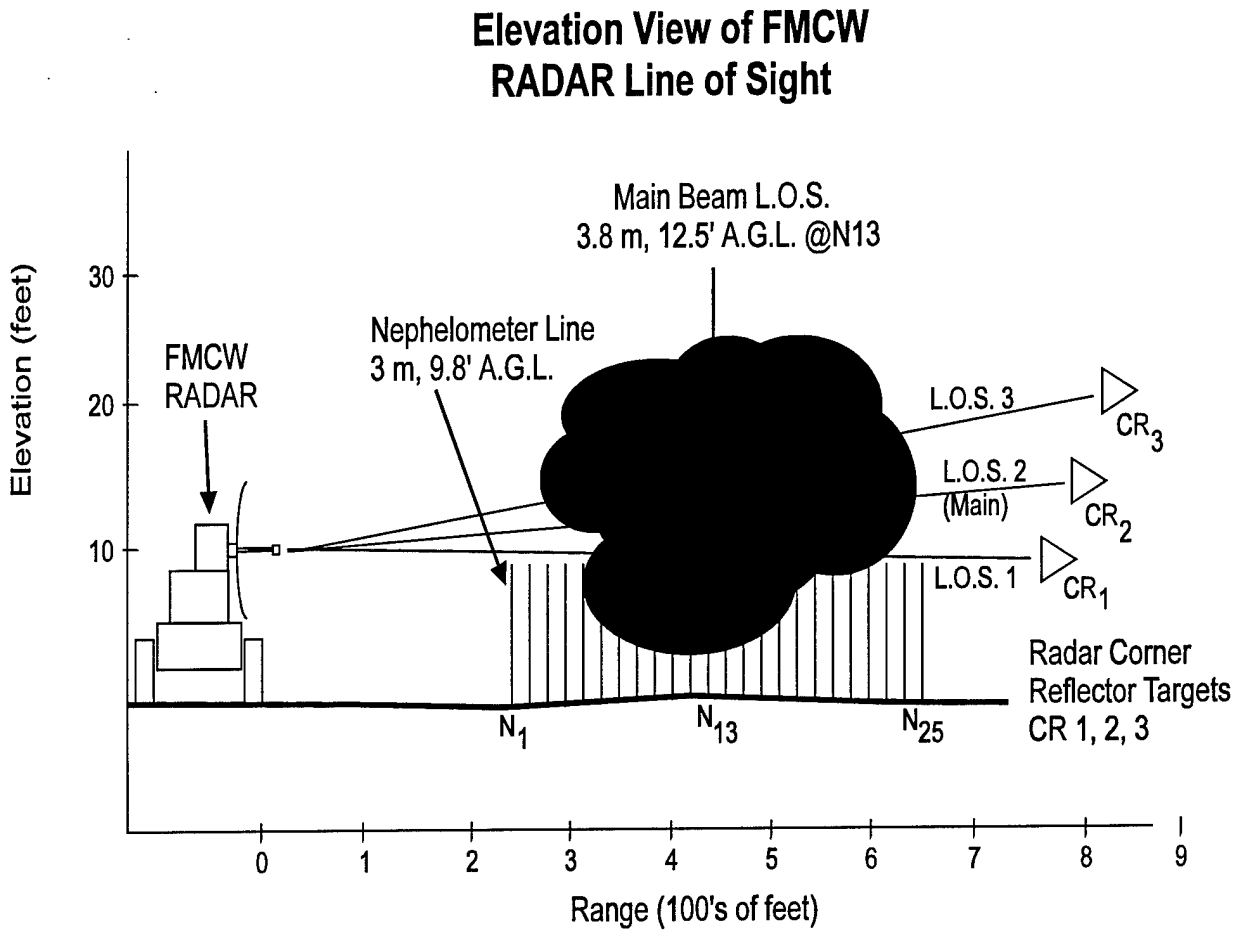

Figure D-4. Elevation (side) view sketch of a typical radar field set-up.

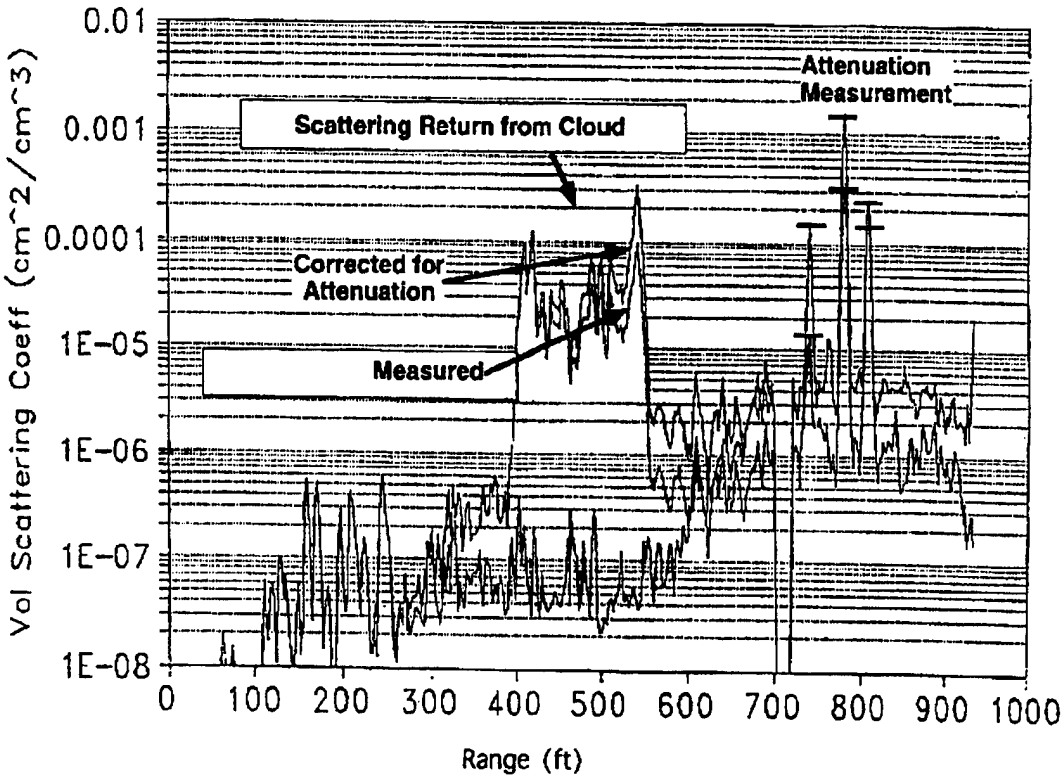

Figure D-5. Typical A-Scope Display for Cloud Attentuation and Scattering Measurement.

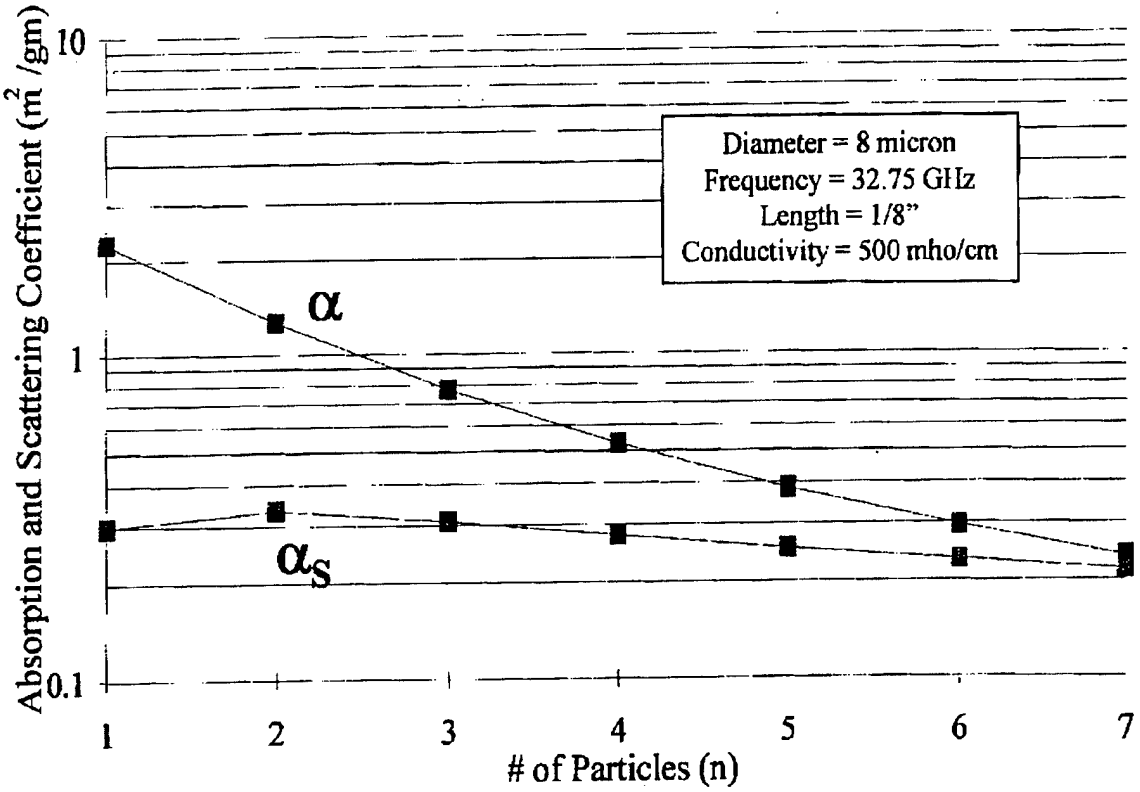

Figure D-6. Calculated α and α_s (m^2/gm) verses number of fibers in a bundle.

not so much influence on the scattering coefficient. In a typical dissemination event there is a "spectrum" of chaff bundles with various "n" values. An important parameter in determining absorption coefficient, is the resistance per unit length of the fiber bundle. Assuming that the material is optimized for single fiber dissemination, a multifiber bundle weighs more and has a lower than optimal resistance per unit length to provide attenuation.

In a practical field measurement or even in a chamber, one does not have a very good way of determining the average number of fibers per bundle. Counting the number of fibers in a bundle under a microscope is very laborious. The calculated results of Figures D-6 show that the scattering cross section per unit mass has a much weaker dependence on the number of fiber, i.e. the clumping number (n) than does the absorption. Since it is laborious to get a good estimate of n from microscopy, mass concentration should be based on corrected scattering data rather than attenuation data.

With a suitably calibrated radar, one measures volume scattering coefficient (m^2/m^3) and then corrects the measured scattering for attenuation such that the attenuation at the far side of the cloud matches that attenuation observed on the corner reflectors. In performing this correction, one naturally arrives at the ratio of scattering and extinction cross sections. The data of Figure D-6 shows that this ratio is clearly a function of how much clumping is present. Reflectivity or "blackness" of a cloud which depends on the ratio of scattering and absorbing cross sections is clearly dependent on the amount of clumping in the cloud.

In material development studies where the reflectivity of the material is of interest or in measurements to evaluate the performance of cloud formations models where mass per unit volume is of interest it is clearly important to perform scattering measurements in addition to the more usual attenuation measurements.

Uncertainties in the GOI technique include those determined by non-random particle orientation, particle length distributions, and particle agglomerations. Data for particle size distributions of millimeter wave and microwave obscurants are extremely limited. Analysis of transmittance data for field dispersions of these obscurants strongly suggests variations in size distributions that result from variations in length (resulting from broken particles) and variations in diameter (agglomerated particles). Data reflecting direct measurement of these parameters in field measurements are sparse or in some cases nonexistent.

5. Data Sources

Sources of experimental data to verify electromagnetic wave propagation models fall into two broad categories: 1) laboratory measurements, and 2) field trials. Data from both sources can be grouped into three categories: 1) material characteristics, 2) electromagnetic wave response characteristics, and 3) figures of merit. Figures of merit are derived from material characteristics and electromagnetic wave responses. Table D-1 provides a summary of the sources of data in these categories. The agencies listed in table D-1 either acquired the data using government facilities or through contractors sponsored by the agency.

Table D-1. Summary of obscurant data sources for evaluation of electromagnetic wave propagation models.

	DATA CLASSES	DATA SOURCES								
		ARL-BED	DPG	ERDEC	WP/EGLIN AFB	ISST	HARC*	UK	CANADA	AUSTRALIA
	MATERIAL CHARACTERISITICS									
1	ELECTRICAL CONDUCTIVITY									
2	DIELECTRIC CONSTANTS			X		X				
3	REFRACTIVE INDICES			X						
4	CHEMICAL COMPOSITION			X						
5	CRYSTALLINE STRUCTURE									
6	DENSITY			X						
7	PARTICLE SHAPE			X						
8	PARTICLE SIZE, SIZE DISTRIBUTION	X	X	X				X	X	X
9	PARTICLE NUMBER DENSITY									
	ELECTROMAGNETIC WAVE RESPONSE									
10	S11 PHASE FUNCTION			X		X		X		
11	MUELLER MATRIX PHASE FUNCTIONS			X		X		X		
12	EXTINCTION CROSS-SECTIONS			X		X		X	X	X
13	RADAR CROSS-SECTION	X	X		X			X		
	FIGURES OF MERIT									
14	VOLUME EXTINCTION COEFFICIENT	X	X	X				X	X	X
15	MASS EXTINCTION COEFFICIENT	X	X	X				X	X	X
16	MASS RADAR COEFFICIENT		X		X	X				
17	DRAG COEFFICIENTS									
18	PARTICLE ORIENTATION			X	X	X		X		
19	CROSS-SECTION RATIO			X	X					
20	FOURIER POWER SPECTRUM				X					

*Note: HARC has not been used for obscurants.

5.1 Facilities

Data acquired by the U.S. Army Research Laboratory (ARL), Battlefield Environment Directorate (BED) are, for the most part multispectral transmittance, stereo imagery for determining obscurant transport and diffusion, point measurement of mass concentration, particle size distribution, and meteorological measurements in support of Smoke Week test programs and other electro-optical sensor evaluation programs.

Dugway Proving Grounds (DPG) has obtained multispectral transmittance, point concentration and dosage measurements for test programs at DPG and for other electro-optical sensor test programs, such as the Smoke Weeks.

Edgewood Research, Development, and Engineering Center (ERDEC) has generated voluminous obscurant data through laboratory chamber measurements, small scale atmospheric tests, and major test programs such as Smoke Weeks. ERDEC has sponsored research for measurements of material characteristics and has developed a small nephelometer capable of Mueller matrix measurements at visible laser wavelengths.

The Air Force represented by Wright-Patterson Air Force Base (AFB) and Eglin AFB has conducted numerous chaff (scattering cylinders) tests in anechoic chambers and under flight conditions. Eglin AFB has provided millimeter wave radar measurements of absorbing cylinder tests conducted during Smoke Week tests.

The Institute for Space Science and Technology (ISST), Space Astronomy Laboratory, Gainesville, FL, operates a 3.1-cm wavelength microwave nephelometer capable of measuring phase functions for irregularly shaped particles scaled for extinction efficiency measurements in the resonant region.

ISST also measures the dielectric constants of the materials used to make the particle models used in the measurements. Phase functions measured in this laboratory have provided detailed data for evaluation of theoretical models of resonant region scattering.

The Houston Area Research Consortium (HARC) have obtained data similar to that of ISST. However, the HARC emphasis has been on measuring bistatic radar cross-sections of object shapes of interest to the military and has not measured obscurants.

Data acquired in the United Kingdom include both laboratory and field measurements with multispectral transmissometers measuring visible and emissive infrared obscurants, and radar systems observing chaff releases. Chemring Ltd, a private contractor, operates a polar nephelometer for the United Kingdom Ministry of Defense that has been used to measure the phase function of individual millimeter wave chaff particles (15-μm diameter by 4 to 8 mm in length) illuminated by a 94-GHz collimated beam. This system is capable of automatically acquiring phase function data for a wide range of particle orientations relative to the collimated incident beam.

The Canadian Defense Research Establishment, Valcartier (DREV) has obtained voluminous multispectral extinction data in a large laboratory chamber, and extensive near infrared lidar signal returns and laser transmittance in field measurements. Data have recently been reported that correlated concentration measurements with integrated back scatter returns.

Data acquired by the Australian Ministry of Defense include a modest number of chamber measurements and field test data for inventory obscurants extinction and for graphite fibers used for millimeter wave obscuration.

5.2 Scattering Properties

For electromagnetic wave frequencies of the order of 100 GHz and lower it is possible to measure single particle scattered wave amplitude and phase as a function of particle orientation relative to the incident beam and scatter angle. There are three known facilities that can accomplish these kinds of measurements:

1. The microwave scattering facility at the Institute for Space Science and Technology,
2. The bistatic microwave scattering facility at the Houston Advanced Research Center, and
3. The United Kingdom 95-GHz polar nephelometer operated by Chemring Ltd.

The ISST microwave scattering facility operates at a wavelength of 3.1835 cm (9.4192 GHz) and obtains measurements of 1) extinction (amplitude and phase) (scattering angle is 0°), 2) angular distribution of scattered amplitude (for 0° elevation and 0 to 172° in azimuth), and 3) scattered intensity versus target azimuth variation for fixed scatter angle and antenna polarization. Figure D-7 shows the ISST microwave scattering facility (*Wang, Microwave Scattering Measurements of Small Particles of Various Target/Array Shapes*, to be published). This facility was designed to acquire data in the resonant scattering region where wavelength is comparable to object dimensions. Thus, data typically reported from this facility are for objects with major and minor dimensions of the order of centimeters. Original applications of these data were tests for theoretical models of irregular particle scattering at much higher frequencies. Scattering object indices of refraction (predominantly plastics) were measured at the scattering facility by measuring the complex dielectric constant using the standing wave technique of Roberts and von Hippel (1946). The dielectric constant is found by analyzing observed shifts in standing-wave maxima/minima positions as well as the voltage standing wave ratio patterns as the dielectric sample is introduced into the wave guide-slotted line. Real indices of refraction for the measurements ranged between 1.1 and 1.8. Imaginary components of the scattering object ranged between 0.005 and 0.2. Data are also reported for aluminum where the refractive index is reported as infinity.

The bistatic radar microwave scattering facility at the Houston Advanced Research Center (HARC) operates with a variety of polarized microwave sources that range in frequency between 2 and 40 GHz. HARC has used both vector network analyzers and narrow band polarized beams. Figure D-8 shows a schematic of the scan geometry of the HARC. The transmitter and receiver antennas are mounted on trolleys. The trolleys can move along their respective support trusses, which are constant radius semicircles. The transmitter truss is fixed with sufficient offset to allow the receiving antennas to rotate about a vertical axis between 0° and 190°. The transmitter antennas always remain at 0° azimuth throughout their entire range of elevation. The range of elevation for the transmit/receive trolleys is 25° to 150°. The scattering object pedestal mount is capable of rotating the object through 400° in azimuth with an uncertainty of $\pm$ 0.05°. HARC was designed to measure bistatic radar cross-sections of objects with major/minor dimensions of the order of centimeters or greater. The scattering object positioned is capable of supporting 500 LB radial loads and 2000 LB axial loads. A Ph.D. dissertation was recently completed on a 12 component error model for HARC (Jersak, 1993). Data are reported for a frequency range of 6 to14 GHz. Jersak's work represents the most complete known error analyses of measurement capability for any of the facilities described in this report. Figure D-9 illustrates the accuracy and precision of calibrated object measurements at HARC and compares the results with theoretical predictions. Theory and experiment agree within fractions of a percent.

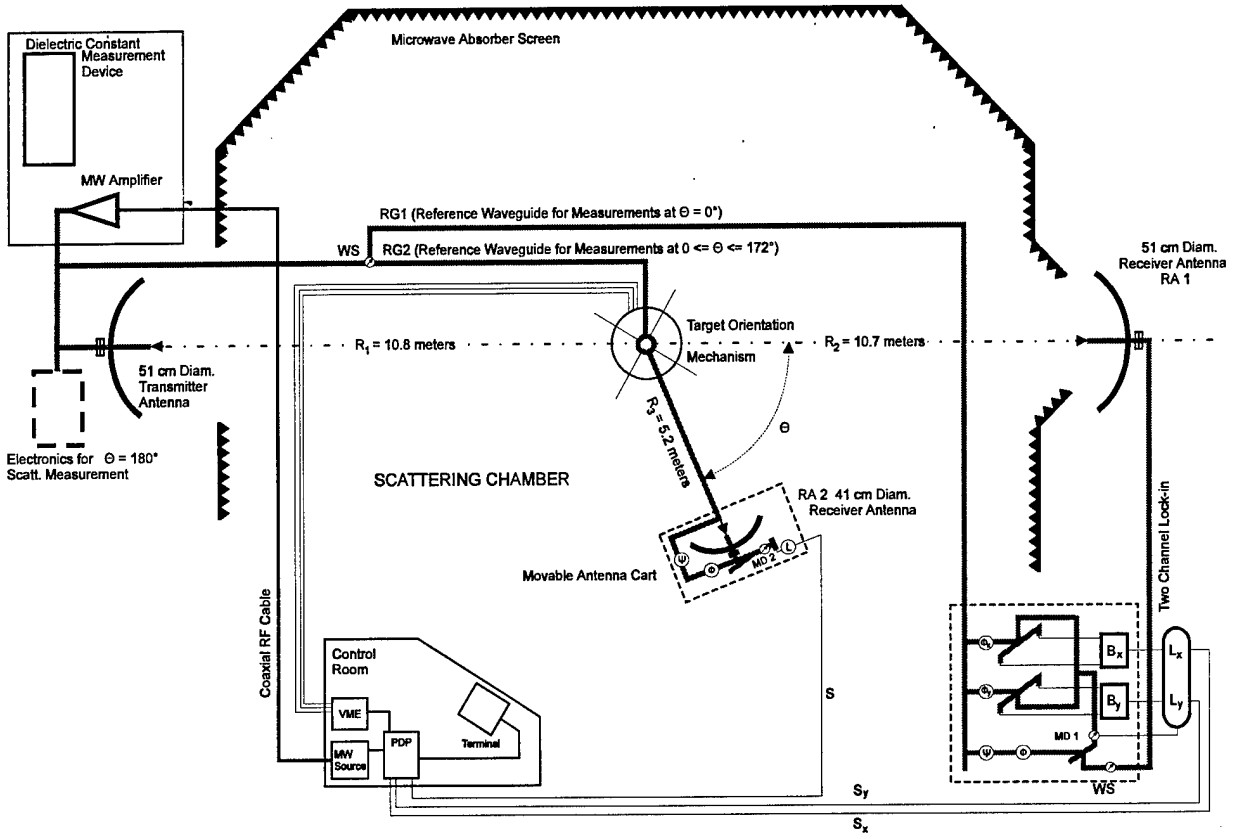

Figure D-7. ISST Microwave Scattering Facility.

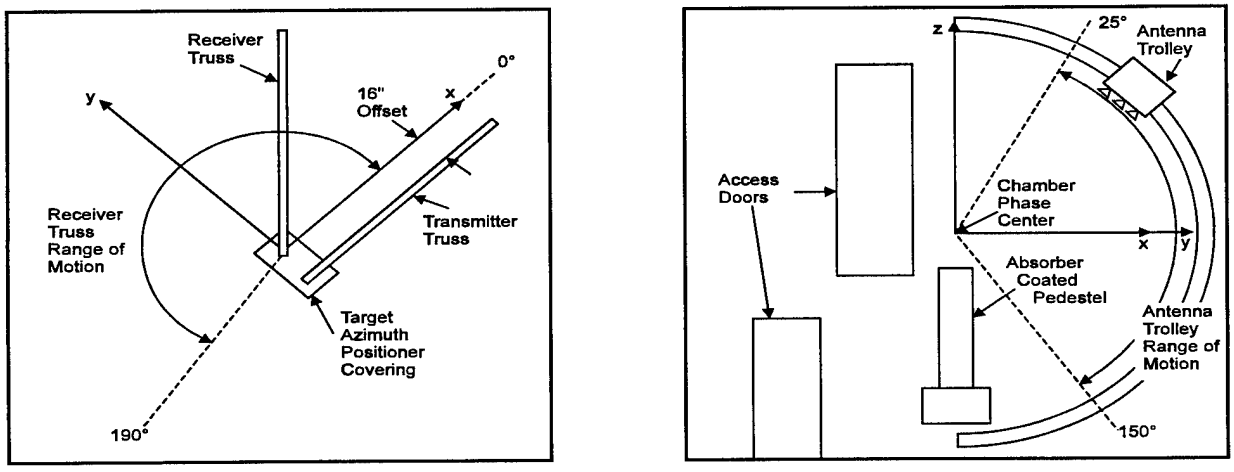

Figure D-8. Sketch of HARC Bistatic Microwave Scattering Facility.

SRCT, ½ " Conducting Sphere, 7-6-94
Time Gate from -0.4 to 0.4 ns, 6" Sphere, Vertical and 22.5° Dihedrals Reference

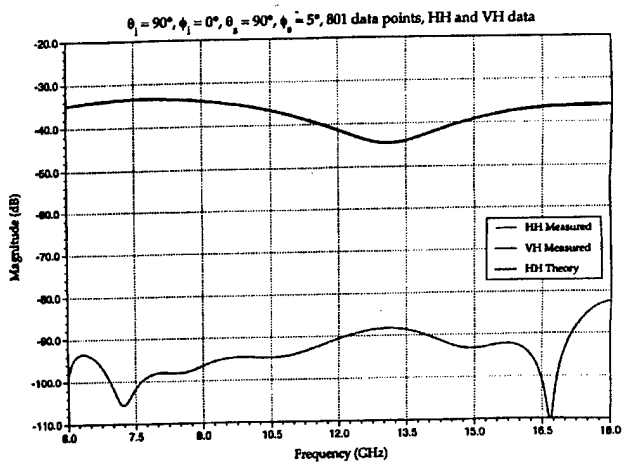

D-9a

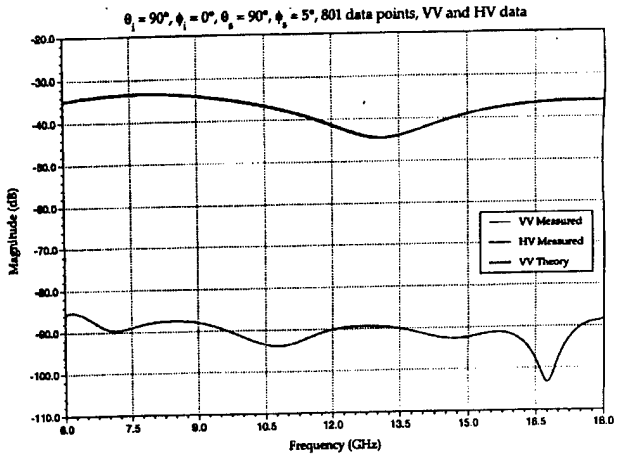

D-9b

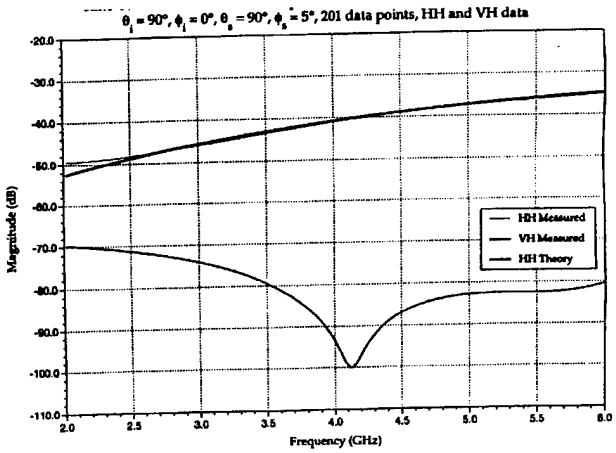

D-9c

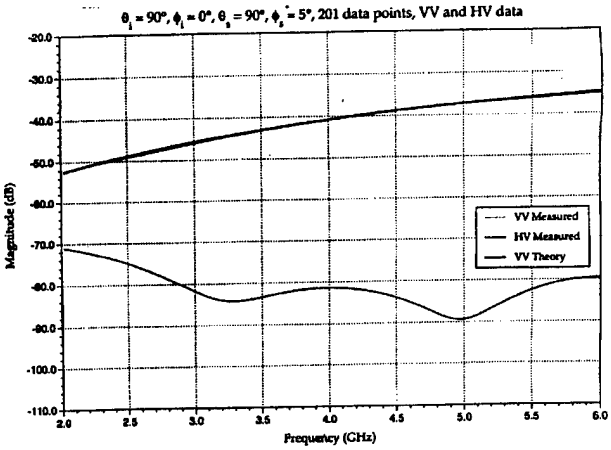

D-9d

Figure D-9. HARC data comparisons.

The United Kingdom polar nephelometer operated by Chemring Ltd uses the highest electromagnetic wave frequency (95 GHz) of the three facilities described in this section. The polar nephelometer uses Gaussian beam mode optics in a polarizing Michelson Interferometer to obtain plane wave illumination of the scattering object placed at the beam waist. The interferometer geometry allows scattered wave phase amplitude in the forward direction to be measured. These data are used to compute the particle extinction cross-section without the use of calibration targets. The largest particle that can be examined with sufficiently uniform illumination is approximately 22 mm. The lower limit in size is defined by the limiting signal to noise ratio which is determined by the particle support system. Past measurements have included aluminum coated glass fibers approximately 4 mm long by 15μm in diameter. The instrument is designed to automatically scan the scattered radiation pattern in the azimuth plane and to position the particle through a full range of orientations relative to the incident beam. Azimuth scan range is approximately 10° to 170°. Figure D-10 shows a schematic of the design of the instrument (Poulson). Figure D-11 shows examples of phase functions measured with the Chemring instrument.

All the nephelometers described in this section are capable of measuring the horizontal and vertical polarization components of the scattered field. It is only necessary to measure these two components to fully characterize the polarization characteristics of the scattered field when both scattered phase and amplitude are measured.

5.3 Particle Orientation Distribution

Nonspherical particles can assume a preferred orientation after dispersal into the atmosphere. For example, it is theorized, and some chaff and snow data show, that cylindrical particles orient in the atmosphere so that the long axis of the cylinder is parallel to the ground. Atmospheric turbulence affects the particle orientation by tilting the particle long axis toward the vertical making the particles fall faster and, as a result, attempt to reorient parallel to the ground. This gives rise to time dependent orientation distributions. For orientation distributions to occur, the particles do not have to be cylindrically shaped. Even raindrops are squeezed into oblate spheroid shapes due to wind resistance as they fall. This shape gives rise to droplet orientation distributions when wind cants the axis of symmetry.

Scattering from irregularly shaped particles depends strongly on the particle orientation relative to the polarization vector of the incident beam. Microwave and millimeter wave transmission through preferentially oriented, naturally occurring, hydrometers is important to the design of communications systems, which may operate in two characteristic polarization modes. The polarization modes must be chosen to optimize transmission and minimize information leakage between the modes. The polarization mode choice strongly depends on particle shape and orientation. Similar effects and problems occur for the design of millimeter wave and microwave sensor systems operating against man-made obscurants. Therefore, particle orientation distributions play a key role in the proper design and application of millimeter wave and microwave sensor systems in the atmosphere and from satellites.

Significant research programs have been conducted to develop theories that predict particle orientation distributions for raindrops. However, very little information has been acquired for orientation distributions of obscurant particles in the atmosphere. This information deficiency is a major gap in data needed to develop and verify propagation models. Millimeter wave and microwave system designers require these data to optimize system performance against obscurant countermeasures. Obscurant developers need these data to develop effective millimeter wave and microwave countermeasures.

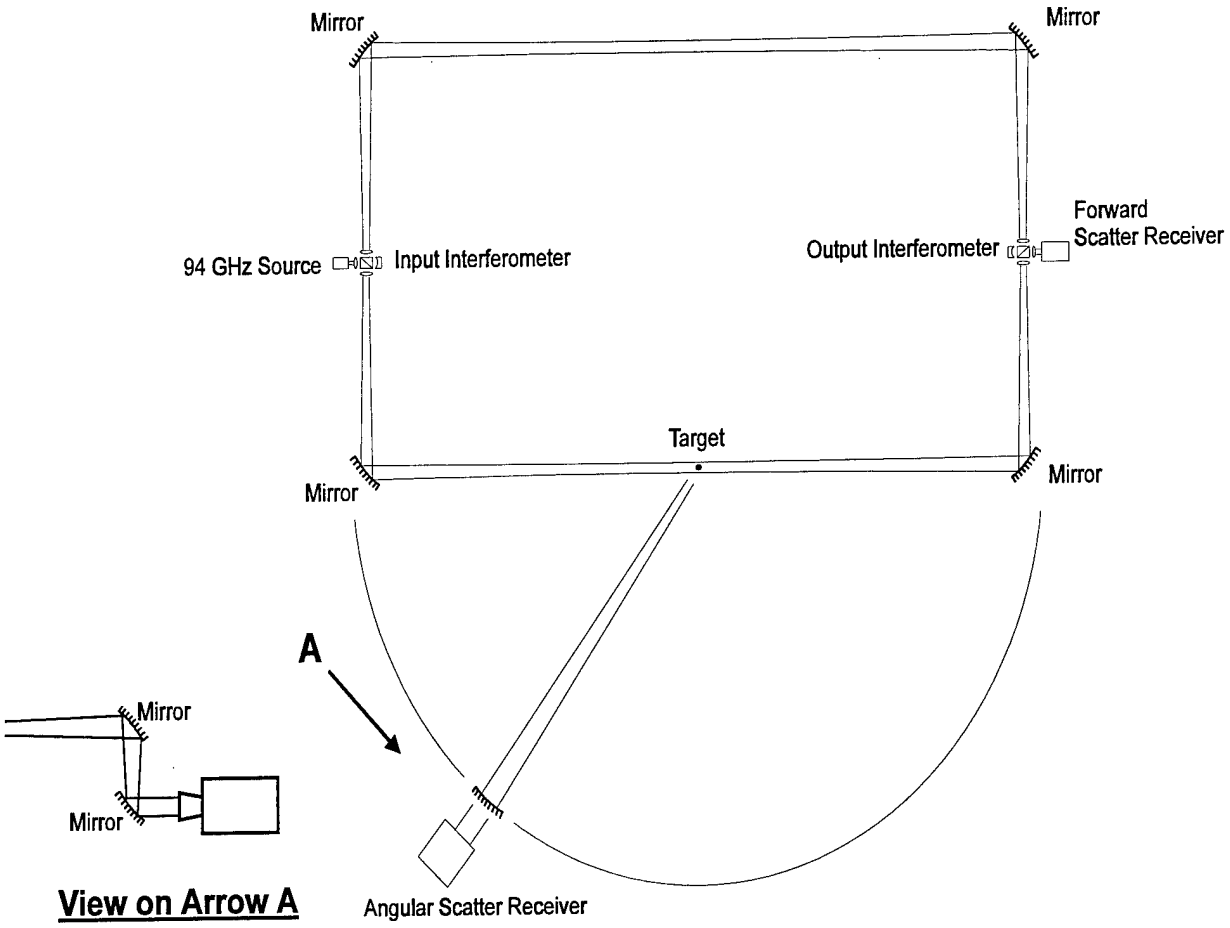

Figure D-10. United Kingdom 94 GHz polar nephelometer.

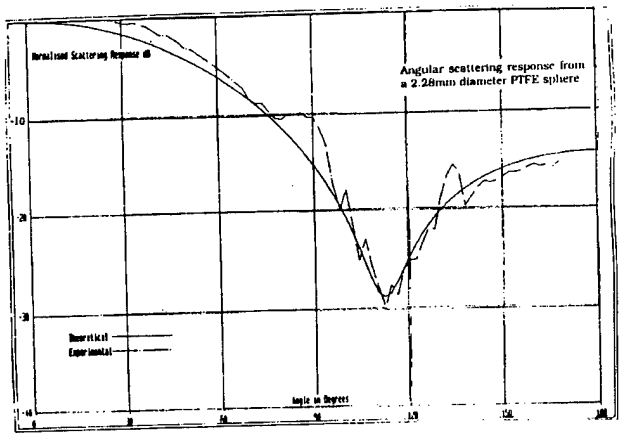

D-11a. 28mm Dia. TFE sphere.

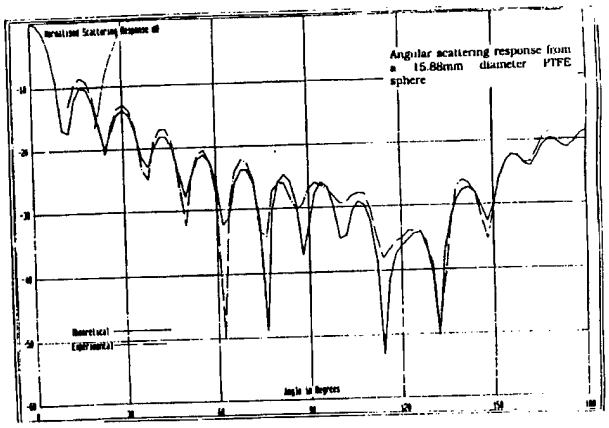

D-11b. 15.88mm Dia. TFE sphere.

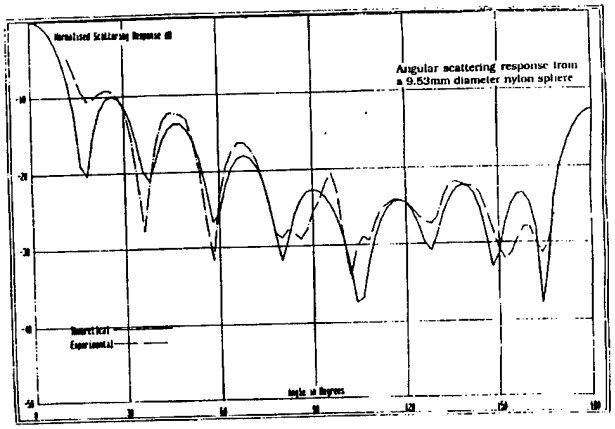

D-11c. 9.53mm Dia. nylon sphere.

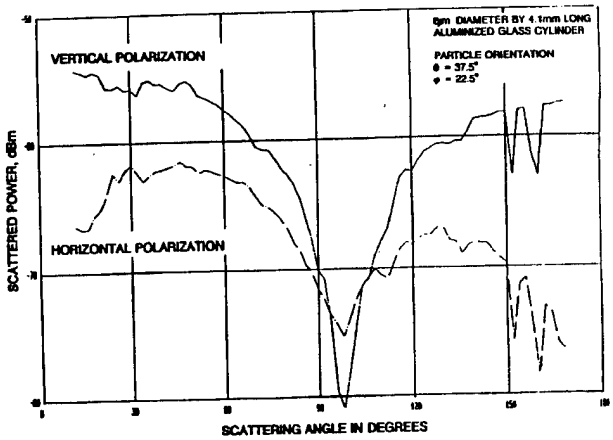

D-11d. 8mm Dia, 4.1mm long spherical glass cylinder.

Figure D-11. Example of Chemring polar nephelometer calibration data.

5.4 Particle Number Density Size Distributions after Atmospheric Release

To estimate transmittance through natural hydrometers or manmade obscurants, it is necessary to know the particle number density size distribution and the numeric spatial distribution along the line of sight between transmitter and receiver. Chamber measurements at ERDEC are taken of particle dosages (time integrated values of mass concentration). Dosage is used to infer concentration in the chamber by assuming a homogeneous distribution in the chamber during the dosage sample time. Chamber measurements are also made of concentration as a function of time using instruments calibrated to respond to concentration for particular obscurant types. When particle size and density are known, particle number density can be estimated from concentration data. When concentration is sufficiently low, individual particles can be counted with calibrated light scattering instruments to measure the particle number density directly for monodisperse millimeter wave obscurants and size distributions for visual and infrared obscurants.

5.5 Material Dielectric Constants

The complex index of refraction is a fundamental input required by virtually all electromagnetic wave scattering models. Detailed spectroscopic data determining material index of refraction to a wavelength of approximately 55 μm are available. For millimeter wavelengths, there are no direct measurements of the dielectric constants for obscurant materials. In this case, the complex index of refraction must be computed from the conductivity. High frequency dielectric constant data can be extrapolated to low frequency data using the Drude theory of metals. In the case of materials with a permanent dipole moment, a modified Debye model can be used for extrapolation. The accuracy of these extrapolations is not known. Data are available of fiber conductivity at millimeter wavelengths. However, transformation equations must be used to infer complex index of refraction from the conductivity measurements.

Measurements of fiber materiameter wavelengths are of materials in tow (continuous) form. These measurements are made in a resonant cavity wherein the cavity Q depends on the conductivity of the fiber material pulled through it (Goldberg). Measurements made by sampling long lengths of tow material show that distributions of conductivity exist for these materials. Uncoated materials have very narrow distributions of conductivity values. However, coated materials (for example, aluminum coated glass, nickel coated graphite, iron coated graphite) yield broad distributions in conductivity values. The photographs shown in figures D-12 to D-13 illustrate why this is so. The figures were kindly provided by Dr. Ira Goldberg, Rockwell International Corp. The figures are scanning electron microscope photographs obtained by Jane Hanamoto of Rockwell of obscurant fiber examples. The figures show conductive layer coated glass and graphite fibers, and uncoated graphite fibers. The photographs reveal uneven coating thicknesses and coating breaks and cracks along the length of the fiber, and striations in the surface of the uncoated fibers.

In figure D-12, the left photograph shows cross-sections of typical 3 μm diameter fibers. The middle photograph shows "dog-bone" cross-sectional shapes from Fortafil Corp. The average diameter is 6 to 7 μm. The right side photograph shows 6 μm diameter graphite fibers coated with nickel produced by Americal Cyanamid. Note the variation in coating thickness which is evident even on this scale.

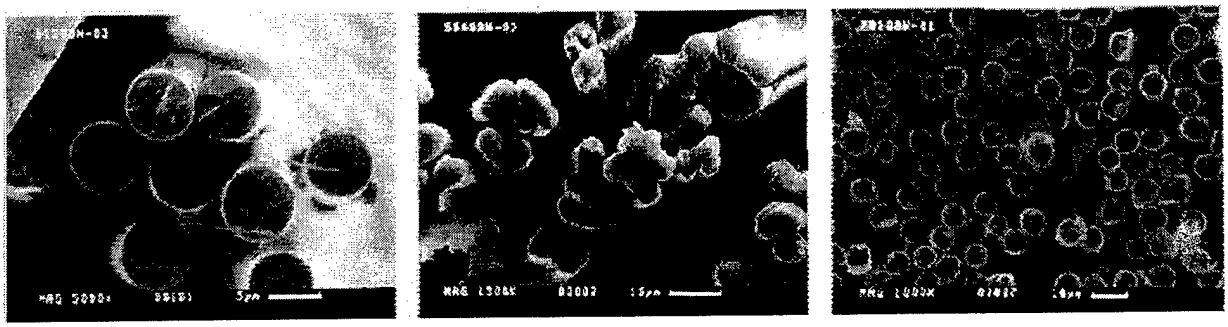

Figure D-12. Three microphotographs of graphite fibers (materials discussed at the CIAOS II workshop) showing end on views of fiber candidates for millimeter wave obscurants.

D-13a

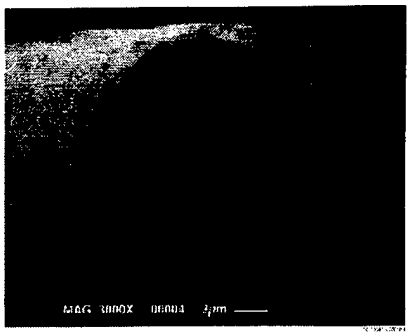

D-13b

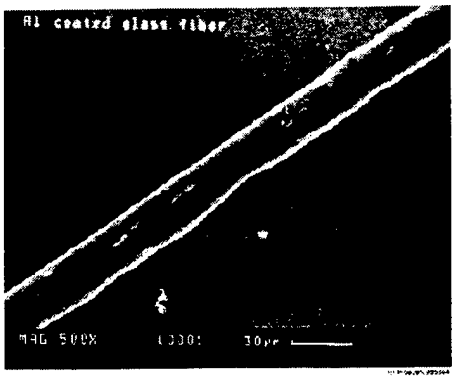

D-13c

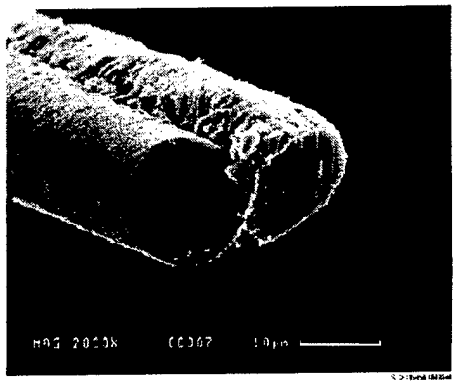

D-13d

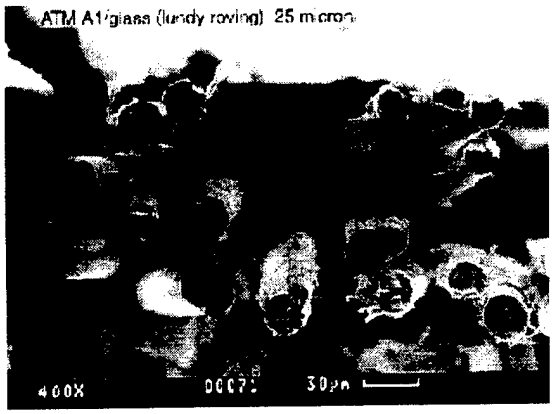

D-13e

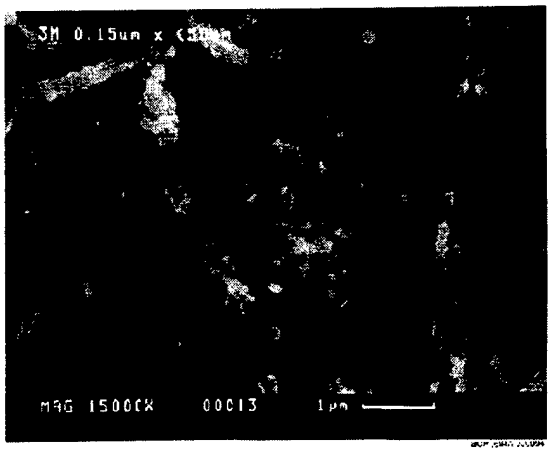

D-13f

Figure D-13. Photomicrographs.

5.6 Obscurant Characteristic Polarizations

For every particle ensemble, there exists an incident wave polarization state in which the polarization is unchanged during transmission (Beckman, 1968). The incident wave polarization state is called the characteristic polarization. Characteristic polarization is a useful parameter for defining the depolarization of electromagnetic waves transmitted through particular types of obscurants and the atmosphere in which they are dispersed.

Characteristic polarization data give sensor designers guidelines for configuring antennas and polarization geometry to optimize sensor performance, the obscurant developer information on optimizing obscurants toward one-way obscuration, and obscurant users information on optimum atmospheric conditions for effective obscurant performance. Virtually no characteristic polarization data for millimeter wave and microwave obscurants exists. It is also important to note the possibility that systems optimized for obscurant polarization effects may be inconsistent with systems optimized for natural meteorological effects.

The effects of particle orientation on the attenuation of polarized transmission in the millimeter wave bands is limited. Experimental data show a strong polarization dependent effect on the mass extinction coefficient. The best examples of these effects are from work performed in the United Kingdom by Edwards, Poulson, and Butters. Figure D-14 plots the measured mass extinction coefficient for horizontally and vertically polarized 35 GHz radiation attenuated by aluminized glass cylinders 25 μm diameter by 3.1 mm in length. These data were measured in a laboratory facility where the fibers fell from rest in still air so that the long axis of the fibers were oriented parallel to the floor. These data, plotted as a function of mass concentration along the transmissometer line of sight, also show potential multiple scatter effects because of the slight decrease in mass extinction as a function of concentration. Figures D-15, D-16, and D-17 show the results of a proof of concept field trial for 25 μm diameter aluminized glass fibers of various lengths disseminated from a RR170 cartridge chaff dispenser for aircraft. The 1.5-mm fibers were loosely packed providing 23 g of obscurant per cartridge. The 4.0-mm fibers could be loaded as aligned packages in the munition to provide a payload of 76 g per cartridge for aluminized glass and 59 g for nickel coated graphite. The transmittances (shown in figures D-15, D-16, and D-17) were produced by firing six cartridges to produce an obscurant cloud that drifted through a transmitted right circularly polarized beam, which was returned to the source using a calibrated trihedral target. Co-polar and cross-polar returns from the target were measured. These data show typical changes in signal levels for a two-way transmission through the cloud with the range gate of the sensor locked on the calibration target. The aluminized glass and nickel coated graphite fibers affect the right polarized signal power differently. The aluminized glass produced an increase in detected signal power after initially decreasing the signal power below the threshold. However, the nickel coated graphite only attenuated the transmitted energy.

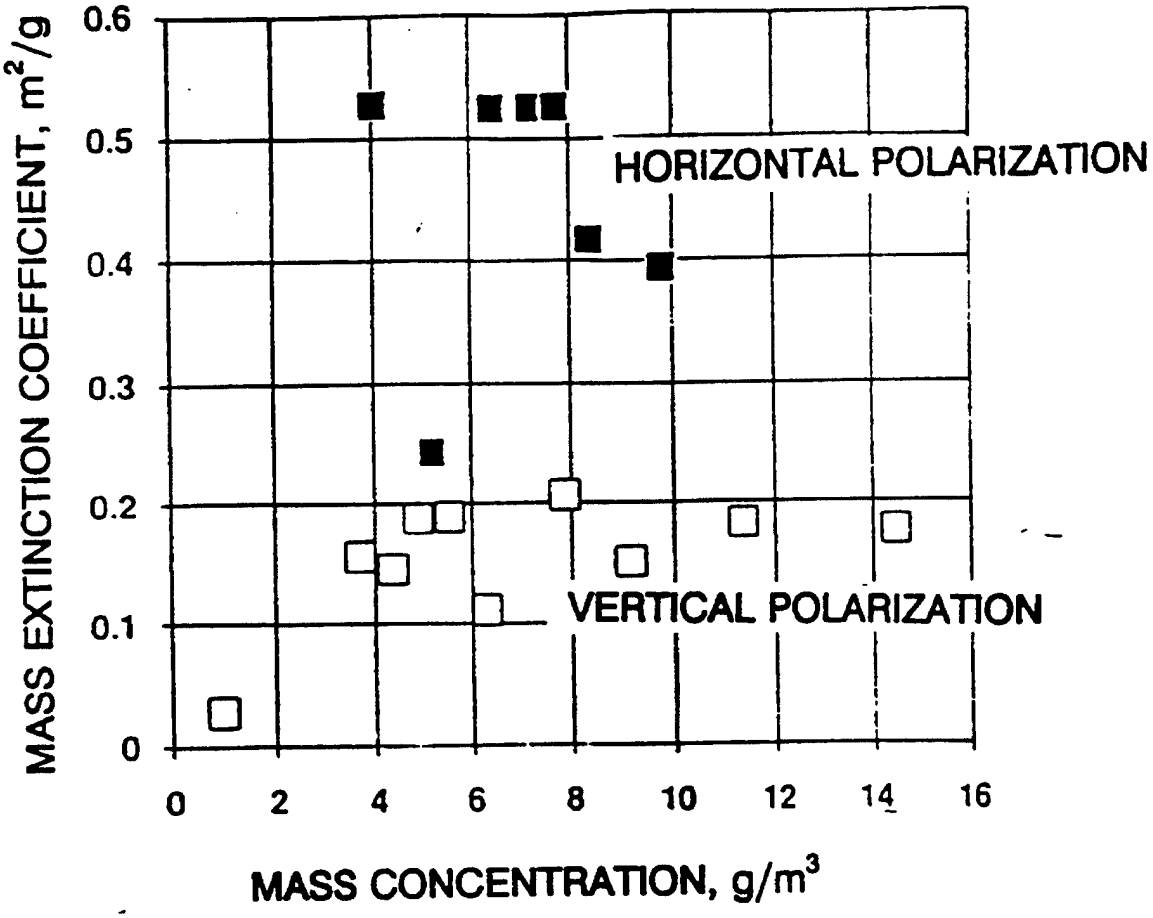

Figure D-14. Laboratory measured 35 GHz mass extinction coefficient as a function of aerosol mass concentration for 25- μm diameter, 3.1-mm long aluminized glass fibers.

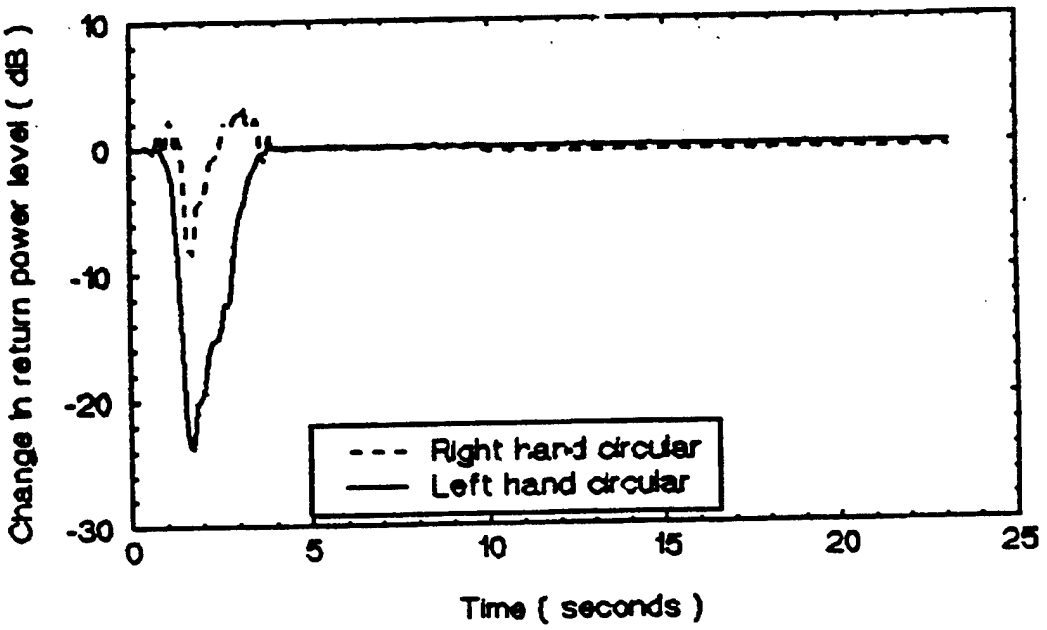

Figure D-15. Change in signal return from a calibrated target due to dissemination of 1.5 mm aluminized glass fibers.

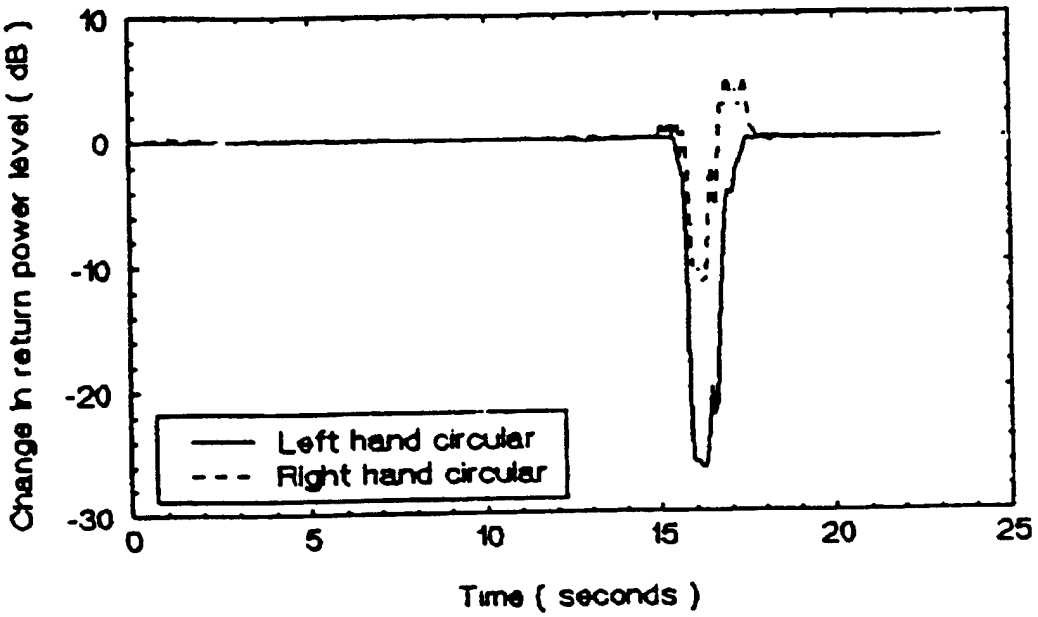

Figure D-16. Change in signal return due to dissemination of 4.0 MM aluminized glass fibers.

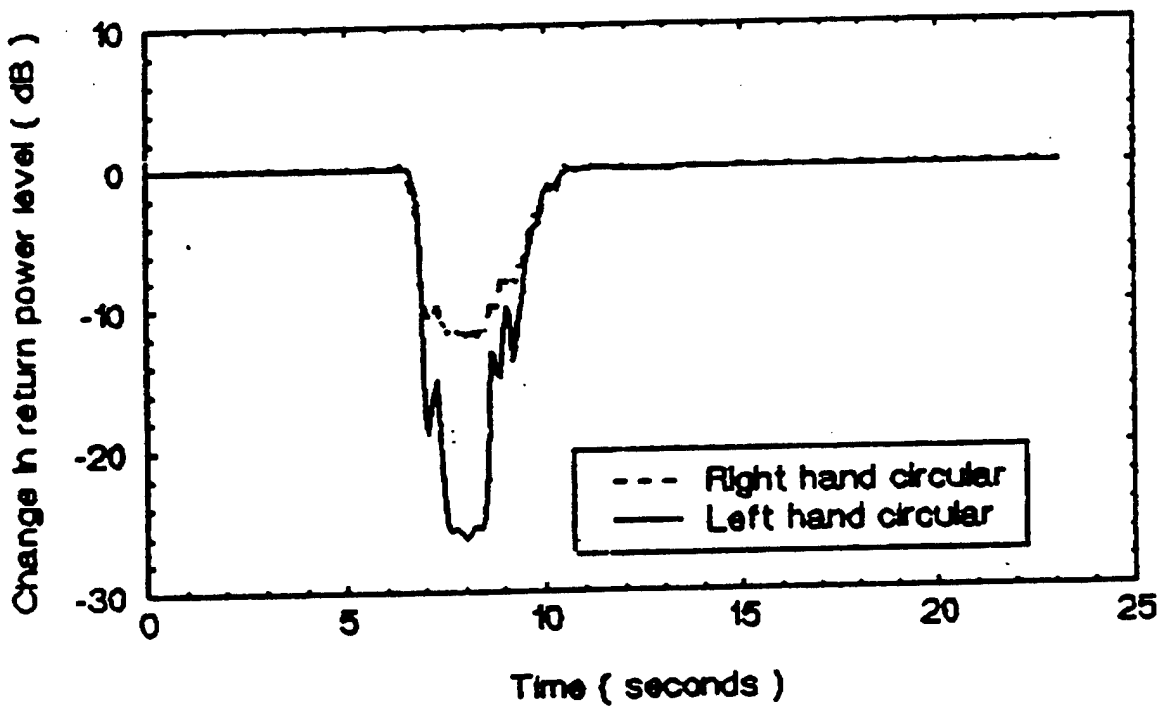

Figure D-17. Change in signal return from a calibrated target due to dissemination of 4.0-mm long coated graphite fibers.

References

Butters, B.C.F., and H. Edwards, 1991, "Measurement of the Mass Extinction Coefficient of Fibers at Millimeter Wave, Infrared, and Visible Wavelengths", Proc. Smoke Symposium XV, U. S. Army CRDEC Report.

Edwards, H. and F.W. Poulson, 1992, "Design and Evaluation of a Millimetric Obscurant Munition", Proc. of Smoke Symposium XVI, U.S. Army CRDEC Technical report.

Oguchi, T., 1983, "Electromagnetic Wave Propagation and Scattering in Rain and other Hyreomentes", Proceedings of the IEEE, Vol. 71(9):1029-1078.

Poulson, G.W. , N.J. Cronoin, N.A. Martin, and B.C.F. Butters, 1990, "A Novel Millimetre Wave Scattering Measurment Facility", Proceedings of Smoke Symposium XVI, Vol I pp 93-96, CRDEC-CR-092.

Roberts, S., and A. Von Hippel, 1946, "A New Method of Measuring Dielectric Constant and Loss on the Range of Centimeter Waves", J. Appl Phys. 17, 610-616.

Wang, R.T., 1988, "Status of the Microwave Scattering Facility (MSF) Upgrade", proceeding 1987 CRDEC Scientific Conference on Obscuration and Aerosol Research, U. S. Army Technical Report CRDEC-SP-88031, Edgewood, MD pp. 323-339.

Distribution

	Copies
NASA MARSHALL SPACE CENTER CODE EL54 ATTN MR JOHNSON HUNTSVILLE AL 35812	1
NASA MARSHALL SPACE FLT CTR ATMOSPHERIC SCIENCES DIV E501 ATTN DR FICHTL HUNTSVILLE AL 35802	1
ARMY STRATEGIC DEFENSE CMND CSSD SL L ATTN DR LILLY PO BOX 1500 HUNTSVILLE AL 35807-3801	1
ARMY MISSILE COMMAND AMSMI RD AS SS ATTN MR WILLIAMS REDSTONE ARSENAL AL 35898-5253	1
ARMY MISSILE COMMAND REDSTONE SCI INFO CTR AMSMI RD CS R DOCUMENTS REDSTONE ARSENAL AL 35898-5241	1
ARMY MISSILE COMMAND AMSMI RD TE F REDSTONE ARSENAL AL 35898-5253	1
DR HANS J LEIBE NTIAITS S3 BOULDER CO 80303	1
MIL ASST FOR ENV SCI OFFICE UNDERSECRETARY OF DEFENSE FOR RSCH & ENGRR&ATE&LS PENTAGON ROOM 3D129 WASHINGTON DC 20314	1

HEADQUARTERS
DAMI POI
WASHINGTON DC 20310-1067 1

ARMY MATERIEL SYS ANAL ACT
AMSXY MP
ATTN MR COHEN
APG MD 21010-5423 1

ARMY CHEM RES DEV & ENGR CTR
SMCCR OPA
ATTN MR PENNSYLE
APG MD 21010-5423 1

ARMY RESEARCH LABORATORY
AMSRL D
2800 POWDER MILL ROAD
ADELPHI MD 20783 1

ARMY RESEARCH LABORATORY
AMSRL OP SD TP
TECH PUB
2800 POWDER MILL ROAD
ADELPHI MD 20783-1145 1

ARMY RESEARCH LABORATORY
AMSRL OP CI SD TL
2800 POWDER MILL ROAD
ADELPHI MD 20783-1145 1

ARMY RESEARCH LABORATORY
AMSRL SS SH
ATTN DR SZTANKAY
2800 POWDER MILL ROAD
ADELPHI MD 20783 1

ARMY RESEARCH OFFICE
DRXRO-GS
ATTN DR FLOOD
PO BOX 12211
RTP NC 27709 1

ARMY ARDEC
AMSTA AR IMC BLDG 59
INFO RESEARCH CENTER
PICATINNY ARSENAL NJ 07806-5000 1

ARMY COMM ELECTRONICS
COMMAND EWRSTA DIRECTORATE
AMSEL RD EW OP
FT MONMOUTH NJ 07703-5206 1

ARMY SAT COMM AGENCY
DRCPM SC 3
FT MONMOUTH NJ 07703-5303 1

6585TH TG AFSC
RX
HOLLOMAN AFB NM 88330 1

ARMY TRADOC ANAL CTR
ATRC WSS R
WSMR NM 88002-5502 1

ARMY RESEARCH LABORATORY
AMSRL B
ATTN MR VEAZY
BATTLEFIELD ENVIR DIR
WSMR NM 88002-5501 1

ARMY RESEARCH LABORATORY
AMSRL BE E
BATTLEFIELD ENVIR DIR
WSMR NM 88002-5501 1

ARMY RESEARCH LABORATORY
AMSRL BE S
BATTLEFIELD ENVIR DIR
WSMR NM 88002-5501 1

ARMY RESEARCH LABORATORY
AMSRL BE W
BATTLEFIELD ENVIR DIR
WSMR NM 88002-5501 1

ARMY RESEARCH LABORATORY
SURV LETH ANALYSIS DIR
AMSRL SL E
WSMR NM 88002-5501 1

ARMY RESEARCH LABORATORY
SURV LETH ANALYSIS DIR
AMSRL SL S
WSMR NM 88002-5501 1

ARMY RESEARCH LABORATORY
SURV LETH ANALYSIS DIR
AMSRL SL C
APG MD 21005-5066 1

DEPT OF THE AIR FORCE
7TH WEATHER SQUADRON
APO NY 09403 1

USAF ROME LAB TECH LIB
FL2810 CORRIDOR W SIT 262
RLSUL DOCUMENTS LIBRARY
26 ELEC PKWY BLDG 106
GRIFFISS AFB NY 13441-4514 1

ARMY FIELD ARTILLERY SCHOOL
ATSF TSM TA SS
ATTN MR TAYLOR
FT SILL OK 73503-5600 1

ARMY DUGWAY PROVING GRND
STEDP MT DA M
ATTN MR CARLSON
DUGWAY UT 84022 1

ARMY DUGWAY PROVING GRND
STEDP MT DA L
DUGWAY UT 84022-5000 1

ARMY DUGWAY PROVING GRND
STEDP MT M L
ATTN MR BOWERS
DUGWAY UT 84022-5000 1

DEFENSE TECH INFO CTR 8725 JOHN J KINGMAN RD SUITE 0944 FT BELVOIR VA 22060-6218	
OPTEC TECHNICAL LIBRARY 4501 FORD AVENUE SUITE 820 ALEXANDRIA VA 22302-1458	1
ARMY FRGN SCI & TECH CTR CM 220 7TH STREET NE CHARLOTTESVILLE VA 22901-5396	1
NAVAL SURFACE WEAPONS CTR CODE G65 DAHLGREN VA 22448-5000	1
NAVAL SURFACE WEAPONS CTR CODE J41 ATTN MR C RUSSELL DAHLGREN VA 22448-5000	1
LOGISTICS CENTER ATCL CE FT LEE VA 23801-6000	1
TACDOWP LANGLEY AFB VA 23665-5524	1
ARMY NUCLEAR & CHEM AGENCY MONA ZB BLDG 2073 SPRINGFIELD VA 22150-3198	1
Record Copy	4
TOTAL	47